Eagle Mountain Lake WPP

Modeling Report

2016

Eagle Mountain Lake Watershed Protection Plan

Modeling Report

Prepared for the

Stakeholders of the Eagle Mountain Lake Watershed

by

Tarrant Regional Water District and Texas A&M AgriLife Research

This project was made possible with funding from the USDA-Natural Resource Conservation Service and the U.S. Environmental Protection Agency.

Additional support and collaboration were provided by
Texas State Soil and Water Conservation Board
Texas Commission on Environmental Quality
Tarrant Regional Water District
Texas A&M AgriLife Research & Extension
Texas Water Resources Institute
Texas A&M University Spatial Sciences Laboratory

2016

Cover photos courtesy TRWD and Dee Ann Littlefield, USDA-NRCS

CONTENTS

This page intentionally blank.

Water Quality Modeling Report for the Eagle Mountain Lake and Watershed

Executive Summary

The modeling efforts described in this report support the Eagle Mountain Lake Watershed Protection Plan, which defines a strategy and identifies opportunities for to implement practices and programs that restore and protect water quality. Water quality reports indicate that, without measures to reverse the trend of increasing eutrophication, Eagle Mountain Lake will likely exceed current nutrient and chlorophyll-a screening levels, and possibly future criteria.

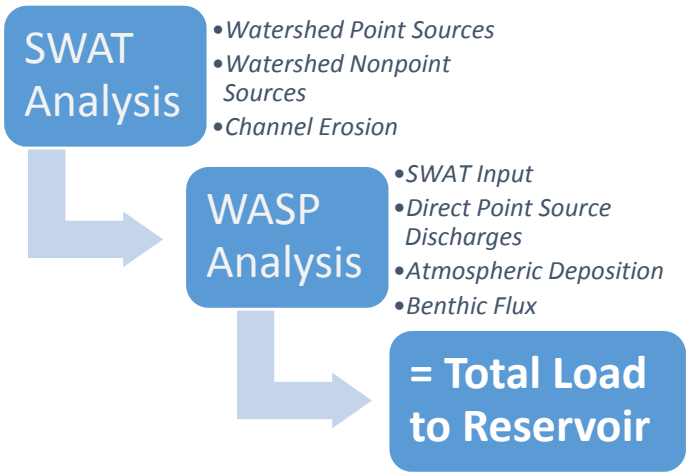

Loadings of nutrients and sediment from point and nonpoint sources in the watershed were estimated using the Soil and Water Assessment Tool (SWAT). The model estimate annual loadings of total phosphorus (TP), total nitrogen (TN), and sediment. Integration of SWAT with the USEPA Water Analysis Simulation Program (WASP) model was then used to estimate the impact of watershed, direct discharges and internal loadings on sediment and nutrient concentrations. The modeling approach is illustrated in more detail in Figure ES-1.

Figure ES-1. Pollutant Load Modeling Approach

The SWAT calibration period was based on the available period of record for two USGS stream gages (08043950 and 08044500) for 1991 through 2004. A base flow filter (Arnold et al., 1995a) was used to determine the fraction of base flow and surface runoff at selected gauging stations.

Validation was performed by applying the same model parameters to a different period (1971-1990).

For station 08044500 flow calibration period, r, N S E (Nash-Sutcliffe Model Efficiency) (Nash and Sutcliffe, 1970), observed mean, and modeled mean were 0.947, 0.913, 7.15 m/s, and 7.04 m/s respectively. For validation period, they were 0.964, 0.921, 8.59 mVs, and 8.50 m/s respectively.

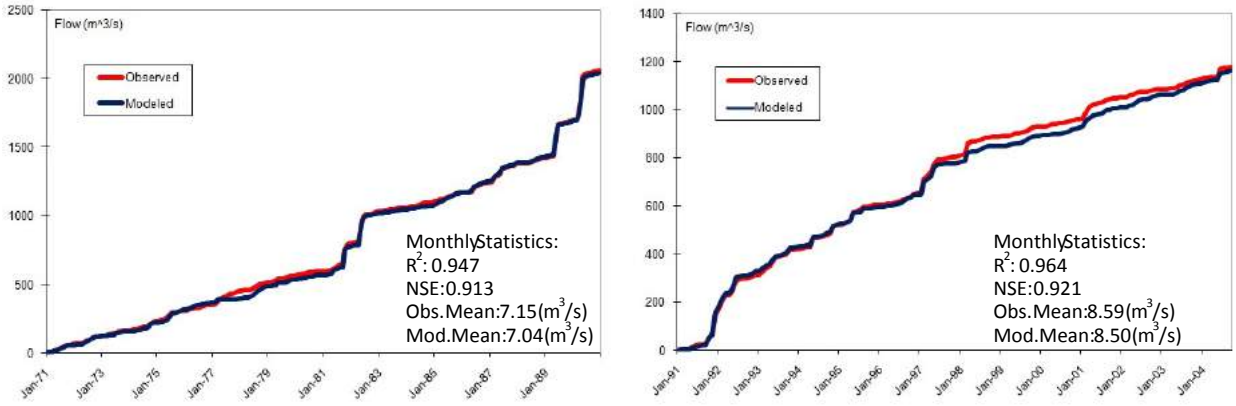

Figure ES-2. The result of flow calibration and validation by accumulated flow at USGS gage station 08044500.

Two sediment survey studies were conducted on Eagle Mountain Lake. The first study was conducted before modeling began and the second study was done during the modeling study. SWAT sediment calibration was done based on the second study conducted by Texas Water Development Board (TWDB 2009). However, the ratio between sediment from channel erosion and sediment from overland erosion was adopted from the study by Allen et al (2006). According to TWDB measurements, the sedimentation rate at the reservoir was 295,822 metric tons/year, which was 45,061 metric tons/year less than the study by Allen et al. Channel contribution was estimated at 98,569 tons/year (33.3%) and 197,313 tons/year (66.7%) from overland erosion. Simulated sediment from SWAT for the 1971 to 2004 period (34 years) was compared to the measured sediment, and appropriate input parameters were adjusted until the predicted annual sediment load from overland and channel erosion was approximately equal to the measured. The calibration was a series of runs to match yearly average sediment yield and it was considered acceptable when the difference was about 10%. Tables ES-1 and ES-2 summarize sediment calibration for overland erosion and for the entire watershed, respectively.

Table ES-1. Calibration and validation for sediment loading from overland flow

	Observed (ton)	Modeled (ton)	Difference (%)
Total (y^{-1})		196,909	-0.2 +4.6
Calibration (1994 – 2004)	197,313	206,294	
Validation (1970 – 1990)		191,748	-2.8

Table ES-2. Calibration and validation for sediment loading at Reservoir

	Observed (ton)	Modeled (ton)	Difference (%)
Total (y^{-1})		290,400	+0.2
Calibration (1994 – 2004)	295,822	263,827	-10.8
Validation (1970 – 1990)		324,880	+9.8

Nutrient calibration consisted of two parts: first, the model was calibrated based on a low flow study conducted August 18, 2004 at 10 sampling sites, and second, using long term tributary monitoring data (1971-2004) collected at five tributaries. Loads from wastewater treatment plants were generated from 12 monthly samples collected by TRWD in 2001 and 2002. There were some discrepancies with observations at some sites but the West Fork 4688 site, located near the lake, showed relatively good correlation between observed and modeled data.

The WASP model was calibrated for a 10-year period (1994-2003) for Eagle Mountain Lake. Nutrient loads to Eagle Mountain came from four (4) sources:

- SWAT was used to estimate the watershed loading to WASP including both nonpoint source (NPS) loading and point source (PS) loading from 7 wastewater treatment plants (WWTPs).
- Point source loading from two plants that directly discharge to the reservoir were input directly to WASP. All WWTP loadings were based on one year of self-reported nutrient data from the plants.
- Benthic flux of nutrients was based upon changes in hypolimnetic concentrations during stratified periods.
- Atmospheric loading was based upon rainfall analysis at Eagle Mountain Reservoir.

Table ES-3 illustrates the comparison of observed and predicted data of important system variables (TN, TP, TN:TP ratio, N-limitation, P-limitation and Chl'a') and revealed a reasonable "fit" for the model and assurance that the fundamental system response to nutrients was correctly simulated.

Table ES-3: Statistical Analysis of EM WASP Model Results

Comparison of Observed and Predicted Medians

	R-square Values		Relative Percent Difference		
Parameter	**Annual**	**Seasonal**	**Annual**	**Seasonal**	**Lab QC**
NH3	0.1622	0.3372	15.2%	42.4%	
NOX	0.5637	0.0121	63.3%	67.2%	
Org N	0.2976	**0.9340**	15.5%	31.4%	
TN	**0.9050**	**0.9361**	12.9%	20.9%	17.2%
OPO4	**0.9209**	**0.7601**	13.1%	37.4%	
Org P	**0.8455**	**0.9430**	22.7%	17.6%	
TP	**0.9345**	**0.9200**	10.0%	15.2%	16.8%
TN:TP	0.6721	0.3183	18.2%	21.4%	28.3%
Chl'a'	0.2332	0.0130	17.7%	26.4%	21.0%
N-limit	0.3315	0.0841	9.0%	11.6%	
P-limit	**0.9704**	**0.8739**	4.1%	14.1%	

Highlighted r-square values significant at p =0.05

There appears to be a co-limitation to nitrogen and phosphorus in Eagle Mountain, meaning that both parameters are at times limiting to algae growth. However given that the third quarter (July-Sep) algae population is made up of greater than 70% nitrogen fixing blue-green algae, it seems reasonable to focus management on just phosphorus. The overall phosphorus budget for 10-years of modeling has an annual load of 167,459 kg/yr with 95% of the phosphorus coming from NPS (watershed) loading, 2% from the 9 WWTPs, 2% from benthic flux, and 1% from atmospheric loading (Figure ES-3).

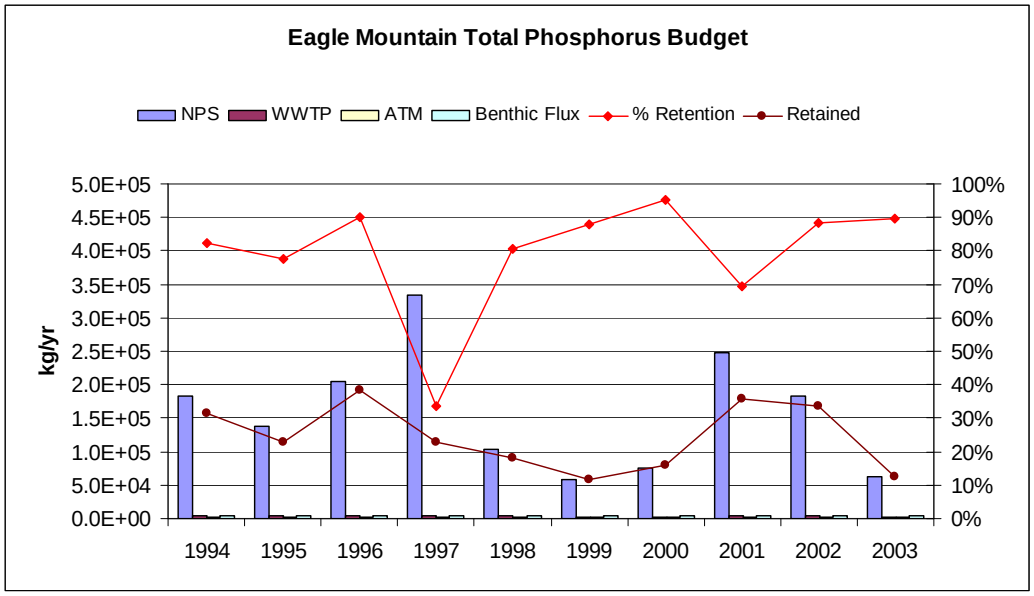

Figure ES-3: Eagle Mountain Nutrient Budget – Total Phosphorus (1994-2003)

Sensitivity analyses show that the reservoir is most sensitive to the watershed loading and benthic flux loading. Systematic reductions from 15% to 65% in watershed loading suggest that loads have to be reduced approximately 30% to have a statistically significant decrease in seasonal Chl'a' concentrations (Figure ES-4).

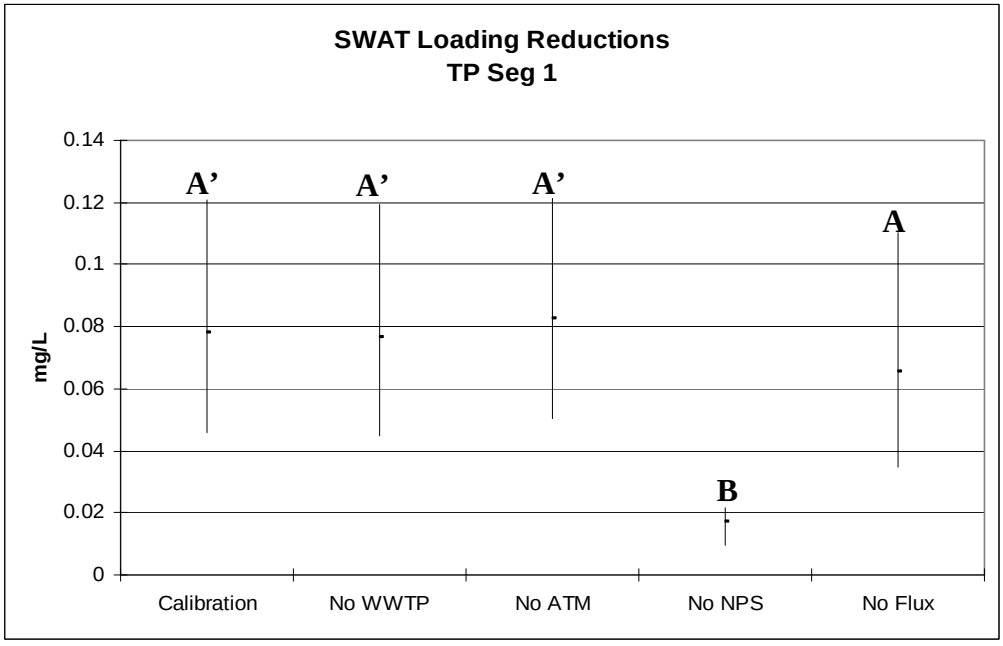

Figure ES-4: Eagle Mountain Reservoir Annual Chl'a' Segment 1 Median and Percentiles (1994-2003)

SWAT Modeling

Taesoo, L., B Narasimhan and R., Srinivasan. Eagle Mountain Watershed: Calibration, Validation, and Best Management Practices Final Report. September 12, 2011

INTRODUCTION

The watershed modeling objective of this project was to use the Soil and Water Assessment Tool (SWAT) to assess the effects of urbanization and other landuse changes on sediment and nutrient delivery to Eagle Mountain Lake. The watershed is located on the West Fork of the Trinity River primarily in Wise County but also partially in Jack, Clay, Montague Parker and Tarrant counties. Eagle Mountain Lake was constructed in 1932 as a water supply reservoir for Tarrant County (Figure 1); the reservoir has a total drainage area of 2,230 km (551,045 acres). All model data in this report, both observed and simulated, includes inflow to Eagle Mountain watershed from Bridgeport Reservoir, also constructed in 1932 (Figure 1). Daily inputs, such as flow, sediment, and nutrients, from Bridgeport Reservoir were represented as a point source in the Eagle Mountain watershed model.

MODEL AND DATA SOURCES

SWAT Model

SWAT is a basin-scale distributed hydrologic model. Distributed hydrologic models allow a basin to be subdivided into many smaller subbasins to incorporate spatial detail. Water yield and pollutant loads are calculated for each subbasin and then routed through a stream network to the basin outlet.

SWAT goes a step further with the concept of Hydrologic Response Units (HRUs). In SWAT, a single subbasin can be further divided into areas with unique combinations of soil and landuse, referred to as HRUs. All hydrologic processes are calculated independently for each HRU. The total nutrient or water yield for a subbasin is the sum of the corresponding constituents from all the HRUs it contains. HRUs allow

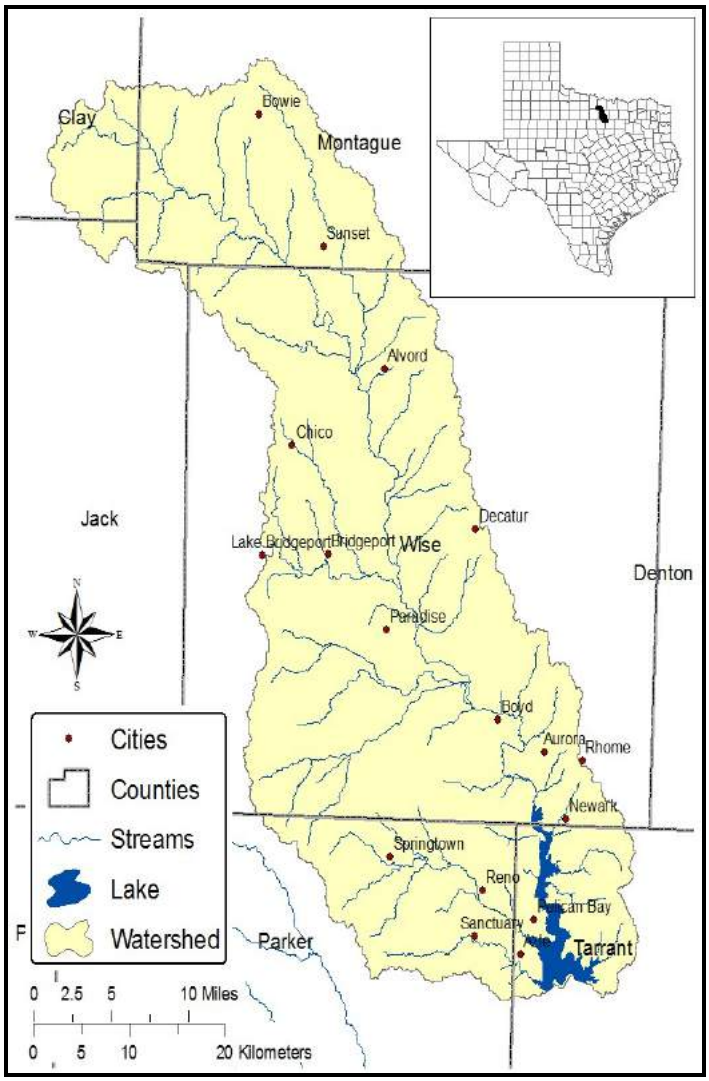

Figure 1. Eagle Mountain Reservoir watershed

more landuse and soil classifications to be represented in a computationally efficient manner, in turn providing greater spatial detail.

SWAT is a combination of applications, ROTO (Routing Outputs to Outlets (Arnold et al., 1995b) and the SWRRB (Simulator for Water Resources in Rural Basins or SWRRB (Williams et al., 1985). Furthermore, several systems contributed to the development of SWRRB including CREAMS (Chemicals, Runoff, and Erosion from Agricultural Management Systems) (Knisel, 1980), GLEAMS (Groundwater

Loading Effects on Agricultural Management Systems) (Leonard et al., 1987) and EPIC (ErosionProductivity and Impact Calculator) (Williams, 1990). SWAT was created to overcome the maximum area limitations of SWRRB, which can only be used on watersheds a few hundred square kilometers in area and has a limitation of ten subbasins. SWAT, in contrast, can be used for much larger areas. The HUMUS (Hydrologic Unit Model for the United States, also known as the HUMUS project (Srinivasan et al., 1998), used SWAT to model 350 USGS six-digit watersheds in 18 major river basins throughout the United States.

SWAT is a continuous simulation model that operates on a daily time step. Long-term simulations can be performed using simulated or observed weather data. The SWAT model is continually updated every few years to include new features and functionality. The current version, SWAT 2005, is widely used both in the United States and internationally. SWAT 2005 is distributed with the full Formula Translator (FORTRAN) source code, allowing anyone to make modifications to the model.

DEM

DEM (Digital Elevation Model) is elevation information created in a digital format. The data was obtained from NRCS (Natural Resources Conservation Service) Data Gateway at 30 meter resolution. The range of elevation in Eagle Mountain watershed is from 186 m to 387 m (610 to 1,270 feet) with average slope of 3.7%.

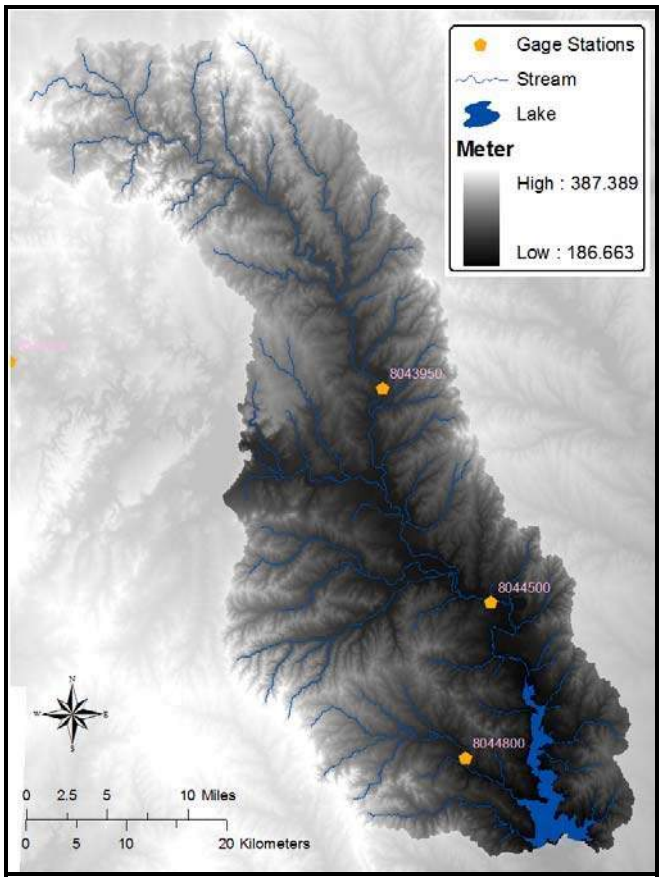

Figure 2. Digital Elevation Model (30m)

Landuse

The National Land Cover Dataset (NLCD) created in 1992 was used as SWAT landuse data input. Due to rapid urban development in the watershed, the Texas A&M Spatial Sciences Lab (SSL) enhanced this data for urban expansion using an aerial photograph from 2003 (Figure 3).

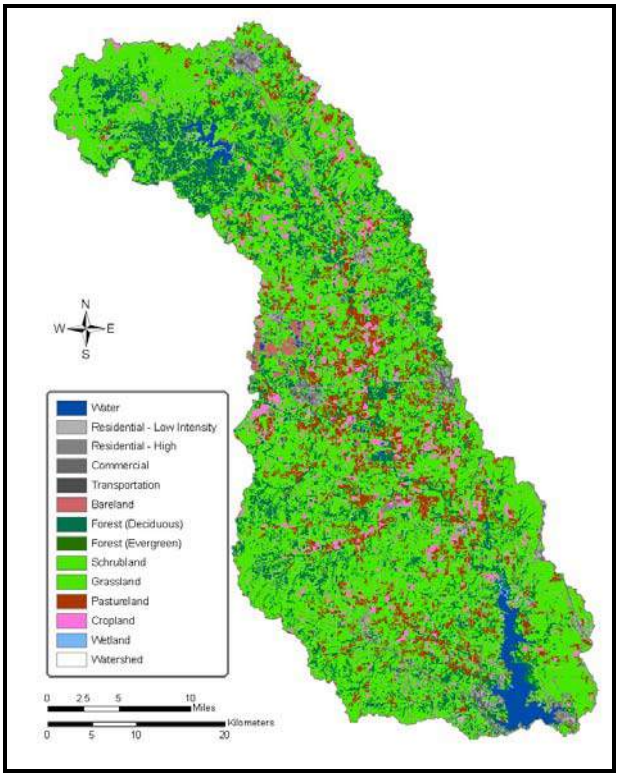

Figure 3. Landuse distribution

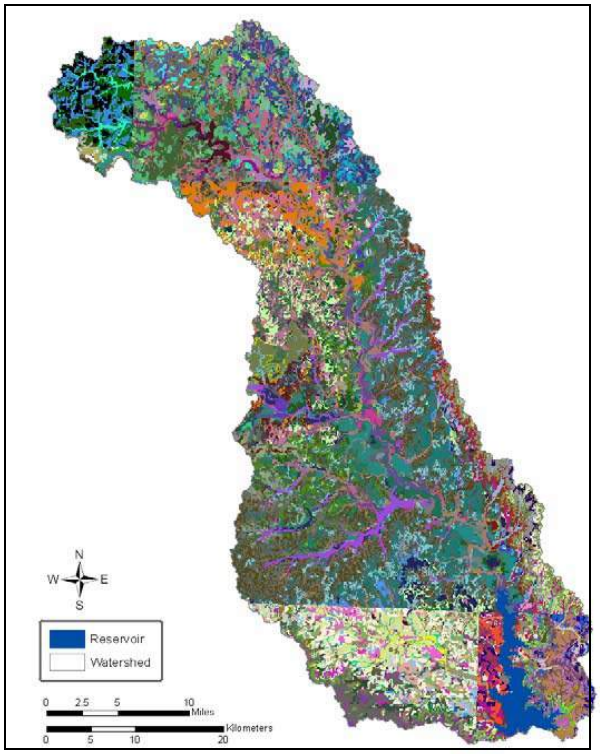

Figure 4. Soil map (SSURGO)

Soil

The soils dataset SSURGO (Soil Survey Geographic), which is the most detailed soils dataset available, was obtained from the NRCS Data Gateway and used as input for the SWAT model. SSURGO dataset includes soil information in each layer, soil type, texture, conductivity, albedo, and so on.

Weather

When National Weather Service stations (shown in Figure 5) lacked precipitation data during the period of record (1950–2004), nearby stations provided substitute data, and SWAT generated missing temperature data.

For rainfall data from 1999–2004, NEXRAD data was used to enhance missing rainfall or to create spatially distributed rainfall with finer resolution. It was done by averaging NEXRAD grid data for all subbasins near an individual climate station.

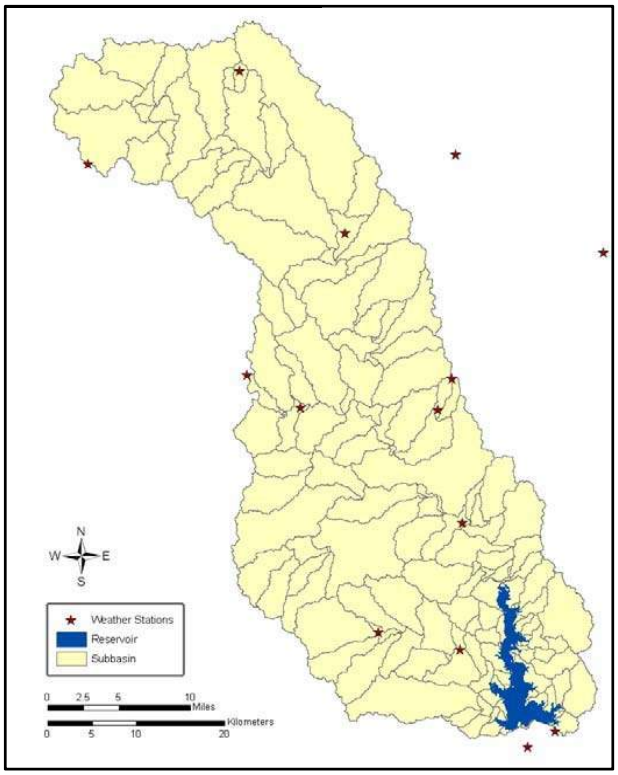

Figure 5. Distribution of weather stations

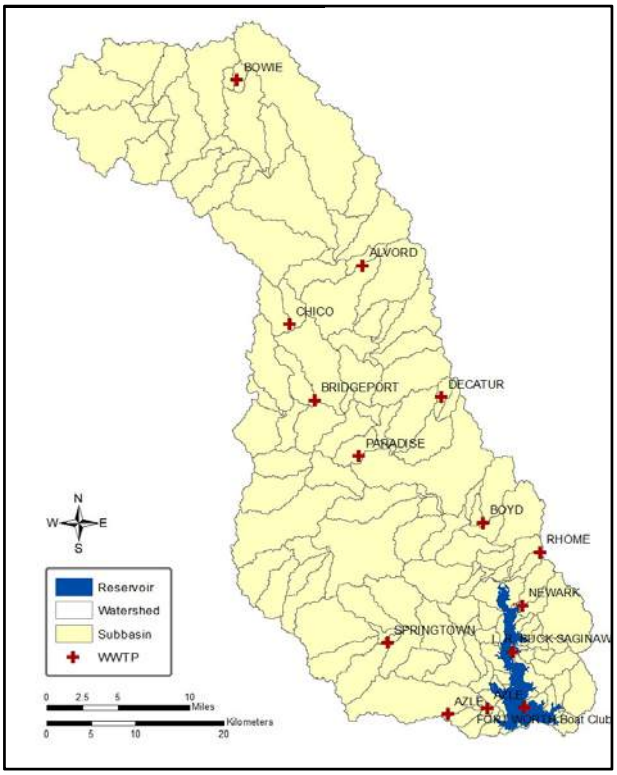

Figure 6. Waste Water Treatment Plants

Point Sources

The Eagle Mountain watershed contained a total of 14 waste water treatment plants (WWTP) distributed across the watershed. Two of these WWTPs discharge directly into the lake (Figure 6). WWTPs voluntarily collected weekly nutrient and flow data for one year, which provided point-source loading inputs. Weekly data have been combined into monthly loadings for each WWTP and then routed through the creeks. Table 1 through Table 11 shows the daily loading (flow, Total N, and Total P) from each WWTP.

Table 1. Daily discharge from WWTP of Alvord

	Daily Loads		
	Flow (m^3)	TN (kg)	TP (kg)
Jan-02	230.90	1.83	0.53
Feb-02	204.40	1.90	0.44
Mar-02	234.68	3.17	0.30
Apr-02	200.61	1.06	0.37
May-02	162.76	0.57	0.45
Jun-02	143.84	0.41	0.44
Jul-02	166.55	1.37	0.68
Aug-02	158.98	2.90	0.60
Sep-02	181.69	1.43	0.26
Oct-02	143.84	1.46	0.22
Nov-01	162.76	1.65	0.10
Dec-01	162.76	1.88	0.23

Table 2. Daily discharge from WWTP of Azle

	Daily Loads		
	Flow (m^3)	TN (kg)	TP (kg)
Jan-02	2882.03	15.10	2.01
Feb-02	2654.35	6.19	1.24
Mar-02	2916.47	10.63	1.00
Apr-02	3536.10	8.08	3.13
May-02	3443.56	3.97	0.86
Jun-02	2428.19	13.26	0.61
Jul-02	1631.41	17.87	0.81
Aug-02	2250.28	3.34	0.41
Sep-02	2102.28	5.98	0.53
Oct-02	3611.05	12.94	1.77
Nov-01	3195.63	7.76	3.15
Dec-01	3272.66	18.84	2.38

Table 3. Daily discharge from WWTP of Bowie

	Daily Loads		
	Flow (m^3)	TN (kg)	TP (kg)
Jan-02	1362.66	26.00	3.92
Feb-02	2258.80	46.76	6.66
Mar-02	2334.50	46.78	7.10
Apr-02	3919.92	77.73	20.05
May-02	2146.19	52.20	7.87
Jun-02	1735.50	42.84	6.03
Jul-02	1552.87	39.68	5.16
Aug-02	1791.90	37.57	5.95
Sep-02	1999.52	47.99	6.40
Oct-02	2119.69	42.44	5.22
Nov-01	1143.12	26.50	3.53
Dec-01	1997.31	41.61	6.34

Table 4. Daily discharge from WWTP of Boyd

	Daily Loads		
	Flow (m^3)	TN (kg)	TP (kg)
Jan-02	262.22	2.60	0.40
Feb-02	314.26	4.97	0.77
Mar-02	335.74	5.36	1.00
Apr-02	341.79	1.27	1.22
May-02	327.19	1.15	0.29
Jun-02	270.73	0.45	0.24
Jul-02	279.61	1.06	0.19
Aug-02	274.05	0.43	0.12
Sep-02	363.19	0.77	0.23
Oct-02	355.90	3.45	0.14
Nov-01	325.43	2.12	0.43
Dec-01	351.77	2.99	1.05

Table 5. Daily discharge from WWTP of Bridgeport

	Daily Loads		
	Flow (m^3)	TN (kg)	TP (kg)
Jan-02	1646.55	25.29	2.44
Feb-02	2117.80	13.23	4.52
Mar-02	2923.10	11.67	2.61
Apr-02	2057.62	15.15	1.58
May-02	2143.35	12.97	1.44
Jun-02	2347.75	24.82	6.31
Jul-02	2283.40	40.05	11.17
Aug-02	2211.48	39.17	6.63
Sep-02	2061.02	41.98	4.91
Oct-02	2167.39	29.69	4.36
Nov-02	2164.17	7.46	2.77
Dec-02	2259.75	25.46	4.85

Table 6. Daily discharge from WWTP of Chico

	Daily Loads		
	Flow (m^3)	TN (kg)	TP (kg)
Jan-02	215.75	5.11	0.99
Feb-02	215.75	5.38	0.90
Mar-02	215.75	5.38	0.94
Apr-02	215.75	4.02	0.86
May-02	215.75	6.21	1.21
Jun-02	215.75	5.34	1.24
Jul-02	215.75	5.22	1.14
Aug-02	215.75	3.91	1.25
Sep-02	215.75	5.47	1.22
Oct-02	215.75	4.46	1.07
Nov-02	215.75	7.29	1.02
Dec-01	215.75	4.24	0.89

Table 7. Daily discharge from WWTP of Decatur

	Daily Loads		
	Flow (m3)	TN (kg)	TP (kg)
Jan-02	1962.99	13.23	3.36
Feb-02	2596.63	31.19	10.32
Mar-02	3003.53	21.81	6.21
Apr-02	3663.10	34.50	5.91
May-02	2748.98	23.65	5.99
Jun-02	3092.48	35.88	14.34
Jul-02	3206.98	89.34	6.82
Aug-02	2654.16	20.01	5.53
Sep-02	2681.79	5.76	0.73
Oct-01	1339.95	15.72	3.94
Nov-01	1402.03	16.50	4.06
Dec-01	1559.49	6.02	1.02

Table 8. Daily discharge from WWTP of Newark

	Daily Loads		
	Flow (m^3)	TN (kg)	TP (kg)
Jan-02	64.35	1.04	0.38
Feb-02	215.28	2.03	0.67
Mar-02	164.09	0.58	0.28
Apr-02	154.34	0.35	0.39
May-02	188.73	0.44	0.38
Jun-02	156.99	2.51	0.74
Jul-02	160.19	3.83	0.88
Aug-02	171.37	3.29	0.82
Sep-02	127.18	2.47	0.50
Oct-02	118.76	2.09	0.31
Nov-02	123.87	0.85	0.53
Dec-01	147.81	1.77	0.59

Table 9. Daily discharge from WWTP of Paradise

	Daily Loads		
	Flow (m^3)	TN (kg)	TP (kg)
Jan-02	56.78	0.63	0.12
Feb-02	60.56	0.53	0.13
Mar-02	90.84	0.79	0.20
Apr-02	79.49	0.70	0.17
May-02	64.35	0.56	0.14
Jun-02	22.71	0.20	0.05
Jul-02	34.07	0.30	0.07
Aug-02	45.42	0.40	0.10
Sep-02	64.35	0.56	0.14
Oct-01	71.92	1.00	0.22
Nov-01	79.49	0.34	0.13
Dec-01	56.78	0.47	0.12

Table 10. Daily discharge from WWTP of Rhome

	Daily Loads		
	Flow (m^3)	TN (kg)	TP (kg)
Jan-02	110.53	0.88	0.29
Feb-02	196.83	0.78	0.09
Mar-02	140.62	1.05	0.24
Apr-02	105.98	0.58	0.14
May-02	213.18	2.08	0.35
Jun-02	134.37	0.93	0.39
Jul-02	200.61	1.94	0.44
Aug-02	215.75	2.09	0.47
Sep-02	219.54	2.12	0.48
Oct-02	215.75	2.09	0.47
Nov-01	120.12	2.49	0.48
Dec-01	121.50	1.73	0.19

Table 11. Daily discharge from WWTP of Springtown

	Daily Loads		
	Flow (m^3)	TN (kg)	TP (kg)
Jan-02	667.45	5.37	1.57
Feb-02	796.69	7.41	1.73
Mar-02	808.13	11.38	1.05
Apr-02	991.71	5.13	1.86
May-02	764.60	2.52	1.92
Jun-02	804.98	2.27	2.49
Jul-02	807.19	6.64	3.33
Aug-02	829.90	15.10	3.14
Sep-02	755.14	5.87	1.06
Oct-02	842.20	8.95	1.30
Nov-01	728.64	7.52	0.48
Dec-01	732.43	8.19	1.06

Sampling and Monitoring Stations

In the Eagle Mountain study, two data monitoring/collecting studies were used for a data source. One was an intensive, short-term, low flow study and the other a continuous, long-term water quality analysis on samples taken from various monitoring sites. For the low flow study, Tarrant Regional Water District (TRWD) collected a total of 14 samples at different locations along the stream network on August 18, 2004. The samples were analyzed for dissolved oxygen, biological oxygen demand, ammonia, phosphorus, Chlorophyll-a, organic nitrogen and nitrate-nitrite concentrations. The SSL then used observed data from 10 of the 14 locations to calibrate nutrients under low flow conditions. The TRWD also set up an independent QUAL-2E model based on the measured channel geometry and hydraulics developed during a dye study. The calibrated QUAL-2E kinetic terms and coefficients were then used as initial estimates of instream water quality parameters in SWAT.

The TRWD has six monitoring sites on main tributaries of Eagle Mountain Lake where they periodically collected grab samples from 1991 to 2004 to test for water quality (Figure 7). For SWAT calibration, data from five monitoring sites were used to modify SWAT's instream model parameters.

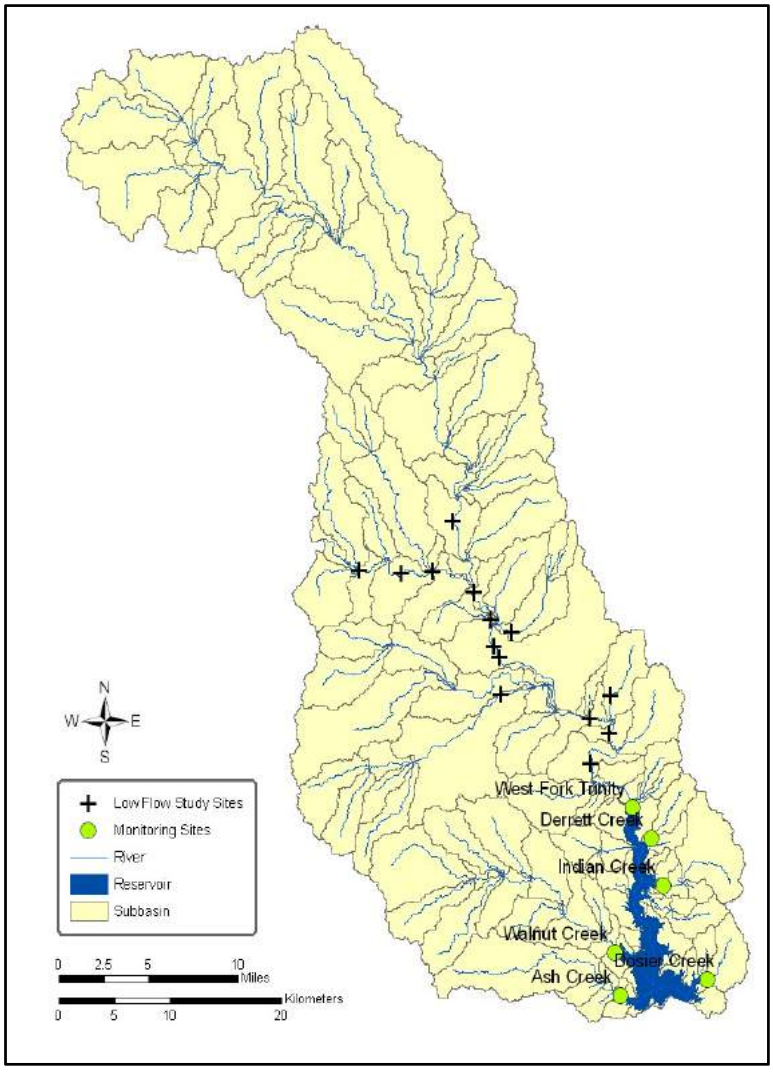

Figure 7. Low flow sampling sites and nutrients monitoring stations

Ponds

The Eagle Mountain Basin contains a total of 56 inventory-sized dams, as defined by the Texas Commission on Environmental Quality (TCEQ). These include NRCS flood prevention dams, farm ponds, and other privately owned dams. Physical data such as surface area, storage, drainage area, and discharge rates for these dams where input into SWAT to allow routing of runoff through the impoundments. Four structures were large enough to be simulated as reservoirs while the rest were simulated as small ponds (Figure 8).

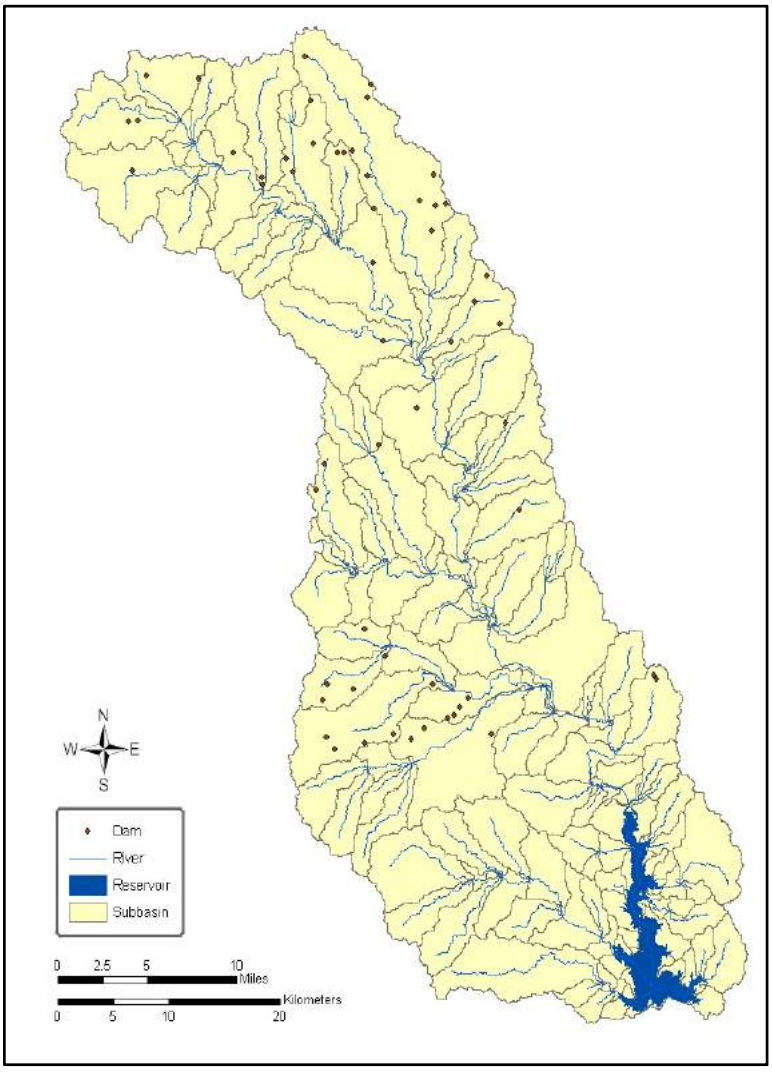

Figure 8. Distribution of NRCS inventory size and other size dams

Lake

Eagle Mountain Lake was built in 1932 and current specification of the lake is summarized in Table 12. The surface area at its principle spillway is 8,694 acres (3,518 ha) and it has the capacity of 190,000 acre-ft of its principle spillway (649.1 feet mean sea level). The surface area at the emergency spillway is 21,853 acres (8,843 ha) and has a capacity of 680,000 acre-ft.

Table 12. Characteristics of Eagle Mountain Lake

Specification	Size	
Surface Area at Principle Spillway	8,694	acres
Volume at Principle Spillway	19	10^4 acre-feet
Surface Area at Emergency Spillway	21,853	acres
Volume at Emergency Spillway	68	10^4 acre-feet

MODEL SET UP AND CALIBRATION

Model Set Up

SWAT 2005 automatically delineated subbasins within the watershed using DEM and a contributing area definition threshold of 500 ha. SWAT used landuse and soil information for spatial variation in the watershed. The total number of subbasins created by the model was 150 and they are shown in Figure 5. There are some subbasins partially submerged by the reservoir. The area under water in each subbasin was calculated and accounted for the effects of submergence in main channel inputs (channel erodibility and channel cover were set to "0.0"). SWAT simulated the land cover for these submerged areas as water.

SWAT's input interface divided each subbasin into HRUs with unique soil and landuse combinations. The number of HRU's within each subbasin was determined by: 1) creating an HRU for each landuse that equaled or exceeded 2% of each subbasin's area, and 2) creating an HRU for each soil type that equaled or exceeded 10% of any of the landuses selected in 1). Using these thresholds, the interface created 1,516 HRUs within the watershed.

Eagle Mountain watershed contained a total of 14 WWTPs from each major city and they are distributed in the basin as shown in Figure 6. Two of these WWTPs discharge directly into the reservoir. WWTPs voluntarily collected weekly nutrient and flow data for one year, which provided point-source loading inputs. This weekly data was converted to monthly loadings for each WWTP and included in the model. The Eagle Mountain watershed contains a total of 56 inventory-sized dams, as defined by the TCEQ. These include NRCS flood prevention dams, farm ponds and other privately owned dams. The physical properties of each pond such as surface area, storage, drainage area, and discharge rates for these dams were input into SWAT to allow routing of runoff through the impoundments. Four ponds were large enough to be simulated as reservoirs while the rest were simulated as small ponds.

Flow Calibration and Validation

The calibration period was based on the available period of record for stream gauge flow. Measured stream flow was obtained from two USGS stream gages (08043950 and 08044500) as

shown in Figure 2 for 1991 through 2004. A base flow filter (Arnold et al., 1995a) was used to determine the fraction of base flow and surface runoff at selected gauging stations.

Appropriate plant growth parameters for brush, native grasses, and other land covers were input for each model simulation. Initial inputs were based on known or estimated watershed characteristics. SWAT was calibrated for flow by adjusting appropriate inputs that affect surface runoff and base flow. Adjustments were made to runoff curve number, soil evaporation compensation factor, shallow aquifer storage, shallow aquifer re-evaporation, and channel transmission loss until the simulated total flow and fraction of base flow were approximately equal to the measured total flow and base flow, respectively.

Validation was performed by applying the same model parameters to a different period (1971–1990). Validation was done in an earlier period than calibration because the landuse dataset used in this model represented land cover in 2001. Therefore, it would be more appropriate to calibrate the model for the period that includes the year of the land cover dataset to represent more accurately.

Figure 9 shows the result of flow calibration and validation at USGS gage station 08044500. For calibration period, r^2, NSE (Nash-Sutcliffe Model Efficiency) (Nash and Sutcliffe, 1970), observed mean, and modeled mean were 0.947, 0.913, 7.15 m^3/s, and 7.04 m^3/s respectively. For validation period, they were 0.964, 0.921, 8.59 m^3/s, and 8.50 m^3/s respectively.

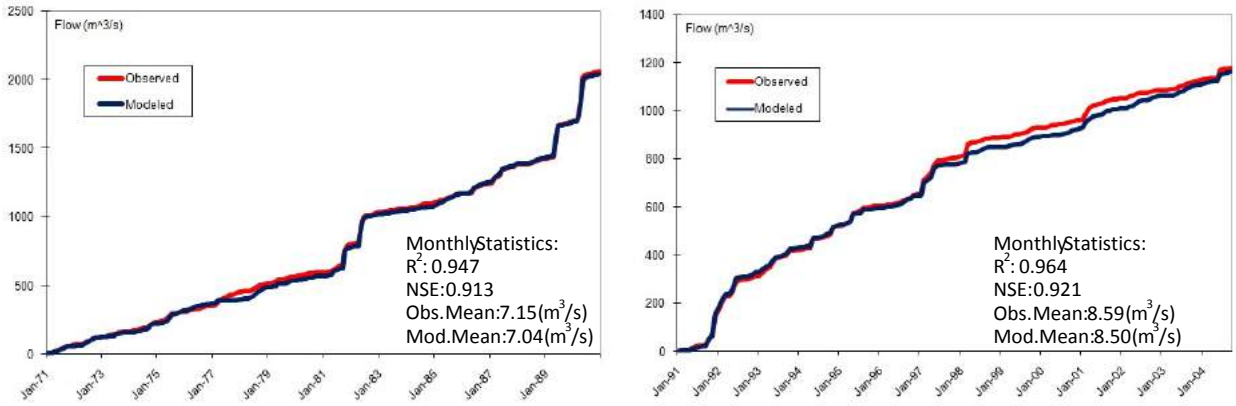

Figure 9. The result of flow calibration and validation by accumulated flow at USGS gage station 08044500.

Sediment Calibration and Validation

Two sediment survey studies were conducted on Eagle Mountain Lake. The first study was conducted before modeling began and the second study was done during the modeling study. SWAT sediment calibration was done based on the second study conducted by Texas Water Development Board (TWDB 2009). However, the ratio between sediment from channel erosion and sediment from overland erosion was adopted from the study by Allen et al (2006).

Sediment calibration was done based on the TWDB study, which used duel frequency sonar. With this technique, the thickness of the post impoundment sediment in the reservoir was estimated, although shallow areas could not be measured due to limited boat accessibility.

Shallow areas full of sediment near the mouth of major tributaries were also not measured with this technique for the same reason.

With these conditions considered, the TWDB sedimentation study was used for calibrating sediment loadings in the SWAT model as it was the most state of the art technology and had finer resolution. However, the ratio between sediment from channel erosion and sediment from overland erosion was adopted from the study by Allen et al (2006).

According to TWDB measurements, the sedimentation rate at the reservoir was 295,822 metric tons/year, which was 45,061 metric tons/year less than the study by Allen et al. Channel contribution was estimated at 98,569 tons/year (33.3%) and 197,313 tons/year (66.7%) from overland erosion.

Simulated sediment from SWAT for the 1971 to 2004 period (34 years) was compared to the measured sediment, and appropriate input parameters were adjusted until the predicted annual sediment load from overland and channel erosion was approximately equal to the measured.

Table 13 and Table 14 summarize sediment calibration for overland erosion and for the entire watershed respectively. The calibration was a series of runs to match yearly average sediment yield and it was considered acceptable when the difference was about 10%. Final values for SWAT input coefficients used in flow and sediment calibration are given in Table 15.

Table 13. Calibration and validation for sediment loading from overland flow

	Observed (ton)	Modeled (ton)	Difference (%)
Total (y^{-1})		196,909	-0.2 +4.6
Calibration (1994 – 2004)	197,313	206,294	
Validation (1970 – 1990)		191,748	-2.8

Table 14. Calibration and validation for sediment loading at Reservoir

	Observed (ton)	Modeled (ton)	Difference (%)
Total (y^{-1})		290,400	+0.2
Calibration (1994 – 2004)	295,822	263,827	-10.8
Validation (1970 – 1990)		324,880	+9.8

Table 15. SWAT input coefficients adjusted for calibration of flow and sediment

Variable	Description	Input Value	Units	File
Coefficients related to flow				
CN2	SCS Runoff curve number (adjustment range)	+5 to -5		*.mgt
ESCO	Soil evaporation factor	0.85		*.hru
GW_REVAP	groundwater re-evaporation coefficient	0.02		*.gw
REVAPMN	Groundwater storage required for reevaporation	1	mm	*.gw
ALPHA_BF	Baseflow alpha factor	0.0431 to 0.0670	$Days^{-1}$	*.gw
CH_N2	Mannings "n" roughness for channel flow	0.125		*.rte
CH_K2	Hydraulic conductivity of channel alluvium	0.5 to 5.0	mm/hr	*.rte
Coefficients related to sediment				
USLE_C	*Minimum "C" value for pastureland in fair condition*	*0.007 - crop.dat*		
SPCON	*Linear parameter for calculating the maximum amount of sediment that can be reentrained during channel sediment routing*	*0.003*	-	*basins.bsn*
SPEXP	*Exponent parameter for calculating sediment reentrained in channel sediment routing*	*0.67*	-	*basins.bsn*
TRNSRCH	*Reach transmission loss partitioning to deep aquifer*	*0.2*		*basins.bsn*
CH_COV	*Channel cover factor*	*0.001 to 0.9*	-	**.rte*
CH_EROD	*Channel erodibility factor*	*0.001 to 0.9*	-	**.rte*

Nutrient Calibration and Validation

Nutrient calibration consisted of two parts: first, the model was calibrated based on a low flow study conducted August 18, 2004, and second, using long term tributary monitoring data.

For the first step in the nutrient calibration of SWAT, parameters were adjusted to agree with measurements at 10 sampling sites where sediment, nutrients, and bio-chemical data were collected under low flow conditions (Table 16). Because it was base flow condition, nutrients discharged from WWTP and channel process were greater portions in the calibration. One of the data problems, however, was that there was a 17 mm rainfall in the northeast part of watershed on Aug 16, 2004, and it may have impacted the data.

In the second step of the calibration, the parameters were adjusted for the remainder of the subbasins using monitoring station data. The simulation period was 1971 through 2004. WWTP loads were generated from one year's worth of monthly data collected by TRWD in 2001 and 2002 and it was assumed that WWTP loadings were constant for each facility.

The output from this simulation was compared to water quality data collected by TRWD from 1991 through 2004 in each major tributary (Ash, Derrett, Dosier, Walnut, and the West Fork of the Trinity River at County Road 4688 as shown in Figure 10). In order to account for daily variability of SWAT, simulated output was averaged for the three days surrounding the day of the measured grab samples. The medians, 25th percentile, and 75th percentile of the 3-day averages from SWAT were compared to the medians, 25th and 75th percentiles of the measured monitoring data samples (Figure 10). The coefficients for all subbasins were adjusted for each watershed to match the observed data. There were some discrepancies with observations at some sites but the West Fork 4688 site, located near the lake, showed relatively good correlation between observed and modeled data. Table 17 summarizes estimated sediment and nutrient loading into the lake as a baseline condition. The baseline condition will be used for BMP analyses in the later chapter of this report.

Table 16. General water quality input coefficients (.wwq) for low flow study and monitoring site calibration

Variable Name	Definition	SWAT-SSL Cal. Coef.	SWAT Default	SWAT Range
LAO	Light averaging option	2	2	2
IGROPT	Algal specific growth rate option	2	2	3 options
AI0	Ratio of chlorophyll-a to algal biomass [µg-chla/mg algae]	10	50	10 - 100
AI1	Fraction of algal biomass that is nitrogen [mg N/mg alg]	0.090	0.080	0.07 - 0.09
AI2	Fraction of algal biomass that is phosphorus [mg P/mg alg]	0.020	0.015	0.01 - 0.02
AI3	The rate of oxygen production per unit of algal photosynthesis [mg O2/mg alg)]	1.500	1.600	1.4 - 1.8
AI4	The rate of oxygen uptake per unit of algal respiration [mg O2/mg alg)]	2.300	2.000	1.6 - 2.3
AI5	The rate of oxygen uptake per unit of NH3-N oxidation [mg O2/mg NH3-N]	3.500	3.500	3.0 - 4.0
AI6	The rate of oxygen uptake per unit of NO2-N oxidation [mg O2/mg NO2-N]	1.000	1.070	1.0 - 1.14
MUMAX	Maximum specific algal growth rate at 20º C [day-1]	2.000	2.000	1.0 - 3.0
RHOQ	Algal respiration rate at 20º C [day-1]	0.300	0.300	0.05 - 0.50
TFACT	Fraction of solar radiation computed in the temperature heat balance that is photosynthetically active	0.440	0.300	0.01 - 1.0
K_L	Half-saturation coefficient for light [kJ/(m2·min)]	0.418	0.750	0.2227-1.135
K_N	Michaelis-Menton half-saturation constant for nitrogen [mg N/lL]	0.400	0.020	0.01 - 0.30
K_P	Michaelis-Menton half-saturation constant for phosphorus [mg P/l]	0.040	0.025	0.001 -0.05
MBDA0	Non-algal portion of the light extinction coefficient [m-1]	1.500	1.000	-
LAMBDA1	Linear algal self-shading coefficient [m-1·(µg chla/l)-1)]	0.002	0.030	0.0065-0.065
LAMBDA2	Nonlinear algal self-shading coefficient [m-1·(µg chla/l)-2]	0.054	0.054	0.054
P_N	Algal preference factor for ammonia	0.100	0.500	0.01 - 1.0

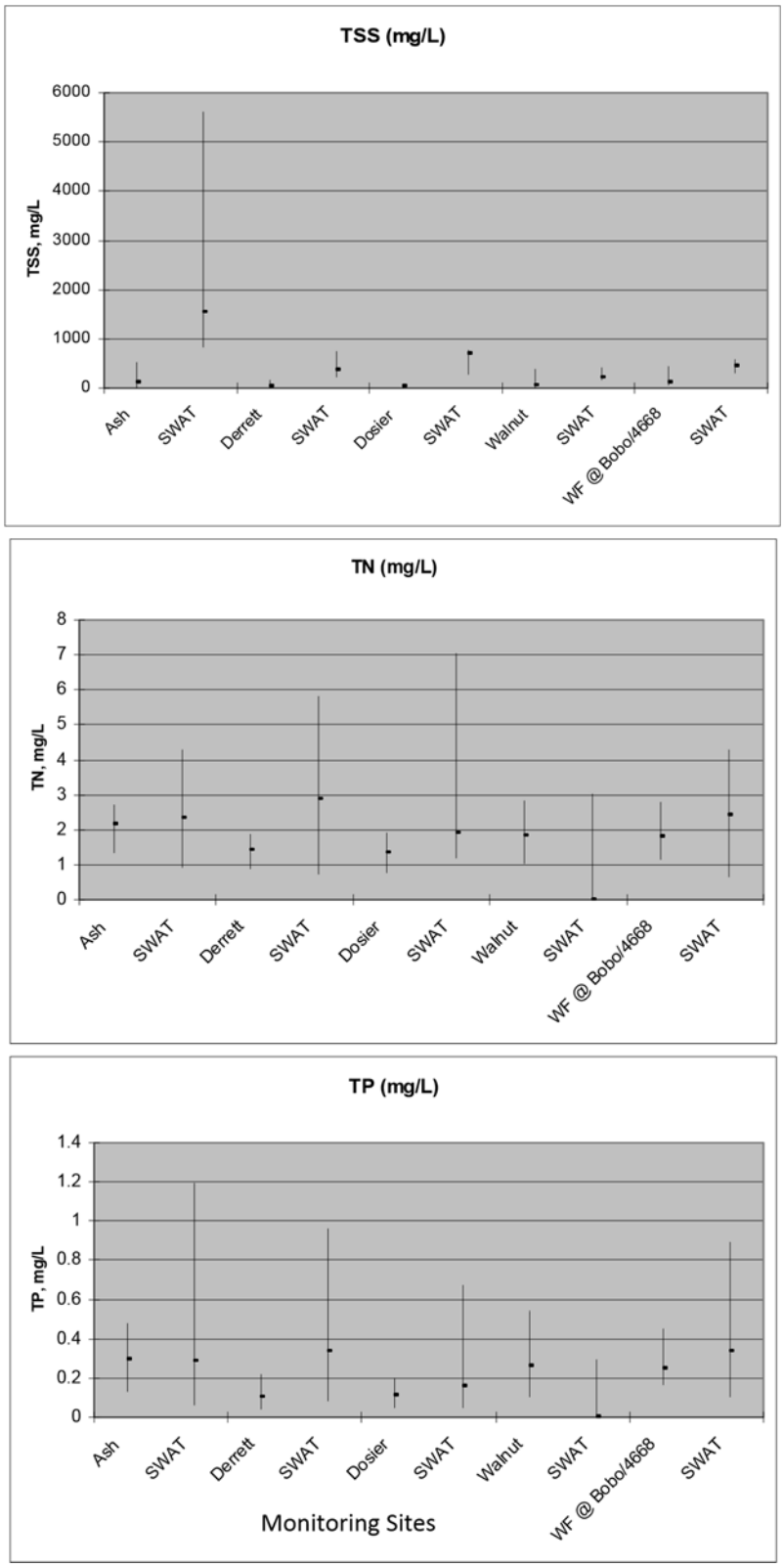

Figure 10. Model calibration for monitoring sites

Table 17. Estimated annual sediment and nutrient loading to Eagle Mountain Lake (Baseline condition) from 1971 to 2004

	Sediment (t/y)*	Total N (kg/y)	Total P (kg/y)
Calibrated model estimation (baseline)	296,400	1,055,220	173,020

* Units are metric units

LOAD ESTIMATES

Average annual load by landuse

Eagle Mountain watershed is composed by 6 landuse categories (Table 18) based on landuse datasets. The largest portion of landuse is occupied by rangeland at almost 60% followed by forest at 17.78%, urban 9.77%, pasture 9.30%, cropland 3.39%, and wetland with 0.04%.

Table 18. Landuse category in Eagle Mountain watershed

Category	Area
Urban	9.77 %
Forest	17.78 %
Cropland	3.39 %
Pasture	9.30 %
Rangeland	59.72 %
Wetland	0.04 %
Total	100.00 %

Figure 11 illustrates sediment and nutrient loading by each landuse category. Channel, which is not in the landuse category, is a major contributor of sediment 46.64%, TN 15.45% and TP 25.05%. Cropland, which accounts for only 3.39% of entire watershed, is another major driver for water quality degradation in the lake contributing 31.16% of sediment, 14.90% of TN and 32.16% of TP. On the other hand, rangeland, which encompasses almost 60% of the watershed, generates relatively less sediment 10.86%, TN 44.10% and TP 14.46%.

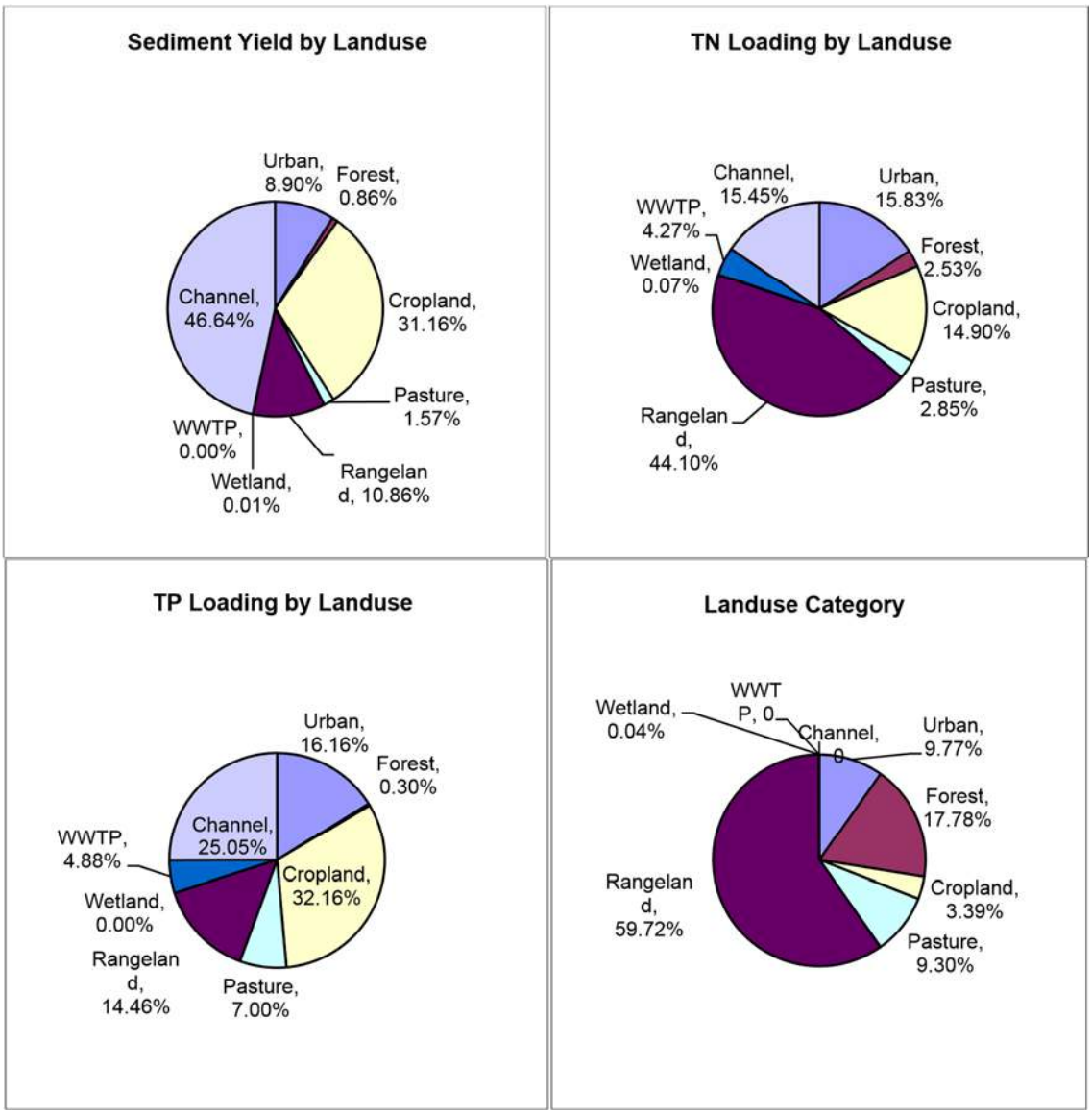

Figure 11. Sediment and nutrients loadings by landuse

Average annual load by subbasin

Sediment and nutrient loading by each subbasin are important to identifying 'hot spots' in the watershed and provides an overview of problems. Figure 12 through Figure 14 show sediment and nutrients loadings by subbasins. There is no significant 'hot spot' to intensively manage for pollutant area, but there is general trend that the eastern and southern parts of the watershed generate relatively more sediment and nutrients (red in maps). Those relatively high yield subbasins are the priorities to be managed by best management practices (BMPs). The next chapter describes how BMPs were simulated and what BMPs were necessary to reduce sediment and nutrient loadings to the lake.

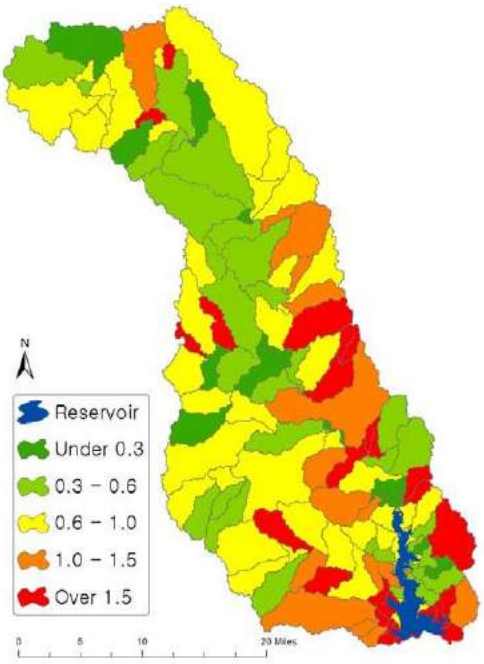

Figure 12. Sediment yield (t/ha) by overland flow predicted by SWAT

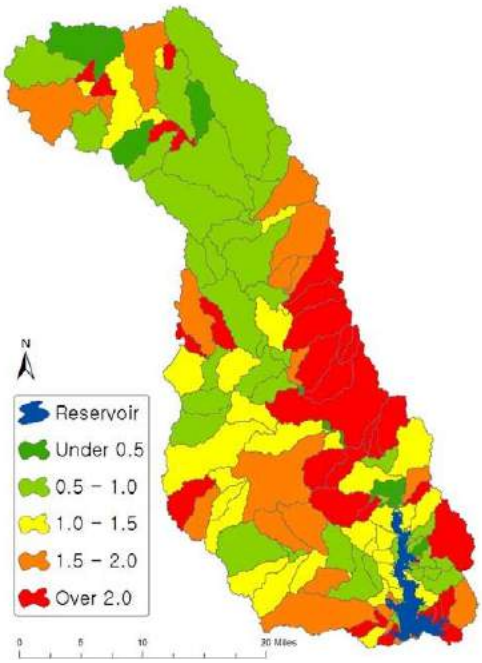

Figure 13. Total Nitrogen loading (kg/ha) by overland flow predicted by SWAT

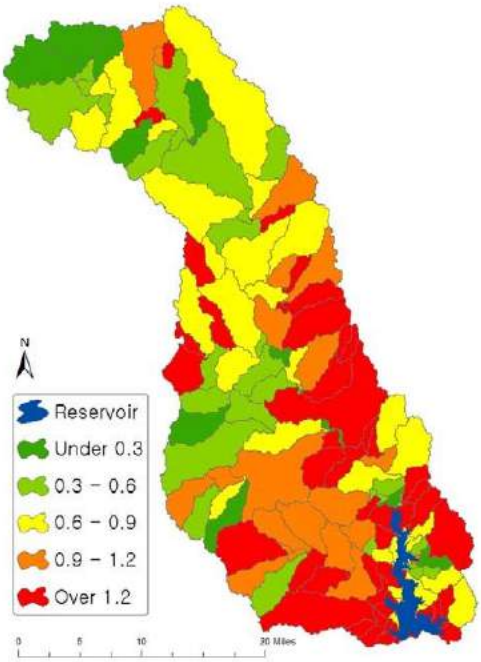

Figure 14. Total Phosphorous loading (kg/ha) by overland flow predicted by SWAT

Channel erosion

Sediment yield from each subbasin was calibrated in SWAT based on the Baylor Sediment Study (Allen et al., 2006) as mentioned earlier. Sediment cores were collected to estimate average density and thickness of sediment at the lake bottom (Allen et al. 2006). In addition, a watershed survey was conducted to identify stream segments with channel erosion problems and to quantify channel erosion using NRCS field assessment techniques such as RAPM. Allen et al. (2006) calculated sedimentation in the reservoir based on the original design volume and compared that to what was found in the 2005 survey and found a sedimentation rate of 427.3 ac-ft/year, which is equivalent to 376,000 ton/year in metric unit. The delta sediment density was 98 lbs/ft^3, pro delta sediment density was 26 lbs/ft^3, and average density was 40.4 lbs/ft^3. Based on the lake sediment survey and the watershed survey, the erosion rate of the Eagle Mountain watershed was estimated at about 340,883 metric tons/yr. Of this, channel erosion contributed about 110,144 metric tons/yr (32.3%) and the rest of the sediment (230,739 metric tons/yr) was attributed to overland erosion (67.7%) (Allen et al. 2006). Simulated sediment from SWAT for the 1971 to 2004 period (34 years) was compared to the measured sediment, and appropriate input parameters were adjusted until the predicted annual sediment load from overland and channel erosion was approximately equal to that measured.

Figures 15 and 16 show the estimation of sediment loading by Baylor's study and SWAT. Each channel in the subbasins was categorized by low, medium, and high depending on the amount of channel erosion. The channel erosion was estimated in the model by difference between sediments coming in from above subbasin and from overland and sediments going out of the subbasin. Differences in the study are mainly due to the fact that higher erosion was estimated at the main channel by SWAT. By estimation of SWAT, most of the channel erosion occurs in the main channel and West Fork sites (shown in red in the map).

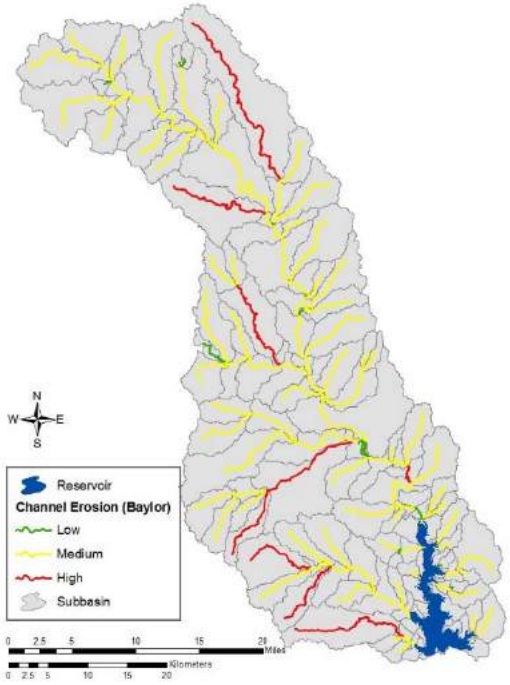

Figure 15. Channel erosion estimation by Baylor

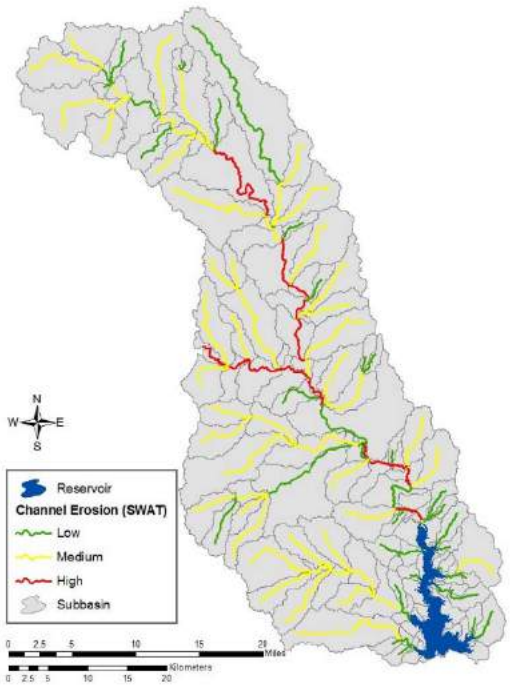

Figure 16. Channel erosion estimation by SWAT

BEST MANAGEMENT PRACTICES SCENARIOS

The SWAT modeling results for Eagle Mountain watershed showed that the annual sediment yield to the lake was about 296,400 metric tons, the annual Total Nitrogen (TN) yield was 1,055,220 kg, and the annual Total Phosphorous (TP) yield was 173,020 kg (Table 17). To reduce the impacts on water quality at the lake, best management practices (BMPs) scenario need to be adopted. Based on the statistical analyses and consent from local stakeholders, the target of TP reduction has been set at 30%. A 30% reduction in TP results in a statistically significant reduction in Eagle Mountain Lake's Chlorophyll 'a' level, a measure of eutrophication. Eighteen BMPs were simulated at the maximum practical rate or at a100% adoption rate in SWAT model, assuming those BMPs were implemented on all suitable land. The 100% adoption rate was also used for sensitivity analyses of each BMP and it provided useful information on the effectiveness of each BMP. To assess the 30% TP reduction goal, each BMP was implemented in the model one at a time until the total TP reduction at the lake reached 30%.

BMPs and Simulation

Eighteen BMPs were implemented in the SWAT model at 100% adoption rate to estimate the effectiveness of the BMPs. Table 19 shows the reduction rate for sediment, TN, and TP by each BMP at 100% adoption rate. The reduction was estimated by implementing each BMP in SWAT model independently and the reduction rate was calculated as the difference in loading from the baseline model (Table 17). The most effective BMP to reduce sediment was riparian buffer (29.4% reduction), for TN the most effective was conversion of cropland to pasture (7.3% reduction) and for TP the most effective was also conversion of cropland to pasture (15.2% reduction).

Table 19. The individual effectiveness of BMPs at 100% adoption rate* as compared to the baseline model

BMPs	Area (ha)	Note	Reduction (%)		
			Sediment	Total N	Total P
1 Filter Strips	7,086	All Croplands	13.0	5.0	12.7
2 Grassed Waterway (10% Cropland)	1,418	Cropland Area in subbasins with more than 10% as cropland	3.8	0.2	3.1
3 Contour Farming	3,499	Cropland larger than 2% of slope	6.7	2.3	6.2
4 Terrace	3,499	Cropland larger than 2% of slope	7.1	2.5	6.8
5 Cropland Nutrient Management	7,086	All Croplands	0.0	-0.2	1.2
6 Cropland to Pasture	7,086	All Croplands	14.2	7.3	15.2
7 Prescribed Grazing	20,300	All Pasturelands	0.5	0.3	1.7
8 Pasture Planting	20,301	All Pasturelands	0.5	0.3	1.7
9 Critical Area Pasture Planting	77,125	Subbasin with more than 75% of Pastureland or Rangeland	1.8	4.6	1.5
10 2000 Ft Buffer	N/A		-4.6	0.7	5.1
11 Riparian Buffer	777	All Channels (Km)	29.4	2.4	3.3
12 Riparian Buffer in Critical Area	84	Channels in High Erosion Category (Km)	14.3	1.3	1.6
13 Graded Stabilization Structures	82,436	All Landuse (except Urban and Water) larger than 3% of slope	4.3	2.8	4.0
14 WWTP Level 2	N/A		0.0	-0.2	0.3
15 WWTP Level 3	N/A		0.0	0.3	0.6
16 Prescribed Burning	26,000	20% of total Rangeland	1.1	0.5	1.8
17 Aerial Herbicide	13,000	10% of total Rangeland	1.1	0.3	1.7
18 FP Sites (Ponds)	N/A	New Ponds in multiple subwatersheds	5.0	5.2	4.4

*Baseline: Sediment – 296,400 t/y, TN – 1,055,220 kg/y, and TP –173,020 kg/y

Cropland BMPs

Croplands are responsible for 31.2% of sediment yield, 14.9% of TN yield, and 32.3% of TP yield although the total area of cropland is only 3.4% of the watershed. Therefore, management practices on croplands are expected to be critical solution to reduce sediment and nutrient loading to the lake.

Terrace (NRCS Practice Code: 600)

Terracing is commonly used to decrease soil erosion by reducing surface runoff (Figure 17). Terraces are series of earthen embankments constructed across the field slope at designed vertical and horizontal intervals based on land slope and soil conditions. Construction of terraces involves a heavy capital investment to move large quantities of earth for forming the earthen embankment. Hence it has to be used only if other low cost alternates are determined to be ineffective.

Figure 17. Terrace

In the SWAT model, terraces were assumed to be constructed only on croplands with slopes larger than 2%. In the Eagle Mountain watershed a total of 3,499 ha (8,645 acres, 1.6% of total watershed) are classified as cropland with at least a 2% slop. For these croplands Universal Soil Loss Equation (USLE) support practice factor (USLE_P) was reduced to 0.5 and curve number (CN2) was reduced by 6 from the calibrated value. These values were selected based on the suggested values from the NRCS National Engineering Handbook and SWAT user manual.

The model results at 100% adoption rates for terracing showed an overall load reduction of sediment 7.1%, of TN 2.5%, and of TP 6.8% (Table 19). These overall reductions were based on the reduction at the lake (off-site), thus the reduction at each subbasin where terraces were implemented (on-site) was much higher. Phosphorus is more tightly attached to sediment, less soluble in water and conservative in nature. Hence, the reduction in sediment translates to almost equal reductions in total P. Whereas nitrogen is much more soluble, volatile to the atmosphere and moves readily in the solute phase; therefore the reduction in total N loading at the lake is proportionately less.

Contour farming (NRCS Practice Code: 330)

Contour farming involves performing critical farming operations (tillage, planting and other operations that disturb the soil) along the contour of the field. To simulate this BMP in SWAT, contour farming was assumed to be implemented on croplands with slope greater than 2%, the same lands simulated with terraces (Figure 18). For these croplands Universal Soil Loss Equation

(USLE) support practice factor (USLE_P) was reduced to 0.5 and curve number (CN2) was reduced by 3 from the calibrated value.

The model results at 100% adoption rates for contour farming showed an overall load reduction of sediment 6.7%, of TN 2.3%, and of TP 6.2% (Table 19). These overall reductions were based on the reduction at the lake (off-site), thus the reduction at each subbasin where contour farming was implemented (on-site) was much higher.

Figure 18. Contour Farming

Conversion of Cropland to Grass – Pasture Planting (NRCS Practice Code: 512)

Soil erosion rate predicted for pasture land is about 0.2 t/ac as compared to 5.35 t/ac from cropland. Therefore, conversion of cropland to pastureland could be an effective BMP for sediment and nutrient control (Figure 19).

Implementation of this BMP was modeled as replacing all cropland into pastureland in the model. The pastureland in the Eagle Mountain watershed was assumed to be fertilized (67 kg N per hectare) every year with two hay cuttings per year on fertilized pasture. The curve numbers were also changed from cropland to pastureland conditions based on National Engineering Hand Book and SWAT user manual.

Figure 19. Pasture Planting

The model results at 100% adoption rate for conversion of cropland to pastureland showed an overall loading reduction at the lake of sediment 14.2%, of TN 7.3%, and of TP 15.2% (Table 19). These overall reductions were based on the reduction at the lake (off-site), thus the reduction at each subbasin where conversion was implemented (on-site) was much higher. This BMP was ranked and the most effective BMP among the cropland BMPs.

Grassed Waterway (NRCS Practice Code: 412)

A grassed waterway is often used to safely discharge the overland runoff to the main channel thus preventing the formation of gullies (Figure 20). The main function of grassed waterways is to reduce channel bottom erosion and flow velocity to protect channel geometry. It can also be used in conjunction with other conservation measures such as terraces to safely convey excess runoff.

Figure 20. Grassed waterway

In this study, grassed waterways were implemented only in subbasins that have at least 10% of croplands in the subbasin. It was simulated in the model by increasing Manning's n roughness coefficient in each subbasin from 0.014 to 0.15 to reflect a good channel cover in the tributary.

The model results for 100% adoption rate of grassed waterway showed an overall reduction of sediment loading to the lake of 3.8%, TN 0.2%, and of TP 3.1% (Table 19). These overall reductions were based on the reductions at the lake (off-site), thus the reduction at each subbasin where grassed waterway were implemented (on-site) was much higher.

Filter Strips (NRCS Practice Code: 393)

Filter strips are strips of dense grass or herbaceous vegetation placed at regular intervals across the slope of the field and at the field edges before discharging the overland flow to a stream (Figure 21). Properly maintained filter strips could effectively trap the sediments and nutrients from the overland flow and creates a good habitat for wildlife and beneficial insects.

Figure 21. Filter strips

SWAT models filter strips as simple edge-of-field vegetation with a trapping efficiency. The trapping efficiency is calculated based on the width of the filter as:

$$trap_{ef} = 0.367 \cdot \left(width_{filterstrip}\right)^{0.2967}$$

For a 15m filter the trapping efficiency is about 82%, i.e. 82% of sediment and nutrients generated from the contributing area to the filter strip is trapped.

The model results at 100% adoption rate for filter strips showed an overall load reduction of sediment at the lake of 13.0%, of TN 5.0% and of TP 12.7% (Table 19). These overall reductions were based on the reduction at the lake (off-site), thus the reduction at each subbasin where filter strips were implemented (on-site) is much higher.

Cropland Nutrient Management (NRCS Practice Code: 590)

Phosphorus is often linked to nutrient enrichment and lake eutrophication. Hence, a reduction in application of mineral phosphorus fertilizer could be an effective BMP to prevent lake enrichment. In the model, cropland nutrient management was implemented by reducing P fertilizer application from 34 kg/ha to 25 kg/ha for all croplands in the watershed.

The model results at 100% adoption rate for cropland nutrient management showed overall load reduction at the lake of sediment was 0.0% and TP 1.2%, and an increase loading of TN of 0.2% (Table 19). These overall reductions were based on the reduction at the lake (off-site), thus the reduction at each subbasin where nutrient management were implemented (on-site) is much higher.

Pasture and Rangeland BMP's

Pasture and rangeland account for the majority of the landuse in the Eagle Mountain watershed (69%). Pastureland occupies 9.3% and rangeland occupies 59.7% of the entire watershed. Fertilizer was applied on pastureland at a rate of 67 kg N per hectare. Based on model simulation, pastureland is responsible for sediment loading of 1.57%, TN 2.85%, and TP 7.0% from entire loading at the lake. On the other hand, the percentages of loadings from rangelands are 10.86% for sediment, 44.1% of TN, and

14.46% of TP.

Prescribed grazing (NRCS Practice Code: 528),
Pasture planting (NRCS Practice Code: 512)

Figure 21. Filter strips

Overgrazing by browsing cattle or machines could impede establishment of healthy and dense grass stands in rangeland and pastures leaving the top soil exposed to erosion. This could be minimized through prescribed grazing. Controlled harvest of vegetation through grazing rotation or prescribed grazing (Figure 22) that allows for establishment of a dense vegetative stand could reduce soil erosion and retain soil nutrients. Further, native or introduced forage species that are well adapted to North Central Texas could be planted periodically to maintain a dense vegetative cover and improve the hydrologic condition of the land. Similarly well adapted perennial vegetation such as grasses, legumes, shrubs and trees could be planted in rangeland with medium to low vegetation cover.

For simulation in the model, pastureland was assumed to be in fair hydrologic condition (USLE_C, cover factor: 0.007). These two BMPs would improve the groundcover of the pasture across the watershed. Implementation of these BMPs was done by reducing the USLE_C factor for pasture across the watershed, which was SWAT's default value for good ground cover of vegetation.

The model results at 100% adoption rate for prescribed grazing and pasture planting showed an overall reduction of sediment loading at the lake of 0.5%, of TN 0.3%, and of TP 1.7% (Table 19).

Grassed waterway (NRCS Practice Code: 412) as critical area pasture planting

Grassed waterway (Figure 20) was implemented on subbasins with at least 75% pastureland or rangeland (77,125 ha). The channel Manning's roughness factor was increased from 0.014 to 0.15 to reflect a good channel cover in the tributary.

The model results at 100% adoption rate for critical pasture planting showed an overall reduction of sediment loading at the lake of 1.8%, of TN 4.6%, and of TP 1.5% (Table 19).

Prescribed Burning

Conducting prescribed burns of rangeland reduces brush thereby allowing greater cover of grass. Grasslands with good cover are less erodible than pastures with brush; therefore, denser grass reduces runoff and sediment entering the waterbody. In the model, rangelands that touch channels were selected to be candidates. Of the total rangeland acreage, only 20% meet this criteria and where therefore eligible for 100% adoption of the BMP. In the model, prescribed burning was represented by decreasing CN by 5 and decreasing C factor from 0.003 to 0.001.

The model results at 100% adoption rate for prescribed burning showed an overall reduction of sediment loading at the lake of 1.1%, of TN 0.5%, and of TP 1.8% (Table 19).

Areal Herbicide Application

Applying herbicide kills brush and other unwanted woody plant and weeds and allows for the revegetation of the land with denser grass, leading to better cover of the soil. For the purposes of this study areal herbicide application was applied only along the main channel in 10% of the rangeland. In the model, the representation of the BMP was the same as prescribed burning, which was decreasing CN by 5 and decreasing C factor from 0.003 to 0.001.

The model results at 100% adoption rate for areal herbicide application showed an overall reduction of sediment loading at the lake of 1.1%, of TN 0.3%, and of TP 1.7% (Table 19).

Channel BMP's

Eagle Mountain watershed has about 777 km of channel. The SWAT simulation shows that about

46.6% of total sediment, 15.5% of total N, and 25.1% of total P are coming from channel erosion. Therefore, control of channel erosion is one of the most important practices to reduce the sedimentation rate and to improve the water quality of the lake.

Riparian Buffers (NRCS Practice Code: 390, 391)

Riparian area is a fringe of land that occurs along the stream or water courses with grass and herbaceous cover. If the riparian buffer, shown in Figure 23, is not adequately established and farming activities continue to the edge of the stream, the banks become unstable resulting in significant sloughing and channel scour. Establishing and maintaining a good riparian buffer, stabilizing channels and protecting shorelines considerably reduce channel erosion.

Figure 23. Riparian Buffer

The riparian buffer was simulated in SWAT by assuming that a good riparian buffer and channel cover (channel cover factor (CH_COV) in SWAT as 0.1) are established along various stream segments with poor riparian buffers and channel cover.

The model results at 100% adoption rate for riparian buffer showed an overall reduction of sediment loading at the lake of 29.4%, of TN 2.4% and of TP 3.3% (Table 19).

Riparian Buffers in critical area (NRCS Practice Code: 390, 391)

Instead of implementing riparian buffer on all channels, implementing them only on critical channels was simulated using the same representation as riparian buffer above. In the Eagle Mountain watershed, there are 84 km of critical channel (categorized as critical in Figure 16), which is about 10.8% of the total channel length.

The model results at 100% adoption rate of riparian buffer in critical areas showed an overall reduction of sediment loading at the lake of 14.3%, of TN 1.3%, and of TP 1.6% (Table 19).

Watershed BMPs

Grade Stabilization Structures (NRCS Practice Code: 410)

Grade stabilization structures (Figure 23) are constructed to control the grade and head cutting in channels. These structures are warranted only if the slope changes abruptly within a short distance. Based on the properties of this BMP, graded stabilization structures in this study were implemented in subbasins with slopes greater than 3%. Some portion of these subbasins and tributary channels could have abrupt slopes, which have to be verified by field investigations. In such circumstances grade stabilization structures could considerably reduce soil erosion.

The effect of grade stabilization structures is to reduce the energy of flowing water due to slope.

Therefore, grade stabilization structures are simulated in SWAT by reducing the slope of the subbasins.

The overland slope that was greater than 3% was reduced to 3%.

The model results at 100% adoption rate for graded stabilization structures showed an overall reduction of sediment loading at the lake of 4.3%, of TN 2.8% and of TP 4.0% (Table 19).

Figure 24. Graded Stabilization Structure

Waste Water Treatment Plant Level II and III

There are a total of 14 (2 of them are discharging directly to the lake) WWTPs in Eagle Mountain watershed (Figure 6). The loading by WWTP level II and III is reduced loading rate by better controlling and processing at each plant. WWTP level II and III as BMPs were simulated based on the discharging information for each level.

The model results at 100% adoption rates for WWTP level II showed an overall reduction of sediment loading at the lake of 0.0%, of TN 0.2% increased, and of TP 0.3% (Table 19). The reason that TN with level II was increased over the baseline was that the current discharge of wastewater is often better than 10 mg/L concentration proposed for Level II.

The model results at 100% adoption rates for WWTP level III showed an overall reduction of sediment loading at the lake of 0.0%, of TN 0.3% and of TP 0.6% (Table 19).

Flood Prevention (FP) Sites (New ponds)

Seventeen FP sites have been planned in Eagle Mountain watershed and have not yet been constructed and were simulated in the SWAT model as a BMP. A pond traps runoff and provides time for sediment to fall out of the water while it controls the volume of runoff downstream. Each subbasin has pond option to be input as a contributing area in SWAT. To represent a new pond, the new area was added onto the area of contributing to ponds in each subbasin based on the contributing area calculated for new ponds.

The model results at 100% adoption rates for contracting new FP sites showed an overall reduction of sediment loading at the lake of 5.0%, of TN 5.2% increased, and of TP 4.4% (Table 19).

BMP Adoption

Implementing BMPs for reduction goal

With TP reduction estimated by SWAT at 100% adoption rate, economic analyses found marginal adoption rates of each BMP and the cost to implement in the watershed. Marginal adoption is the difference between the most likely adoption rate and the current adoption rate in the field. Table 20 shows the rank of BMPs by least cost and their marginal adoption rate.

Based on the economic analyses, BMPs were implemented into the SWAT model until total annual TP reduction reached 30% at the lake. Below is the summary of the methodology for SWAT simulation.

a) Implement least cost BMP on subbasin with highest TP loading (subjected to BMP condition)
b) Run SWAT and calculate TP load reduction at the lake

If total TP reduction of 30% for the watershed is not reached, go to the next lowest cost BMP and implement on subbasin with highest TP loading

The results show that a total of 13 BMPs are necessary to achieve a 30% TP reduction annually at the lake (Table 20). Sediment, TN, and TP shown in Table 20 are accumulated reduction as each BMP was implemented in order. There are two BMPs that were not simulated in SWAT, P Inactivation with Alum and the wetland on the West Fork of the Trinity River. The reduction rates from P Inactivation with Alum was independent of SWAT model, therefore, the reduction rate was simply subtracted from the previously implemented BMP.

Table 20. Implementation of BMP by the order of cost until the TP reduction reaches at 30%

		Reduction (%)		
BMP	**Adoption Rate**	**Sediment**	**Total N**	**Total P**
Graded Stabilization Structures	25%	1.3	1.2	2.1
Filter Strips	25%	7.0	3.5	6.0
Grassed Waterway	10%	7.0	3.4	7.8
Herbicide Application	5%	9.6	5.6	8.5
2000 Ft Buffer	60%	8.1	6.1	12.3
Terrace	10%	8.5	6.3	14.0
Conversion Cropland to Pasture	25%	10.6	7.2	20.5
Prescribed Burning	4%	10.8	7.3	21.3
P Inactivation with Alum	100%	24.6		
10FP Site	100%	14.9	12.3	28.8
Prescribed Grazing (Pasture Planting)	25%	15.0	12.4	29.1
Brush Management	20%	15.3	11.1	29.4

Spatially distributed effectiveness

The effectiveness of each BMP was simulated not only to reach the TP reduction goal (30%) but also analyzed for spatially distributed impacts. Every time a BMP was simulated/ implemented as shown in Table 20, TP loading maps were re-drawn for subbasin level assessment. Figure 25 shows the sequential, spatially distributed effectiveness of each BMP. The series of maps shows TP reduction in each subbasin compared to the baseline simulation for TP reduction in each subbasin. TP reductions in each subbasin were accumulated reduction as each BMP was added one at a time. Some red colored subbasins remain on the map even with the implementation of 13 BMPs. The reason that no BMPs were implemented in these subbasins was those subbasins did not have chances for BMPs to be implemented due to the condition of the subbasins and the criteria of BMPs.

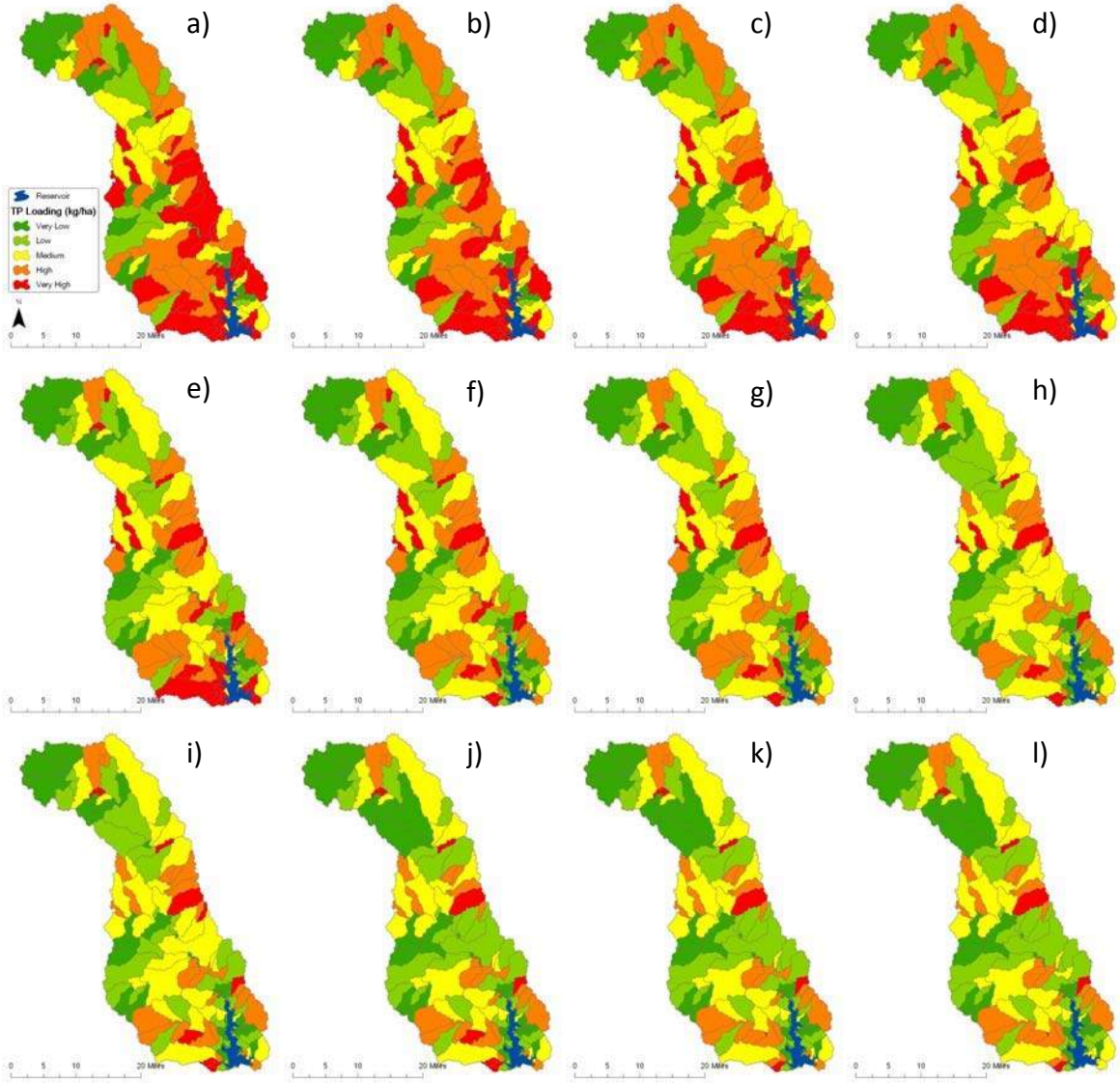

a): *baseline,* ***b):*** *Graded stabilization structures,* ***c):*** *b) + Filter strips,* ***d):*** *c) + Grassed waterway,* ***e):*** *d) + Herbicide application,* ***f):*** *e) + 2000 ft buffer,* ***g):*** *f) + Terrace,* ***h):*** *g) + Conversion cropland to pasture,* ***i):*** *h) + Prescribed burning,* ***j):*** *i) + FP sites,* ***k):*** *i) + Prescribed grazing.* ***l):*** *k) + Brush management*

Figure 25. Spatially distributed effectiveness of BMPs

REFERENCES

Allen, P.M., J. A. Dunbar, S. Prochnow, and L. Zygo. 2006. *Eagle Mountain: Stream Erosion and Reservoir Volume Evaluation*. Baylor University and SDI Inc. April 2006.

Arnold, J.G., P.M. Allen, R.S. Muttiah, G. Bernhardt. 1995a. Automated Base Flow Separation and Recession Analysis Techniques. *GROUND WATER*, Vol. 33, No. 6, November-December.

Arnold, J.G., J.R. Williams, D.R. Maidment. 1995b. A Continuous Water and Sediment Routing Model for Large Basins. *American Society of Civil Engineers Journal of Hydraulic Engineering*. 121(2): 171-183.

Knisel, W.G. 1980. *CREAMS, A Field Scale Model for Chemicals, Runoff, and Erosion From Agricultural Management Systems*. United States Department of Agriculture Conservation Research Report No. 26.

Leonard, R.A. Knisel, W.G., and Still, D.A. (1987), 'GLEAMS: Groundwater Loading Effects of Agricultural Management Systems,' *Transactions of ASAE*, vol. 30, pp. 1403-1418.

Nash, J. E. and Sutcliffe, J. V., 1970, River flow forecasting through conceptual models: Part I - A discussion of principles, *Journal of Hydrology*, 10, 282-190.

Srinivasan, R., T. S. Ramanarayanan, J. G. Arnold, and S. T. Bednarz (1998), Large area hydrologic modeling and assessment. Part II: Model application, *J of American Water Resource*. Assoc., 34(1), 91-101.

Texas Water Development Board. 2009. *Volumetric and Sedimentation Survey of Eagle Mountain Lake*, February 2008 Survey. Surface Water Resources Division. January 2009.

Williams, J. R. 1990. The erosion-productivity impact calculator (EPIC) model: A case history. *Phil. Trans. Royal Soc. London* 329: 421-428.

Williams, J.R., A.D. Nicks, and J.G. Arnold. 1985. Simulator for Water Resources in Rural Basins. *J. Hydraulic Engineering*, ASCE, 111(6): 970-986.

WASP Modeling

Berge, M., M. Ernst, and J. Owens. Eagle Mountain Lake WASP Model Development and Calibration Results Technical Memorandum. March 20, 2011

INTRODUCTION

The USEPA Water Analysis Simulation Program (WASP) is a powerful water quality model that can be used to predict and interpret water body responses to various nonpoint source loads and point source pollution. This model was selected by the Tarrant Regional Water District (TRWD) to predict the changes in water quality over time due to the introduction of point source loadings such as WWTP discharges and NPS loading from the watershed, benthic flux and atmospheric deposition. The Eagle Mountain WASP model was calibrated based on a 10-year time period starting January 1, 1994 and ending December 31, 2003.

A 20-year trend of Chlorophyll A (Chl'a') in Eagle Mountain Lake is shown in Figure 1. The trend in Chl'a' in Eagle Mountain over the past 20 years has a significant positive slope with an annual rate of increase of 3.69%. TRWD plans to use the calibrated WASP model to interpret changes in water quality within Eagle Mountain that may occur based on the implementation of various nutrient-loading schemes and/or best management practices (BMPs) in order to protect the future water quality of the reservoir.

This memo documents the current results of the Eagle Mountain WASP model development and calibration. The file name is **EM94_03_cal.wif** with a corresponding postprocessor **High_Low_Close_EMcal.xls**.

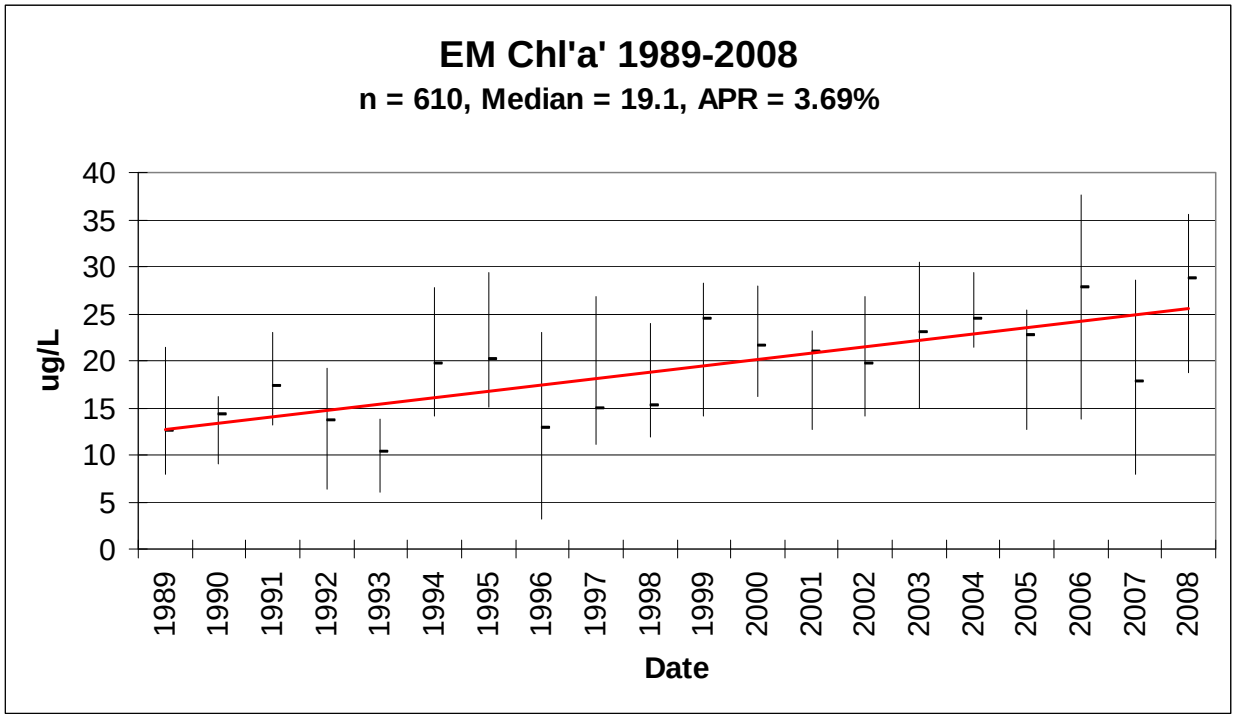

Figure 1: 20-Year Trend of Chl'a' in Eagle Mountain Lake (3.69% APR)

MODEL AND DATA SOURCES

Physical Depiction of Eagle Mountain Lake in WASP

The WASP model simulates the transformations and transport of water quality variables using mass balance computations for each unique segment defined for the water body. Therefore, the user must segment or discretize the water body according to the physical, chemical and reactive properties of the water body as well as the users modeling goals. For example, if the user is interested in gross lake response to pollution, large segmentation may be appropriate if physical and chemical data allows for such segmentation. An example of such an instance would be for a small, shallow water body that does not exhibit stratification due to temperature or oxygen gradients. For the Eagle Mountain segmentation in WASP, temperature stratifications along with physical characteristics of the lake such as depth and incoming tributary flows, were used as a basis for the segmentation. An existing segmentation scheme was utilized for this project that has been used with previous Eagle Mountain modeling efforts.

The Eagle Mountain segmentation consists of 17 segments. Segments are defined either as surface or subsurface segments. Surface segments have unique properties because they serve as contact between the reservoir and the atmosphere (evaporation/precipitation) and they serve as entry points for point source and non point source nutrient loadings from the adjacent watershed areas. In addition, the surface segments define the photic zone in the model to a depth of 6 feet (ft), which represents the approximate depth to which light can penetrate the reservoir. For the Eagle Mountain segmentation, the surface segments are defined as the 6 main thalweg segments 1-6, which includes the West Fork cove segment, and 4 additional cove interface segments 14-17. The surface segments (horizontal segmentation) in the Eagle Mountain WASP model are depicted in Figure 2.

Vertical or subsurface segmentation excluding the cove/tributary segments (14-17) for the Eagle Mountain WASP model is depicted in Figure 3. These subsurface segments define the remaining areas of Eagle Mountain Lake below 2 meters (6 ft). Subsurface segments 7-11 characterize the Eagle Mountain WASP model to the depth of the typical thermocline of approximately 7 meters. Subsurface segments 12 and 13 define the two hypolimnetic segments in the Eagle Mountain WASP model. Each surface and subsurface segment is physically and hydraulically connected to adjacent and adjoining segments where appropriate, by vertical and/or horizontal interfaces.

Dispersion

Due to large segment interfacial areas in the Eagle Mountain WASP model, horizontal and vertical dispersion serves as an important transporter of mass in the Eagle Mountain WASP model. Horizontal dispersion was estimated from the 4/3 Power Law used routinely in historic TRWD water quality models. Horizontal dispersion ranged from 0.6935 m^2/sec to 7.235 m^2/sec throughout horizontal segment interfaces in the model. Vertical dispersion between the surface segments and underlying subsurface segments (2 - 7, 3 - 8, 4 - 9, 5 - 10, and 6 - 11) were arbitrarily set at a high rate (0.001 m^2/sec) to ensure uninhibited mixing vertically between segments. Based on Eagle Mountain field data and characteristics, TRWD has no information or reason to suspect that the surface segments do not mix freely with subsurface segments below the surface. This segmentation scheme was created to facilitate better algal growth modeling in the model.

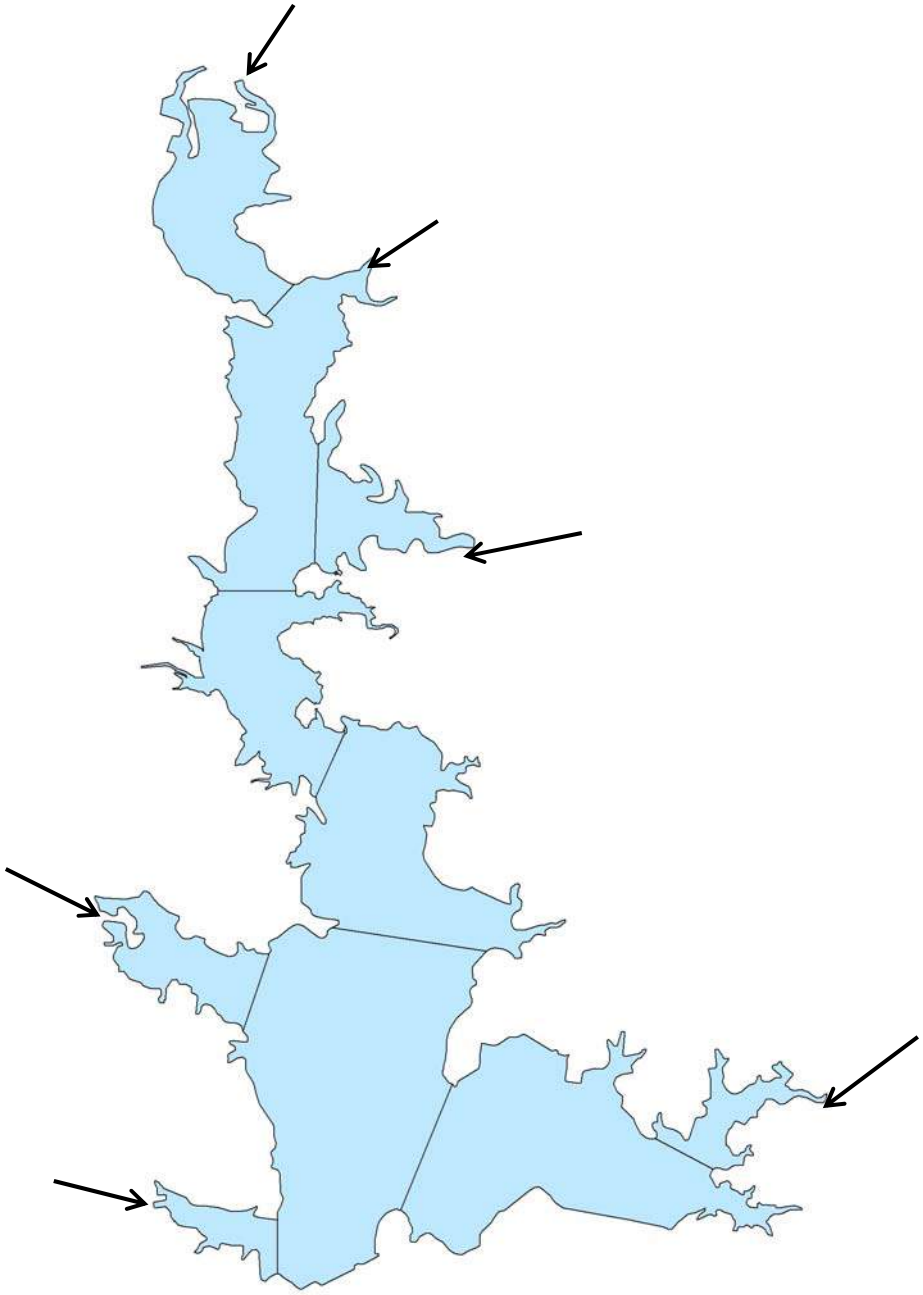

Figure 2: Horizontal (Surface) Segmentation of Eagle Mountain

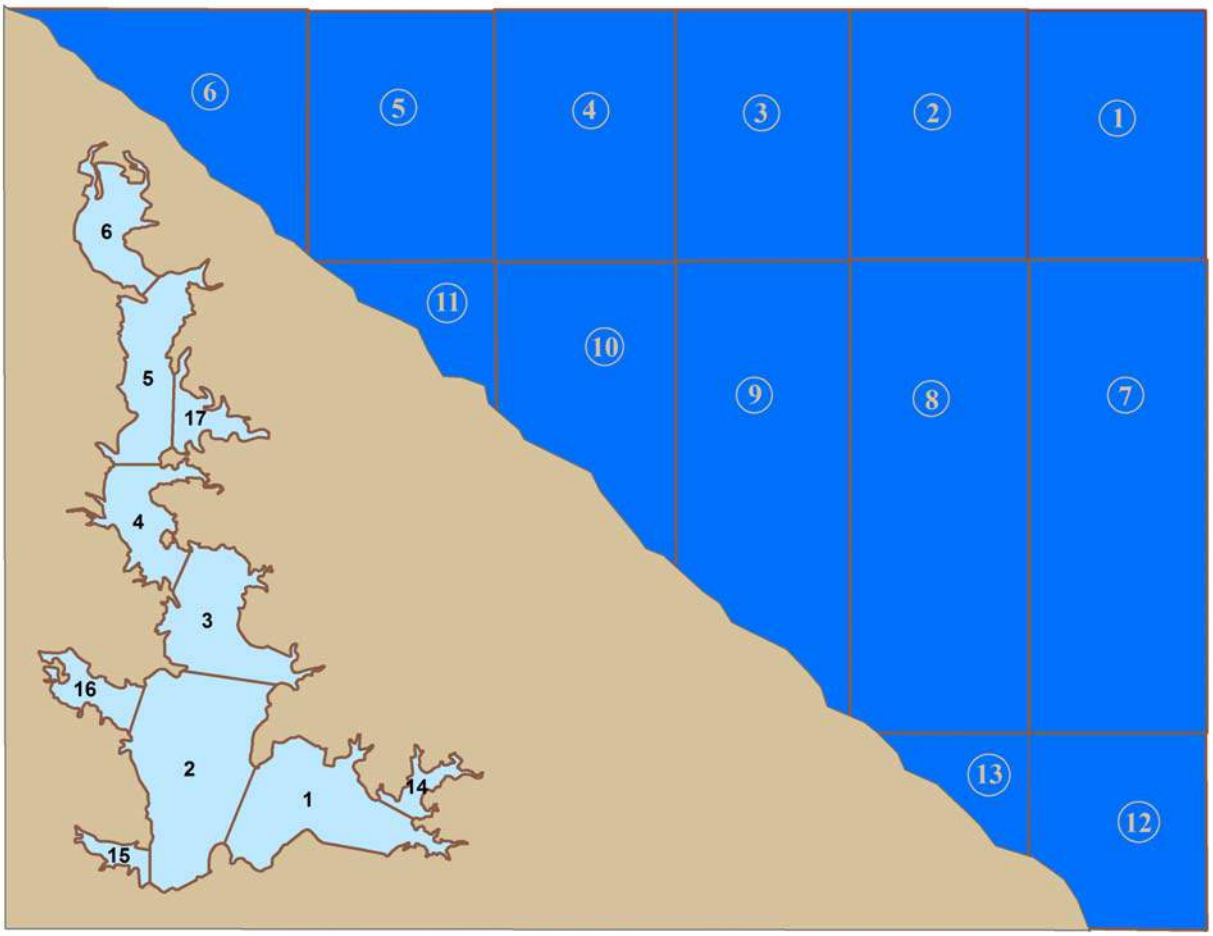

Figure 3: Vertical (Subsurface) Segmentation of Eagle Mountain Lake

Hypolimnetic dispersion coefficients for subsurface segments 7-12 and 8 -13 were initially estimated using Thomann and Mueller's (1987) temperature differential technique. However, due to the paucity of data for several locations, a consistent time function for each subsurface and hypolimnetic subsurface segment (7-12 and 8 -13) proved difficult. Observation of temperature plots from Eagle Mountain field data comparing one (1) meter below the surface to one (1) meter above the reservoir floor illustrated that there are distinct temperature differentials each summer and minimal mixing between these subsurface segments (7-12 and 8-13). Based on these temperature plots, TRWD determined the time frame of the temperature differentials for each year at Eagle Mountain Sampling Station 7 (EM-07) and applied typical lake vertical dispersion rates listed by Chapra (1997) for each time frame of each respective year. These rates varied from 0.0005 m^2/sec for well-mixed time periods to 0.00001 m^2/sec for summer stratification time periods. Figure 4 presents the step function where dispersion is maximum in the winter and minimum in the summer. Dissolved oxygen and temperature profile data was used to calibrate summer time vertical dispersion rates. For example, if the data showed weak stratification and limited hypolimnetic anoxia, the vertical dispersion could be increased in this summer period to allow more mixing and better simulate the observed data. These rates and duration simulate the stratification period well.

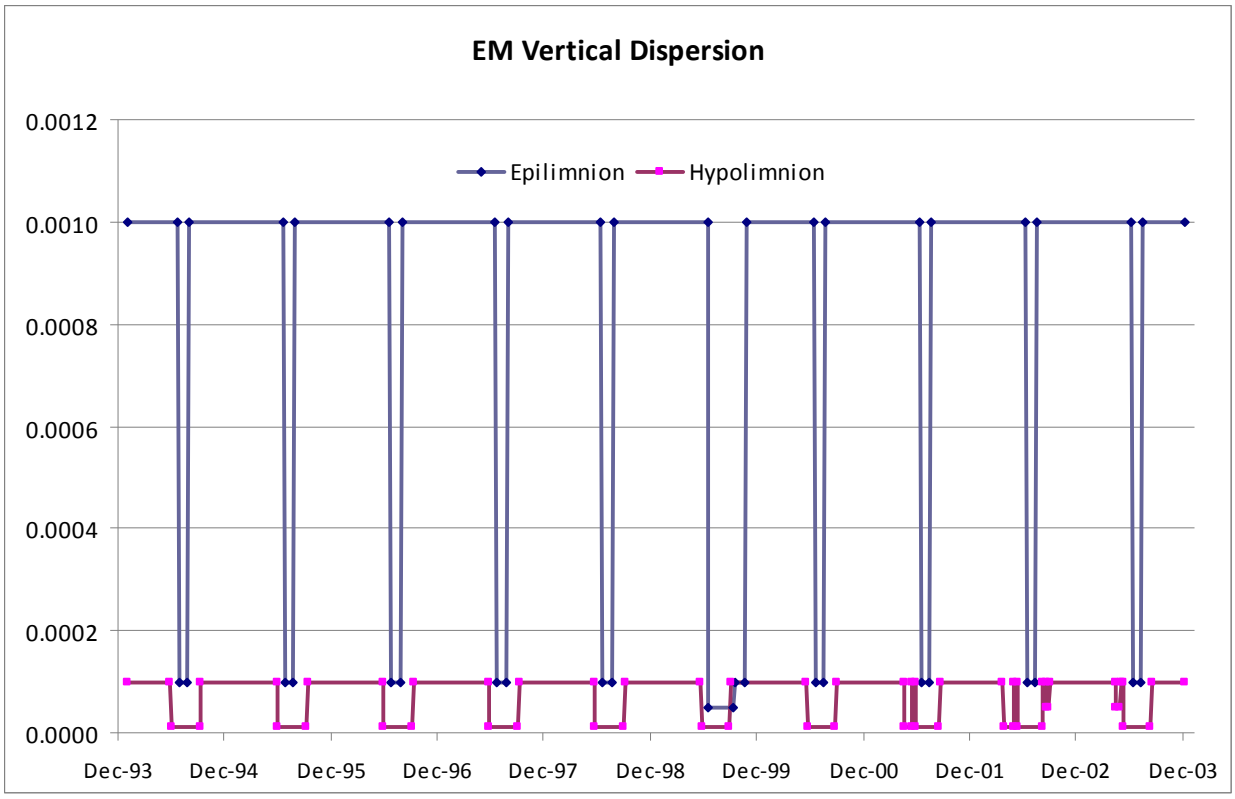

Figure 4: Vertical Dispersion for Hypolimnetic Segments in WASP Model

Hydrodynamics

In order to accurately model the transport and transformation of the nutrients in a water body, it is crucial that the hydrodynamics be represented within the model accurately. For this effort, an external hydrodynamic flow model developed by Alan Plummer and Associates, Inc. (APAI) was utilized. This program utilizes the external flows to the system (precipitation, evaporation, pumpage, discharge, and tributary inflows) as recorded by TRWD and the corresponding geometry of each segment to solve for the advective flows between adjacent segments. The program specifies a matrix solution employing the criteria of minimum kinetic energy and the solution is input into the appropriate flow field for each segment in WASP.

Figure 5 presents the hydrology in Eagle Mountain from 1980 to 2009. Note the low inflow and corresponding low water levels in Eagle Mountain from 1999 to 2001 for the WASP simulation time-period. This decrease in water surface elevation from 1999 to 2001 is consistent with a higher period of nutrient retention in the reservoir because of the decrease of spillage from the reservoir. This is also presented later in this memorandum in the results discussion.

During the start of the WASP simulation time-period, Eagle Mountain was near full capacity. The lake volume in January 1994 was 177,970 ac-ft, which is 98% of the full conservation pool volume. Per the APAI flow balance solution, the DV segments are those capable of volume changes in order to force the flow exchange between respective segments, while the remaining segments maintain a constant volume. The matrix flow balance solution developed by APAI uses this initial volume and is capable of changing the capacity of the reservoir to mimic that found during the actual time period modeled. Table 1 provides the initial volumes of the 17 reservoir

segments used during the model simulation time-period. DV segments (12 and 13) are highlighted in blue.

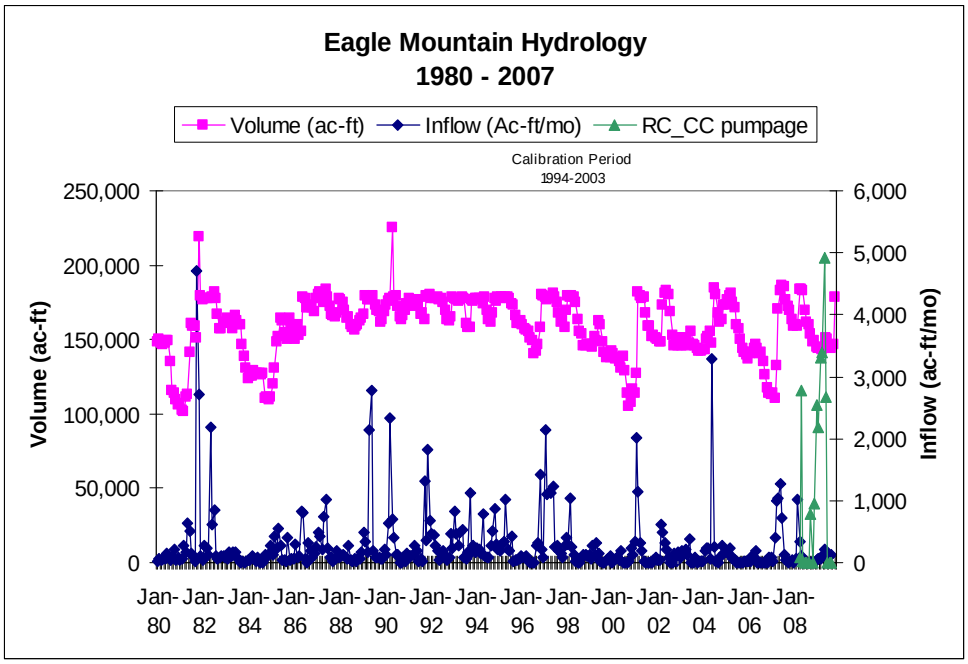

Figure 5: Eagle Mountain Hydrology (1980-2009)

Table 1: Eagle Mountain Initial Segment Volumes for WASP Model

Wasp Seg	Actual Volumes cubic m
1	1.18E+07
2	1.65E+07
3	8.64E+06
4	5.41E+06
5	7.54E+06
6	3.37E+06
7	3.24E+07
8	3.99E+07
9	2.24E+07
10	1.01E+07
11	8.16E+06
12	2.64E+07
13	1.57E+07
14	5.05E+06
15	1.79E+06
16	4.67E+06
17	4.31E+06
Total	**2.24E+08**
Ac-ft	181792

Settling Rates

The physical settling of particulate matter in any reservoir is an important transport phenomenon of nondissolved nutrients and often leads to a distinct longitudinal gradient or slope in concentration. Only 3 of the 8 state variables were assigned settling velocities. Table 2 presents the average fraction dissolved for both organic nitrogen and organic phosphorus in each segment. This data was estimated from limited laboratory measurements of total and filtered samples. As a side note, we have found organic N to have a greater fraction in the dissolved state than organic P. The fraction of organic nitrogen that was determined to be in the undissolved phase (varied from segment to segment based on field data) was given a settling velocity of $2.3x10^{-6}$ m/sec (0.20 m/day). Algae were given a rate of 5.0×10^{-7} (0.04 m/day) and the fraction of organic phosphorus that was in the undissolved phase were given a settling velocity of $2.8x10^{-6}$ m/sec (0.24 m/day). Organic phosphorus was given a higher settling velocity because it binds with inorganic clay readily, while organic nitrogen is more often associated with organic matter. The longitudinal profiles of observed data support this position.

Table 2: Percent Organic Nitrogen and Phosphorus Dissolved

Summary Table		
Segment	OP	ON
1	0.34	0.67
2	0.31	0.65
3	0.24	0.69
4	0.19	0.54
5	0.29	0.62
6	0.12	0.52
7	0.46	0.68
8	0.28	0.59
9	0.16	0.55
10	0.13	0.59
11	0.44	0.56
12	0.27	0.68
13	0.35	0.64
14	0.38	0.80
15	0.43	0.60
16	0.50	0.57
17	0.33	0.52
Median:	0.31	0.59

Environmental Time Functions

WASP requires the input of time functions for important environmental functions such as temperature, incident light, light extinction, photoperiod and wind. For this type of water-quality modeling, water temperature, light extinction and incident light are critical components of the nutrient cycle. Three graphs have been created below to demonstrate how the temperature and light functions were determined for the WASP calibration effort. The first graph, Figure 6 presents the two of the three temperature curves that were used to determine temperature time functions for the Eagle Mountain WASP model. As shown in Figure 6, Curve 1 represents the main body of the reservoir and Curve 2 represents the deeper portions of the reservoir.

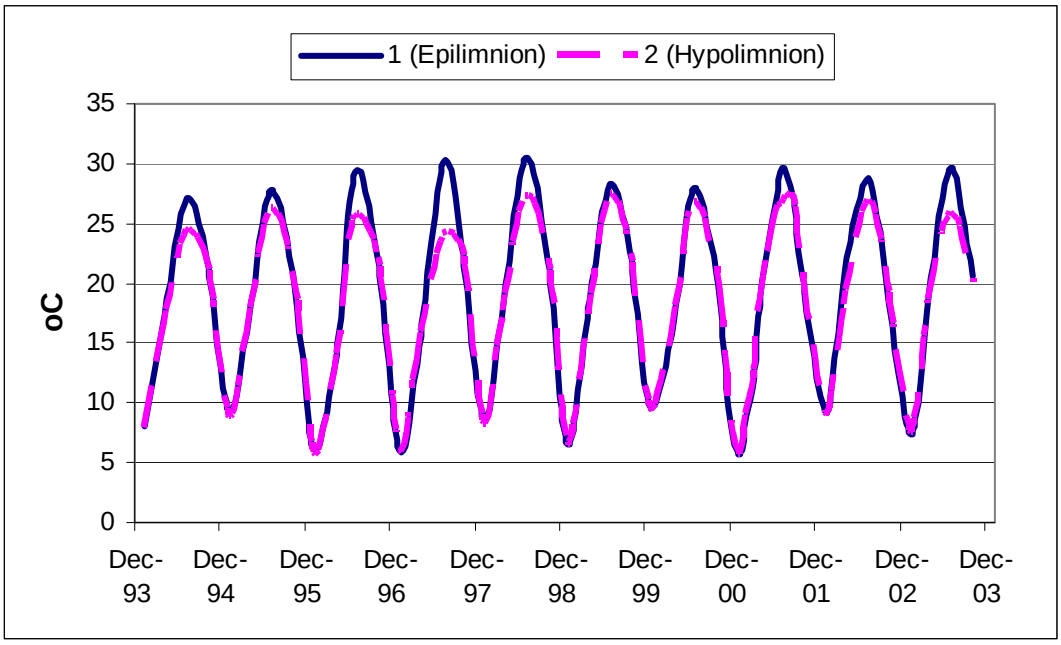

Figure 6: Selected WASP Temperature Curves 1 and 2

Light extinction due to non-algal turbidity is an important time function because the waters of Eagle Mountain are relatively turbid and this greatly affects algae modeling in WASP. Five (5) light curves were used to represent the longitudinal gradient from the turbid north end of Eagle Mountain to the relatively clearer waters in the southern end near the dam. Figure 7 presents two (2) of these selected light extinction curves. The "inlet segment" curve represents the north end area of Eagle Mountain, while "intake segment" curve represents the southern end of the lake near the dam. For this effort, the light extinction coefficient (Ke') was calculated using the following formula (Ernst 1995):

$$Ke' = 0.9020/z - 0.0045(Chl'a')$$

Where z is the secchi depth in meters and Chl'a' is in ug/L.

The incident radiation curve that was used in his effort is based on National Oceanic and Atmospheric Administration (NOAA) data and has been used in numerous District models. Figure 8 presents the incident radiation curve that was used for the WASP calibration model.

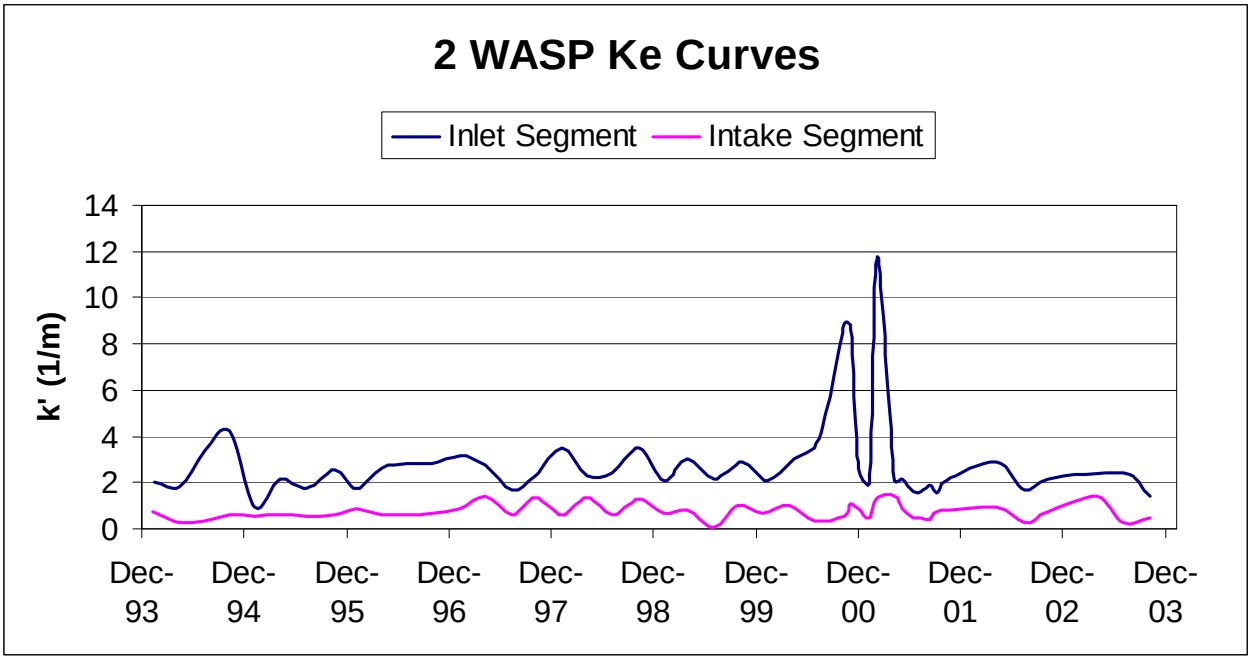

Figure 7: Selected WASP Light Curves 2 and 4

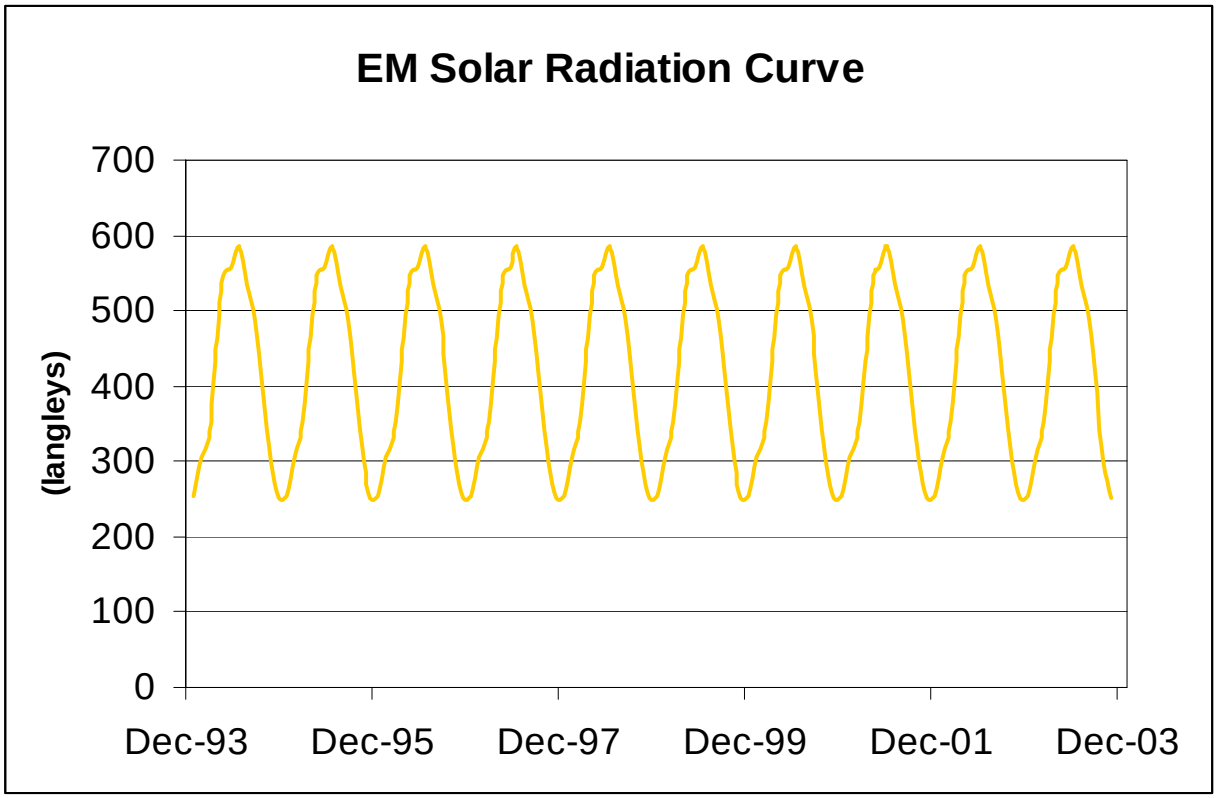

Figure 8: Solar Radiation Curve

WATER-QUALITY MODELING WITH WASP

WASP 6.2 consists of two stand-alone programs that include a hydrodynamic version and a water quality program. These two programs can be used alone or in conjunction with each other. The hydrodynamic program simulates the movement of water, while the water quality program simulates the movement and interaction of pollutants within the water. For the purposes of this effort, WASP 6.2 was used only for the water quality component of the modeling. As discussed in the previous section, TRWD utilized a hydrodynamic program developed by APAI for the District.

The principal of the WASP model is the conservation of mass. This applies to both the water quality and the hydrodynamic programs in WASP. In WASP, the nutrient enrichment, eutrophication, and dissolved oxygen (DO) depletion processes are simulated using the EUTRO sub-routine program. Several physical-chemical processes can affect the transport and interaction among the nutrients, phytoplankton, carbonaceous material, and DO in the aquatic environment. The principal kinetic reactions for the nutrient cycles (state variables) in WASP are presented in Figure 9.

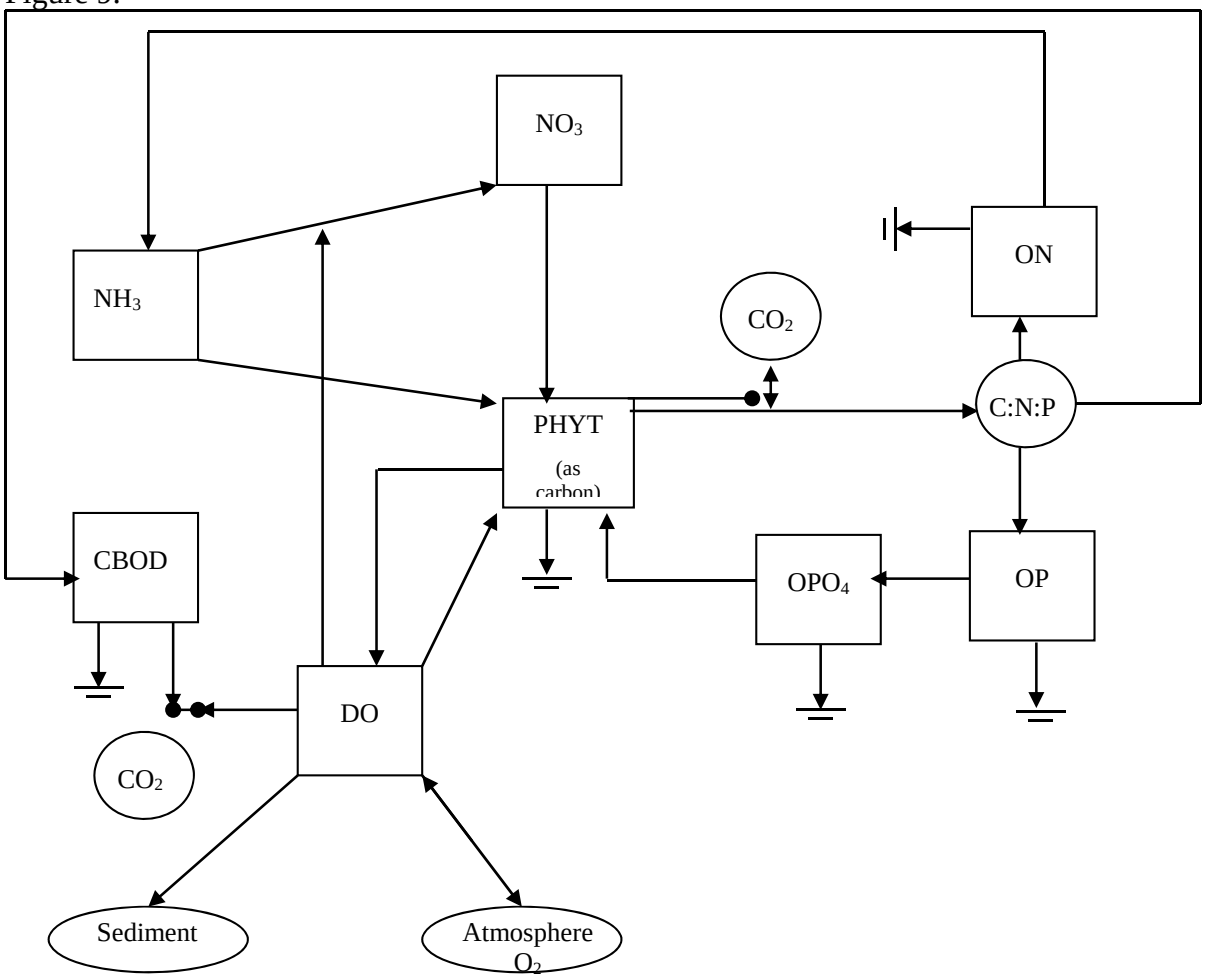

Figure 9: EUTRO State Variable Interactions in WASP

Nutrient Loading

The Eagle Mountain WASP model includes four (4) types of nutrient loading systems:

1. Lakeside Point Source Loading
2. Atmospheric Deposition
3. Benthic Flux Loading
4. Watershed Loading (Point and Non-Point Sources)

Lakeside Point Source Discharges

This nutrient loading system includes two WWTPs that discharge treated effluent directly to Eagle Mountain: Fort Worth Boat Club (FWBC)) and Larry Buck RV Park. FWBC collected weekly nutrient discharge data from October 2001 through January 2002. This data was used to calculate the annual load of nutrients to Eagle Mountain in kilograms/day (kg/d). Since nutrient discharge data was only available for one time period in the simulation period, this data was summarized and repeated for the 10-year simulation for the calibration model. There was no nutrient discharge data available for Larry Buck RV Park. Due to similarities in plants, the nutrient concentration data from FWBC was combined with weekly flow data reported to TCEQ from the plant to calculate nutrient loads to the lake. Again, the one year data set was recycled for the 11-year simulation period for the respective months. WASP requires the load to be expressed as kg/day. No flow data is associated with the WWTP load data input to the model. Parameters used to calculate loads that were input into WASP includes NH_3, NO_X, ON, OPO_4 and OP. Referring back to Figures 2 and 3, FWBC point source nutrient data was applied to segment 1 and Larry Buck RV Park data was applied to Segment 5 in the Eagle Mountain WASP model. Table 3 presents the one-year of nutrient loading data for FWBC and Larry Buck RV Park.

Table 3: Lakeside Point Source Loading

	FWBC WWTP Monthly Average Loads (kg/day)						Larry Buck RV Park Monthly Average Loads (kg/day)				
Month	ORG N	ORG P	NO_x	OPO_4	NH_3		ORG N	ORG P	NO_x	OPO_4	NH_3
Jan	0.03	0.02	0.56	0.09	0.024		0.01	0.01	0.12	0.02	0.005
Feb	0.03	0.04	0.38	0.06	0.011		0.01	0.01	0.09	0.01	0.003
Mar	0.03	0.04	0.39	0.06	0.012		0.01	0.01	0.09	0.01	0.003
Apr	0.03	0.04	0.40	0.07	0.012		0.01	0.01	0.09	0.01	0.003
May	0.02	0.04	0.36	0.06	0.011		0.01	0.01	0.09	0.01	0.003
Jun	0.02	0.03	0.26	0.04	0.008		0.00	0.01	0.06	0.01	0.002
Jul	0.02	0.03	0.31	0.05	0.009		0.01	0.01	0.09	0.01	0.003
Aug	0.01	0.02	0.19	0.03	0.006		0.01	0.01	0.09	0.01	0.003
Sep	0.01	0.02	0.21	0.03	0.006		0.00	0.01	0.06	0.01	0.002
Oct	0.03	0.06	0.63	0.09	0.011		0.01	0.01	0.15	0.02	0.002
Nov	0.04	0.02	0.16	0.06	0.010		0.01	0.00	0.04	0.01	0.002
Dec	0.01	0.08	0.43	0.04	0.011		0.00	0.02	0.09	0.01	0.002

Atmospheric Loads

Nutrient loading from the atmosphere was calculated using precipitation and nutrient data (NH_3, NO_X, ON, and OP) provided by the District from rainwater analysis. This data was compared to literature estimates and found to be very similar. The loads where then converted to a constant daily rate and applied to the model (all surface segments). The calculated rates are presented in Table 4.

Table 4: Global Atmospheric Deposition Rates for Eagle Mountain WASP Model

Variable	Rate (mg-m^2/day)
Atmospheric Deposition of Nitrate	0.913
Atmospheric Deposition of Ammonia	0.829
Atmospheric Deposition of Orthophosphate	0.048
Atmospheric Deposition of BOD	0.0
Atmospheric Deposition of Organic Nitrogen	1.142
Atmospheric Deposition of Organic Phosphorus	0.048

Benthic Flux

Benthic flux in the form of ammonia (NH_4) and orthophosphate (OPO_4) was added to the two hypolimnetic segments (12, 13, 14). Initially the rates were based on sediment sampling and Nurnburg's (1988) regression equation and literature (Erickson and Auer, 1998), but analysis of intensive survey data from two summers allowed estimation of release rates from Hypolimnetic increase in concentration. These rates of increase and the duration of the phenomena were used in the model. WASP allows the user to apply benthic flux as a time-variable phenomenon and in the Eagle Mountain system, flux was applied from April through September when observed data showed increases in both ammonia and dissolved phosphorus in the hypolimnion. Table 5 presents the constant flux rates that were used for the Eagle Mountain WASP calibration model.

Table 5: Benthic Ammonia and Phosphate Flux Loading in Eagle Mountain WASP Model

WASP Segment	Benthic Ammonia Flux (mg-m^2/day) 1994-2003	Benthic Phosphorus Flux (mg-m^2/day) 1994-2003
12	22	4
13	22	4

Watershed loads

Nutrient loading from the watershed include both PS discharges from 11 WWTPs located in the Eagle Mountain watershed, and overland flow from approximately 800 square miles. These combined nutrient loads from the watershed were estimated using the SWAT model and supplied to WASP via an external NPS file. The nutrient loads for all 8 state variables were entered as kg/d.

Kinetics

Presented in Table 6 are the kinetic rates used in the Eagle Mountain WASP calibration model. All values are within the suggested literature ranges. Important kinetic parameters are the Michaelis-Menton half saturation constants and the nutrient to carbon ratios. These directly affect algal modeling and growth in WASP. The nitrogen half saturation constant of 0.0485 mg/L was based on Cedar Creek bioassays performed by Sterner and Grover (1998). The phosphorus half saturation constant of 0.007 mg/L P was calibrated in the model. The nitrogen to carbon ratio of 0.15 and a phosphorus to carbon ratio of .022 was fit to the Eagle Mountain model during calibration and is within the range of commonly used values in the literature. These ratios suggest a stoichiometry of 6.82 N: P, which is biased toward less nitrogen-limitation. This was determined to be appropriate because it best represents Eagle Mountain and its large proportion of nitrogen fixing blue-green algae. Kinetics that favor a 10 to 1 or higher N: P ratio are most representative of green algae growth requirements and underestimate the late summer Chl'a' in Eagle Mountain and similar TRWD reservoirs. Ideally, a WASP model that allows simulation of two algal groups would circumvent this problem, but this technology for WASP is not available at this time.

Table 6: Kinetic Constants for Eagle Mountain Calibration and Validation Model

WASP Kinetic Constant Type	**Avg. Range**	**Eagle Mountain**	***Units***
Nitrification Rate @ 20º C	0.001 – 0.2	0.17	day $^{-1}$
Nitrification Temp Coeff.	1.02 – 1.08	1.04	NA
Half Saturation: Nitrification Oxygen Limit	0.5 – 2.0	1.0	mg O_2/L
Denitrification Rate @ 20º C	0 – 0.09	0.03	day $^{-1}$
Denitrification Temp Coeff.	1.02 – 1.09	1.06	NA
Half Saturation: Denitrification Oxygen Limit	0 – 2.0	2	mg O_2/L
Phytoplankton Growth Rate @ 20º C	1.0 – 3.0	2.0	day $^{-1}$
Phytoplankton Growth Temp Coeff.	0 – 1.07	1.04	NA
Phytoplankton Light Formulation Switch (1 = DiToro)	NA	1 = DiToro	NA
Phytoplankton Max Quantum Yield Constant	NA	NA	NA
Phytoplankton Self Shading Extinction	NA	NA	NA
Phytoplankton Carbon::Chlorophyll Ratio	0 – 200	50	mg carbon/mg chla
Phytoplankton Optimal Light Saturation	0 – 350	200	Ly/day
Phytoplankton Half Saturation Constant: Nitrogen	0.01 – 0.06	0.0485	mg-N/L
Phytoplankton Half Saturation Constant: Phosphorus	0.0005 – 0.05	0.007	PO_4-P/L
Phytoplankton Endogenous Respiration Rate @ 20º C	0 – 0.5	0.05	day $^{-1}$
Phytoplankton Respiration Temp Coeff.	1.0 – 1.08	1.045	NA
Phytoplankton Death Rate Non-Zooplankton Predation	0 – 0.25	0.05	day $^{-1}$
Phytoplankton Zooplankton Grazing Rate	0 – 5	NA	L/cell-day
Nutrient Limitation Option (0 = Min; 1 = Multiplicative)	0, 1	0	NA
Phytoplankton Decay Rate in Sediments @ 20º C	0 – 0.02	0.02	day $^{-1}$
Phytoplankton Decay Rate Temp Coeff.	1.0 – 1.08	1.08	NA
Phytoplankton Phosphorus::Carbon Ratio	0 – 0.24	0.024	mg P/mg C
Phytoplankton Nitrogen::Carbon Ratio	0 – 0.43	0.15	mg N/mg C
Phytoplankton Half Saturation for N and P	0 – 1.0	0	NA
BOD Decay Rate @ 20º C	0.05 – 0.4	0.1	day $^{-1}$
BOD Decay Rate Temp Correction	1.0 – 1.07	1.04	NA
BOD Decay Rate in Sediments @ 20º C	0.0004 – 1.0	1.0	day $^{-1}$
BOD Decay Rate in Sediments Temp Coeff.	1.0 – 1.08	1.08	NA
BOD Half Saturation Oxygen Limit	0.5 – 1.0	1.0	NA
Waterbody Type for Wind Driven Aeration	1.0 – 3.0	NA	NA
Oxygen::Carbon Stoichiometeric Ratio	0 – 2.67	2.67	mg O_2/mg C
Reaeration Rate Constant @ 20º C	0.5 – 3.0	1	day $^{-1}$
Reaeration Rate Option (sums Wind and Hydraulic Ka)	0 – 1.0	NA	NA
Dissolved Organic N Mineralization Rate @ 20º C	0.02 – 0.075	0.035	day $^{-1}$
Dissolved Organic N Mineralization Temp Coeff.	1.0 – 1.08	1.045	NA
Organic N Decay in Sediments @ 20º C	0.0004 – 0.01	0	day $^{-1}$
Organic N Decay in Sediments Temp Coeff.	1.0 – 1.08	1.045	NA
Fraction of Phytoplankton Death Recycled to ON	0 – 1.0	1.0	NA
Dissolved Organic P Mineralization Rate @ 20º C	0 – 0.22	0.064	day $^{-1}$
Dissolved Organic P Mineralization Temp Coeff.	1.0 – 1.08	1.045	NA
Organic P Decay in Sediments @ 20º C	0.0004 – 0.01	0	day $^{-1}$
Organic P Decay in Sediments Temp Coeff.	1.0 – 1.08	1.08	NA
Fraction of Phytoplankton Death Recycled to OP	0 – 1.0	1.0	NA

SETUP AND CALIBRATION

This section presents the results of the Eagle Mountain 10-year WASP model calibration.

Figures 10 through 20 present and compare the median results of the WASP calibration model to observed Eagle Mountain water quality data for variables NH_3, NO_X, ON, TN, OPO_4, OP, TP, TN/TP ratio, nitrogen limitation, phosphorus limitation and Chl'a' in segments 1, 2, 3, 4, 5, and 6, respectively for the 11-year simulation time-period. Calibration concentrated on achieving overlapping observed and predicted data percentiles for each segment and mimicking the longitudinal trends (gradients) of each parameter. We feel this model does an adequate job at both.

Table 7 provides statistics for each of the annual calibration figures and for seasonal (April – September) calibration (figures not included here). R-square results were significant for TN and TP, both annually and seasonally, demonstrating a good basis for the model. R-square values were not significant for Chl'a' but the Relative Percent Difference calculation suggest that the error in observed and predicted data was similar to the difference we have seen in duplicates sent in for laboratory analysis. We feel this is as good as we can expect with a single algae group model. The excellent fit for P implies that this may be a good parameter for BMP evaluation.

Table 7: Statistical Analysis of EM WASP Model Results

Comparison of Observed and Predicted Medians

	R-square Values		Relative Percent Difference		
Parameter	Annual	Seasonal	Annual	Seasonal	Lab QC
NH3	0.1622	0.3372	15.2%	42.4%	
NOX	0.5637	0.0121	63.3%	67.2%	
Org N	0.2976	**0.9340**	15.5%	31.4%	
TN	**0.9050**	**0.9361**	12.9%	20.9%	17.2%
OPO4	**0.9209**	**0.7601**	13.1%	37.4%	
Org P	**0.8455**	**0.9430**	22.7%	17.6%	
TP	**0.9345**	**0.9200**	10.0%	15.2%	16.8%
TN:TP	0.6721	0.3183	18.2%	21.4%	28.3%
Chl'a'	0.2332	0.0130	17.7%	26.4%	21.0%
N-limit	0.3315	0.0841	9.0%	11.6%	
P-limit	**0.9704**	**0.8739**	4.1%	14.1%	

Highlighted r-square values significant at p =0.05

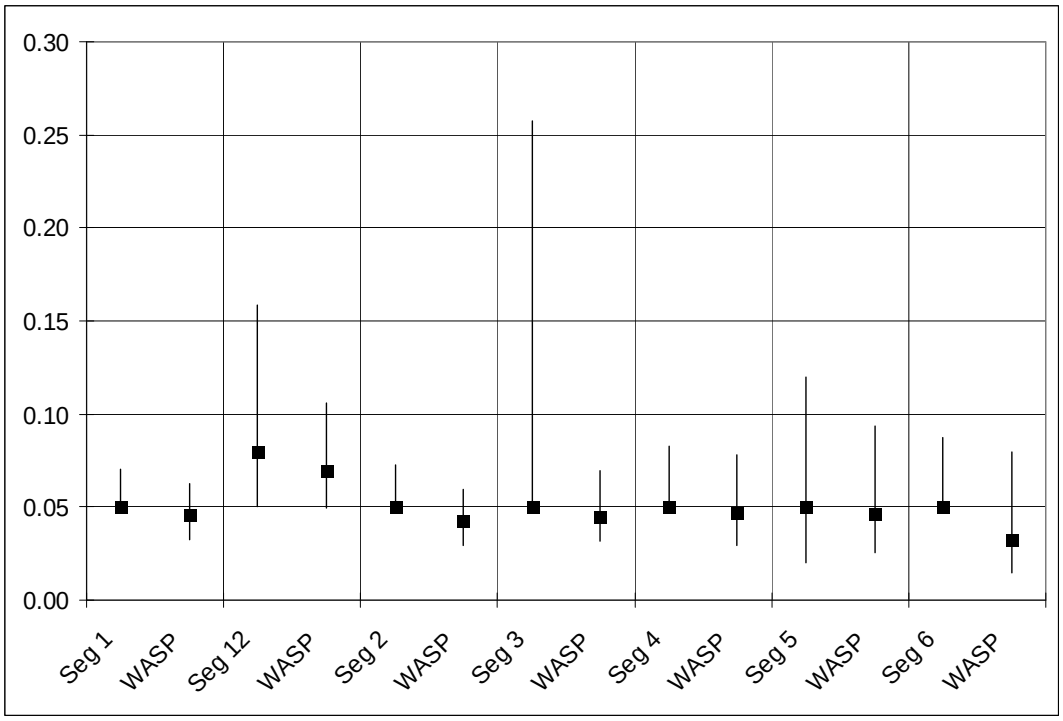

Figure 10: Eagle Mountain NH3 (1994– 2003) Median + 25th Percentiles

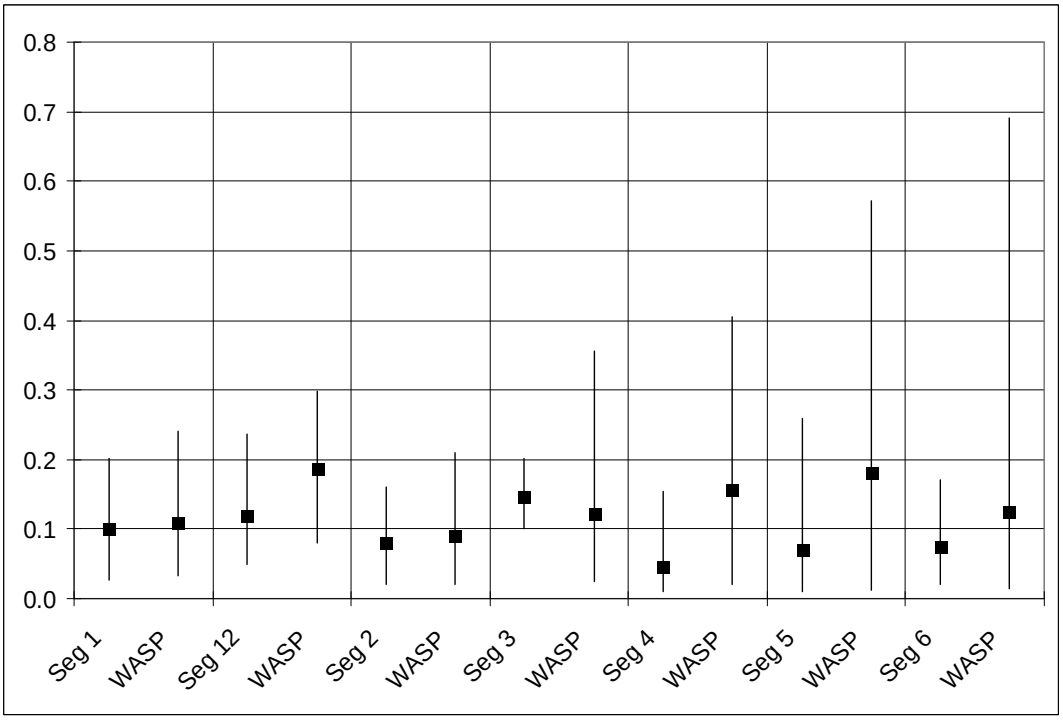

Figure 11: Eagle Mountain NOx (1994– 2003) Median + 25th Percentiles

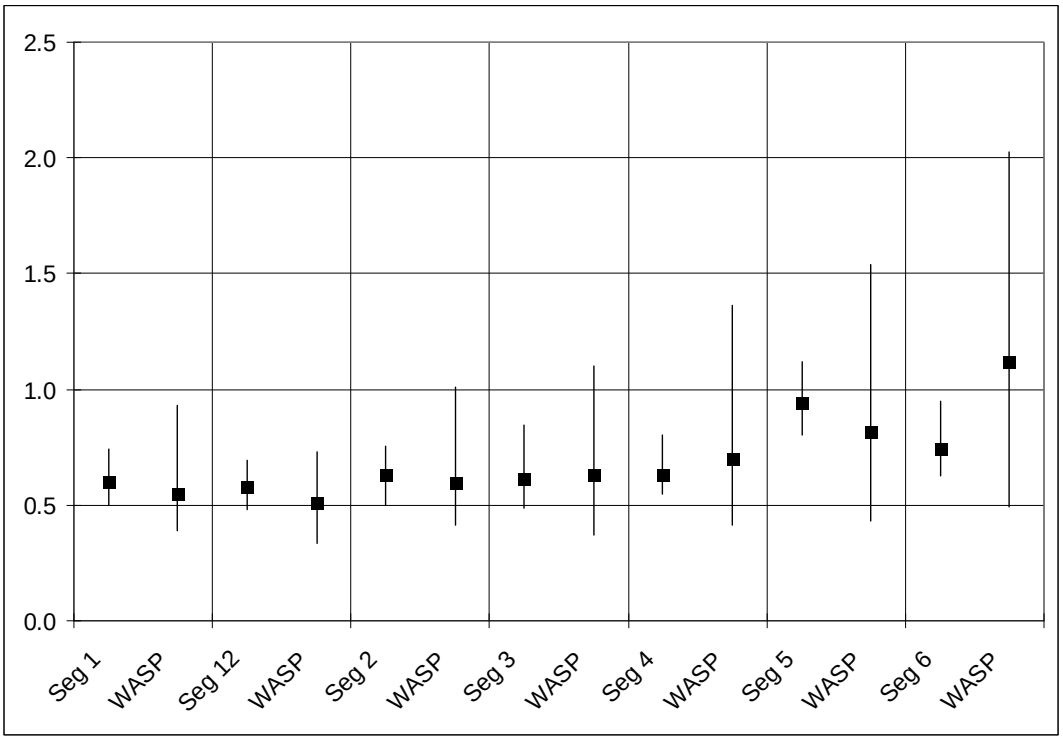

Figure 12: Eagle Mountain Organic Nitrogen (1994 – 2003) Median + 25th Percentiles

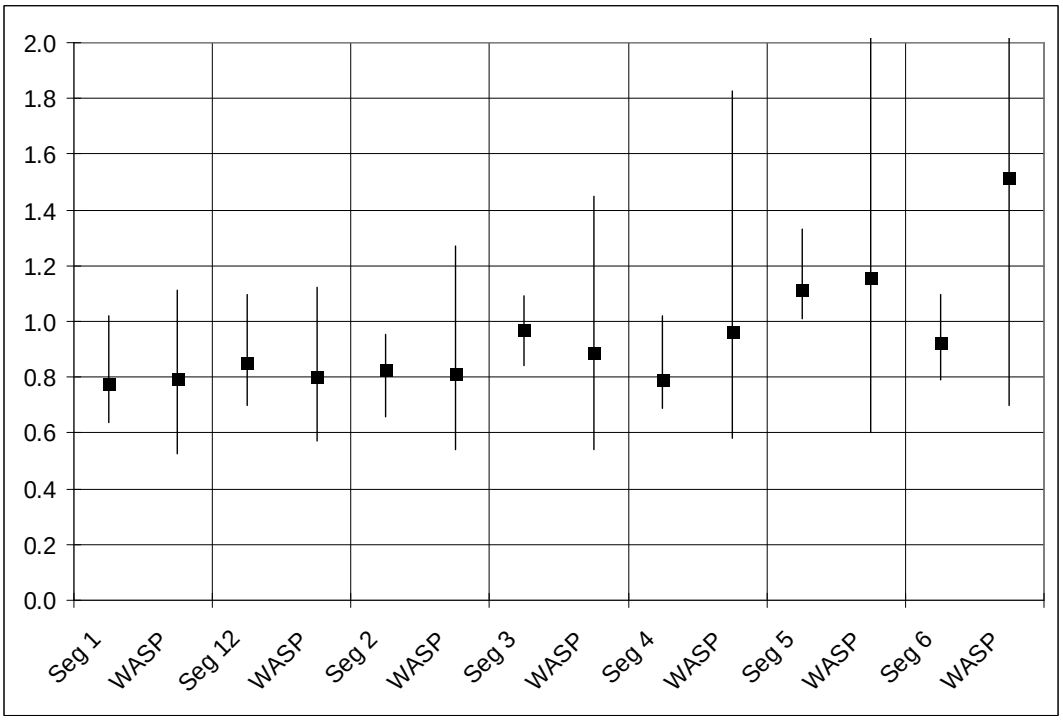

Figure 13: Eagle Mountain Total Nitrogen (1994 – 2003) Median + 25th Percentiles

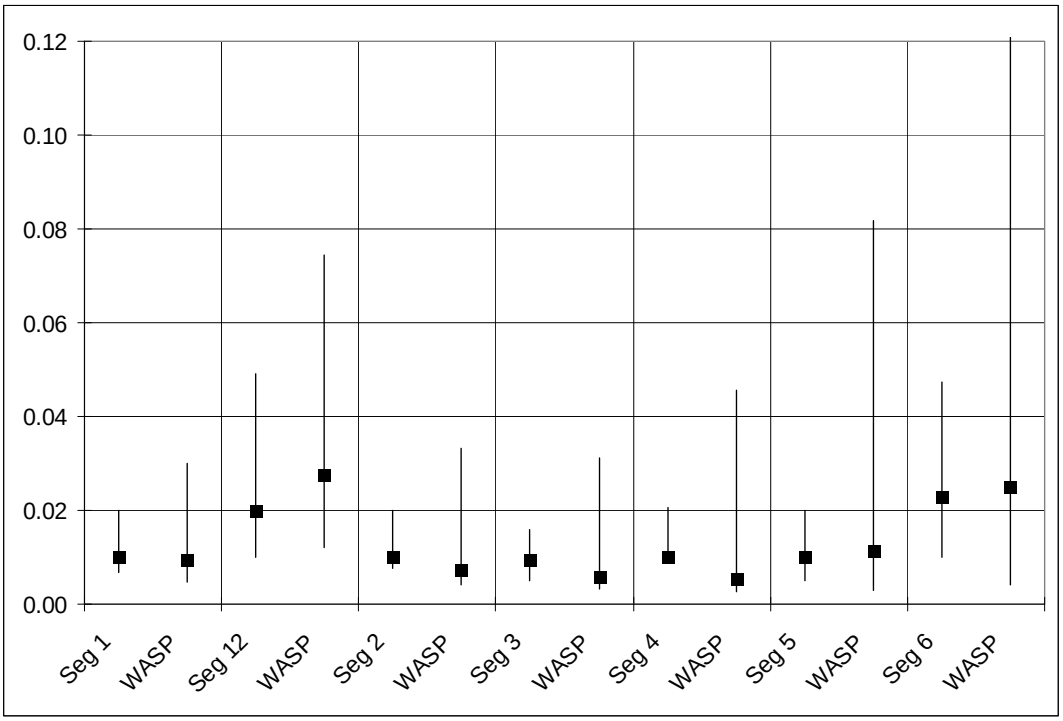

Figure 14: Eagle Mountain OPO4 (1994 – 2003) Median + 25th Percentiles

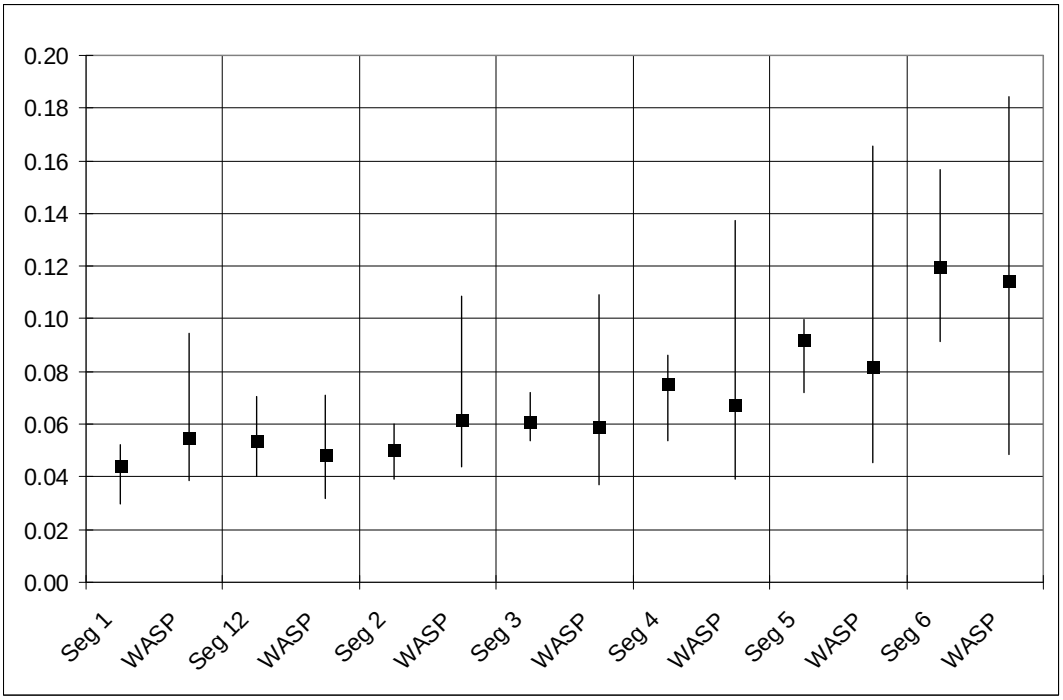

Figure 15: Eagle Mountain Org P (1994 – 2003) Median + 25th Percentiles

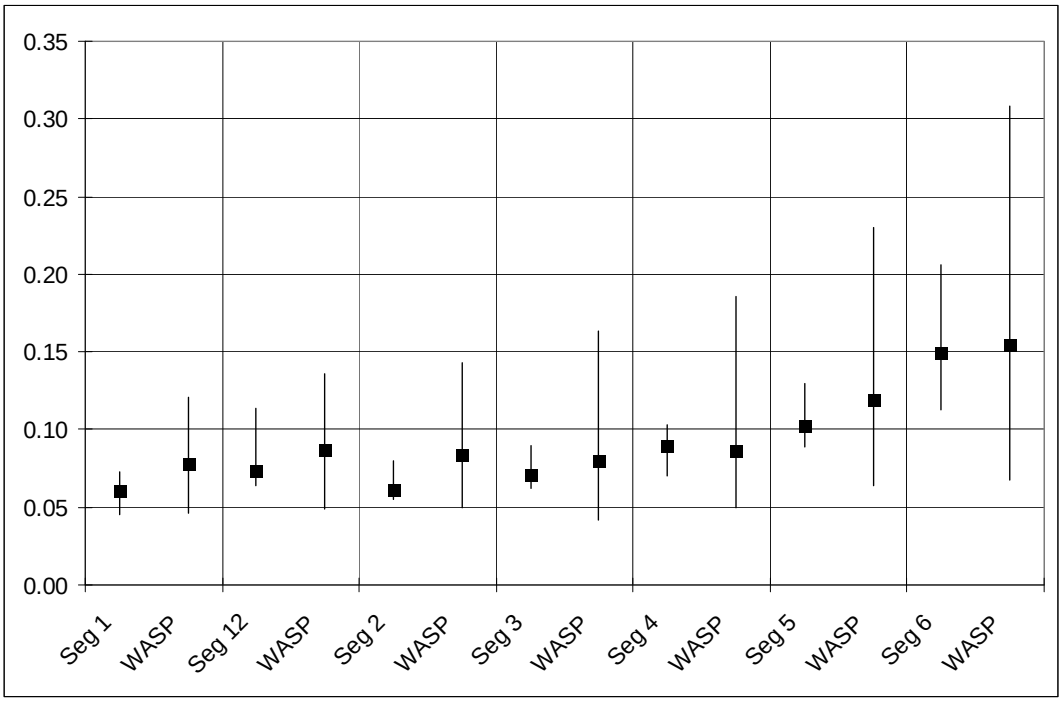

Figure 16: Eagle Mountain Total Phosphorus (1994 – 2003) Medians + 25th Percentiles

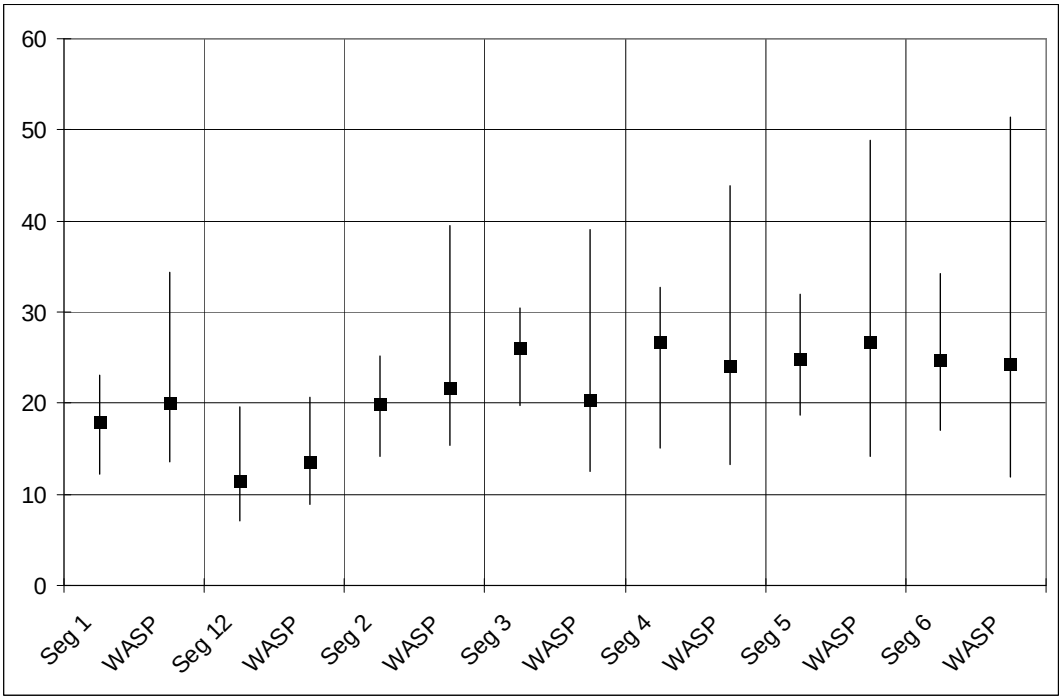

Figure 17: Eagle Mountain Chlorophyll-a (1994 – 2003) Medians + 25th Percentiles

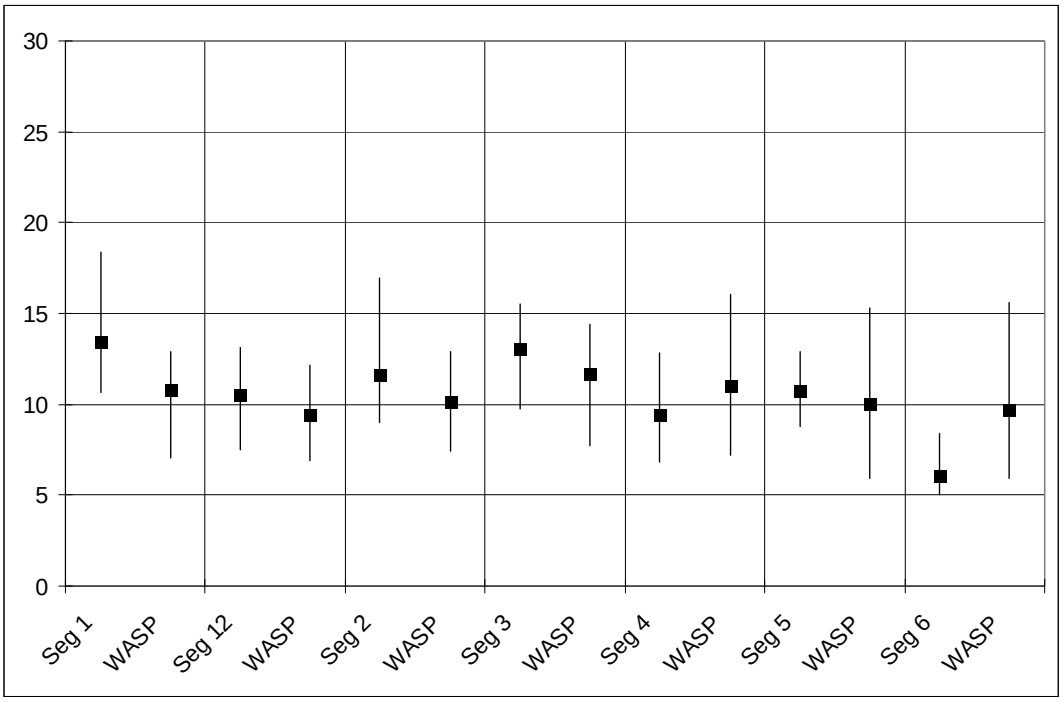

Figure 18: Eagle Mountain TN/TP Ratio (1994 – 2003) Medians+25th

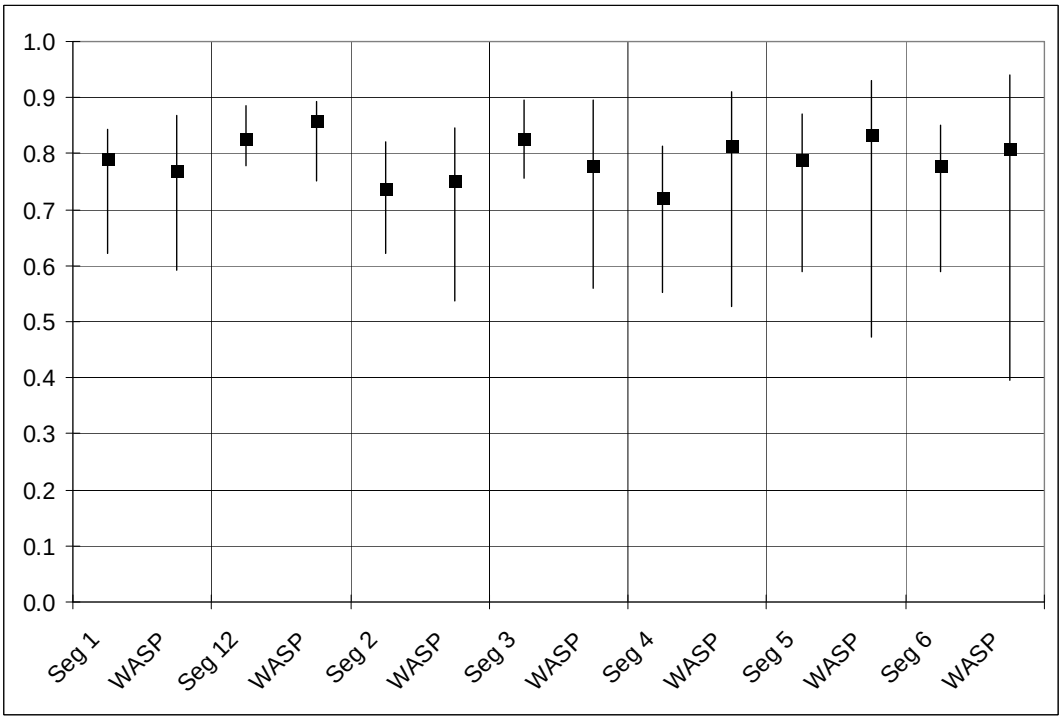

Figure 19: Eagle Mountain Nitrogen Limitation (1994 – 2003) Median + 25th Percentile

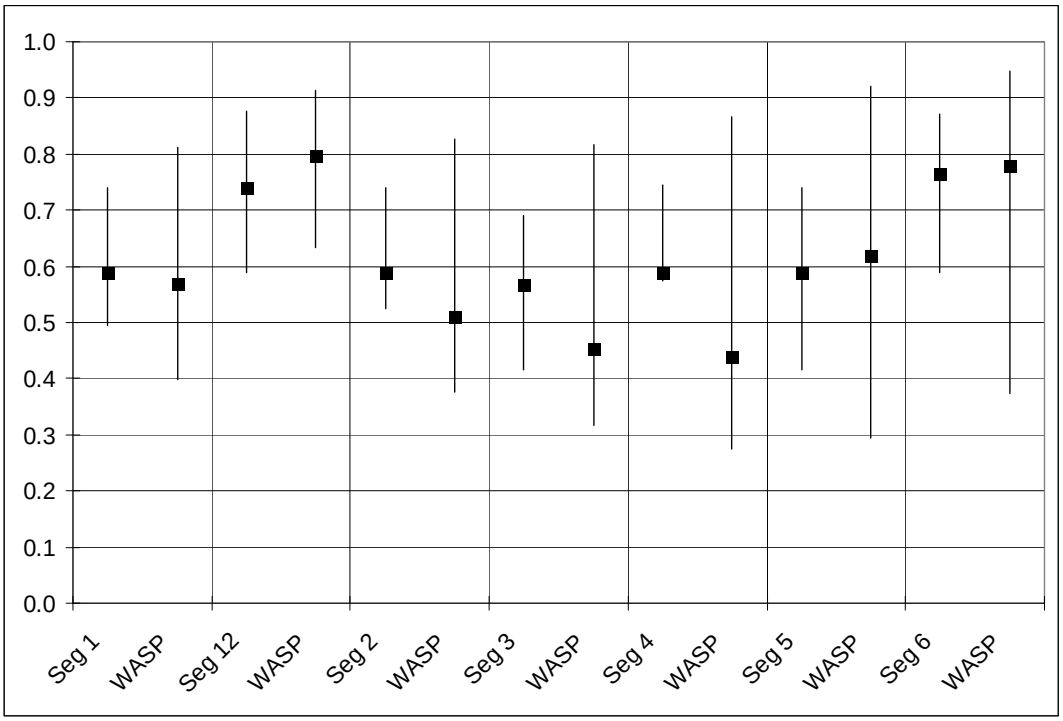

Figure 20: Eagle Mountain Phosphorus Limitation (1994 – 2003) Median + 25th Percentile

Eagle Mountain Nutrient Balance

An annual and 10-year mass balance of the nutrients coming into Eagle Mountain, leaving Eagle Mountain and the percent retained by the lake was calculated using all sources of incoming nutrients for the calibration period (1994-2003). Using the incoming nutrient data along with the inflows and outflows from the reservoir, the percent of nutrients retained by Eagle Mountain was calculated as:

Retention = Benthic Flux + ATM Load + Lakeside PS Load + Watershed Load - Outflow

Figures 21 and 22 represent the nutrient budget for TN and TP, respectively. The red line across the graphs represents the percent of nutrients retained. As can be seen from Figures 22 and 23, the highest periods of retention in Eagle Mountain occurred during the low flow period in 1999 and 2000. Conversely, the lowest amount of retention occurred in the year with the highest inflow. The average 11-year nutrient budgets for TN and TP for Eagle Mountain are presented in Figures 23 and 24 respectively. For Total Phosphorus the average annual loading is 167,459 kg/yr, broken down as follows: NPS 159,000 kg/year, WWTP 3486 kg/year, Atm 1216 kg/year and benthic flux 3390 kg/year.

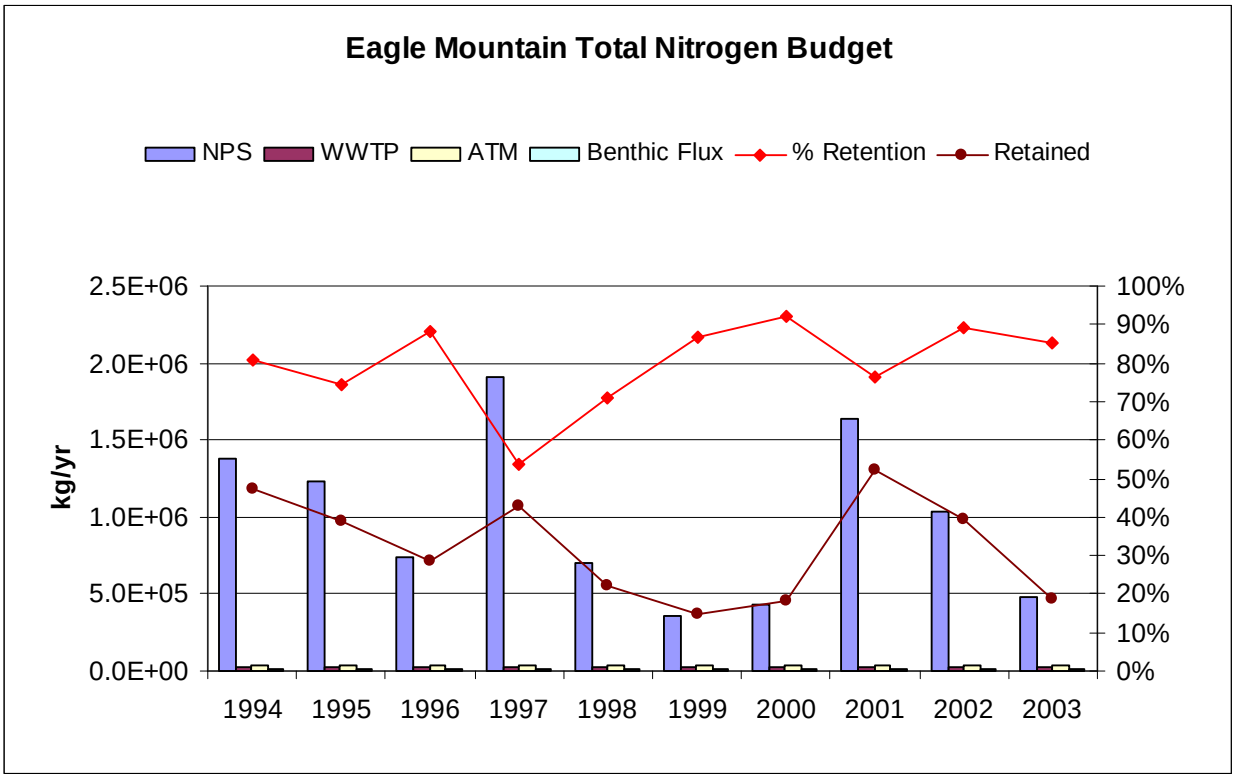

Figure 21: Eagle Mountain Nutrient Budget – Total Nitrogen (1994-2003)

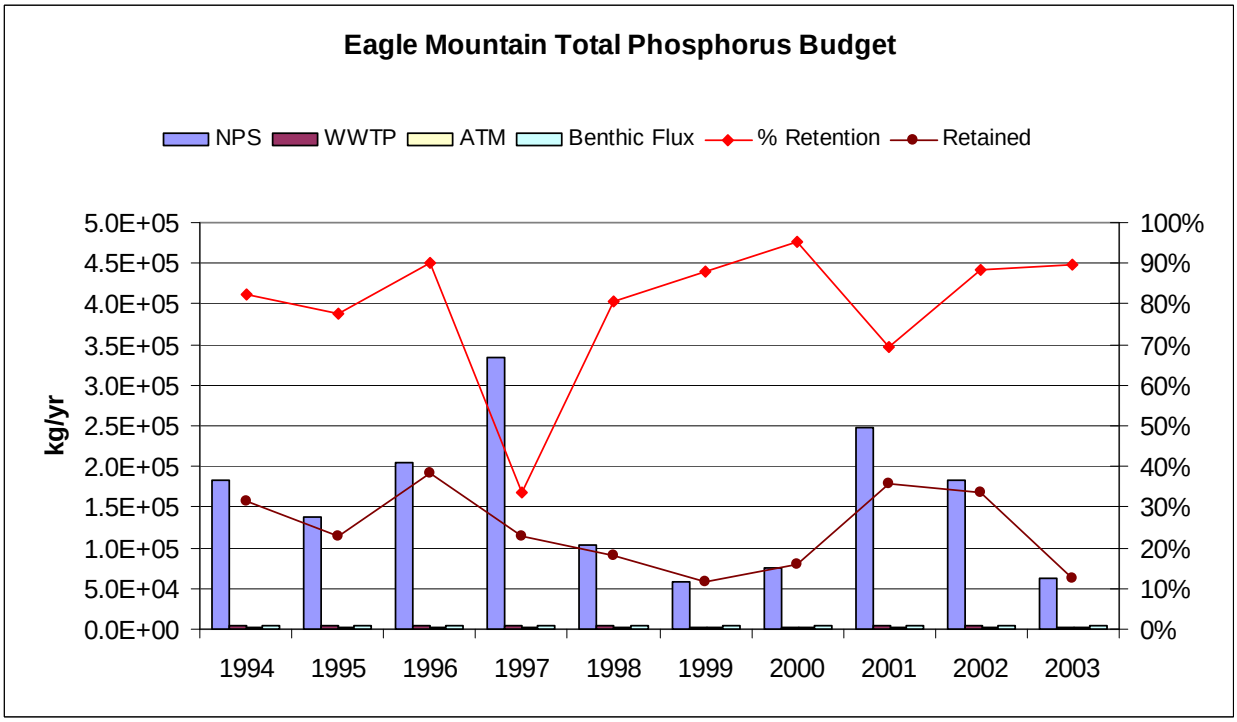

Figure 22: Eagle Mountain Nutrient Budget – Total Phosphorus (1994-2003)

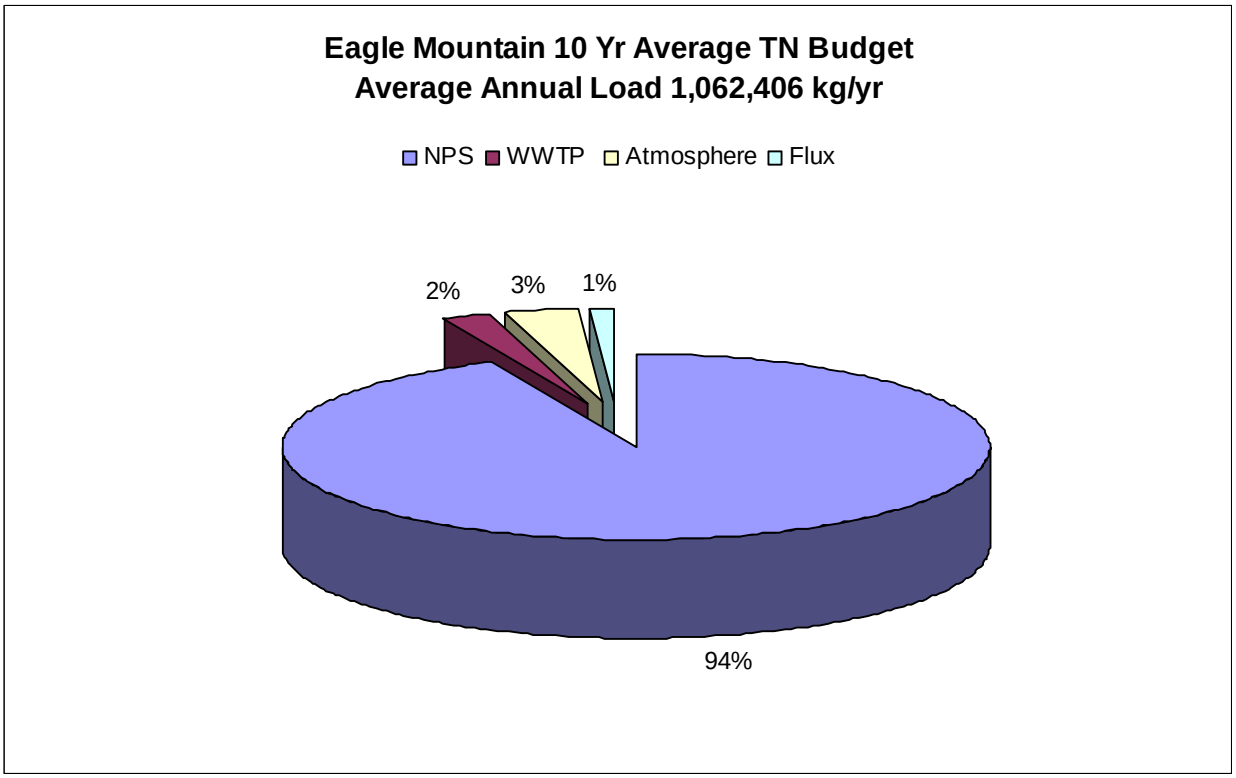

Figure 23: Eagle Mountain Average 10-Year Total Nitrogen Budget

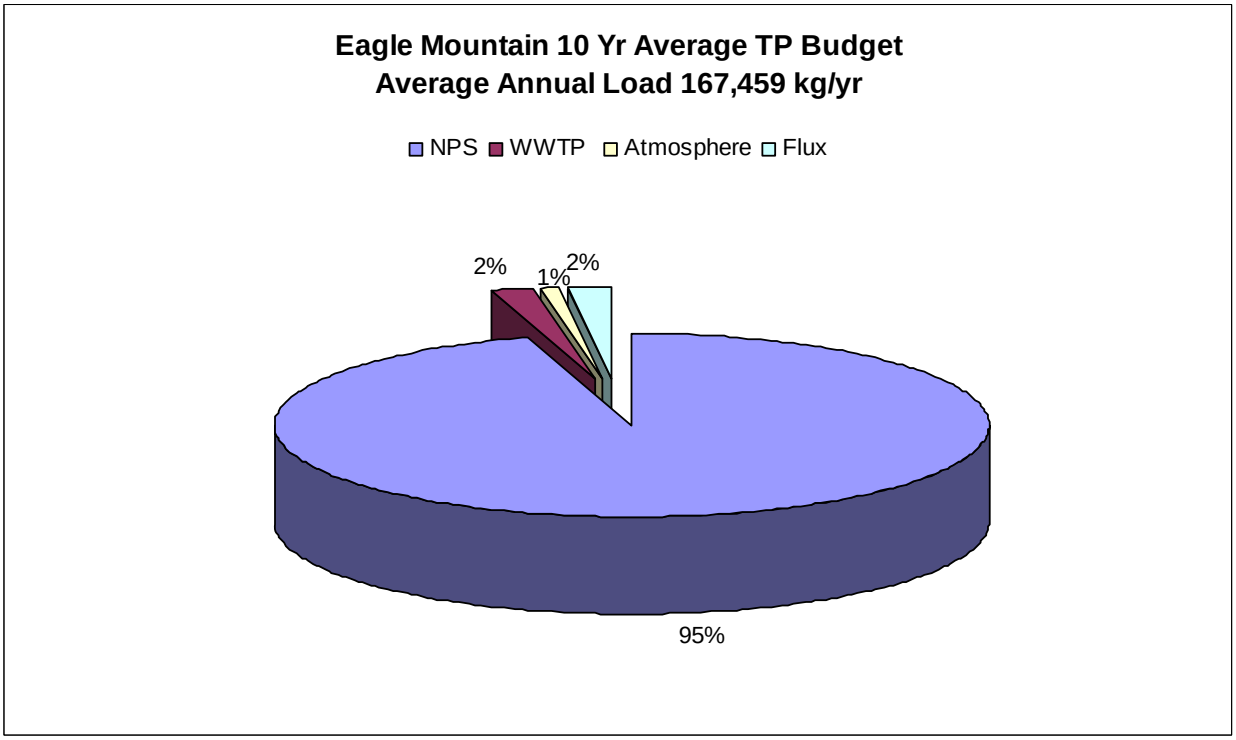

Figure 24: Eagle Mountain Average 10-Year Total Phosphorus Budget

Sensitivity Analysis

The response of the calibrated WASP model to five (5) nutrient loading scenarios was evaluated independently by systematically shutting each off. The response of algae (Chl'a') growth during the calibration period for segment 1 is presented in Figure 25. The first bar on the graph represents the calibrated WASP model; the second bar represents the response of Chl'a' if the WWTPs in the external SWAT watershed file and the two (2) WWTPs with direct input to the reservoir are shut off; the third bar represents the response of Chl'a' if atmospheric deposition of nitrogen and phosphorus are switched off; the fourth bar represents the response of Chl'a' if the SWAT external watershed load is shut off; and the fifth bar represents the response of Chl'a' if benthic flux is switched off. Likewise, the same sensitivity analysis was conducted for segments 1 to test the sensitivity of TP concentrations in the calibrated model as presented in Figure 26. Statistical testing with a Kruskal-Wallis Multiple Comparison test (alpha = 0.05) shows all simulations that are not significantly different from the calibration as having the same letter designation (i.e. A). These results, suggest that watershed loading is the most important contributor to Chl'a' growth.

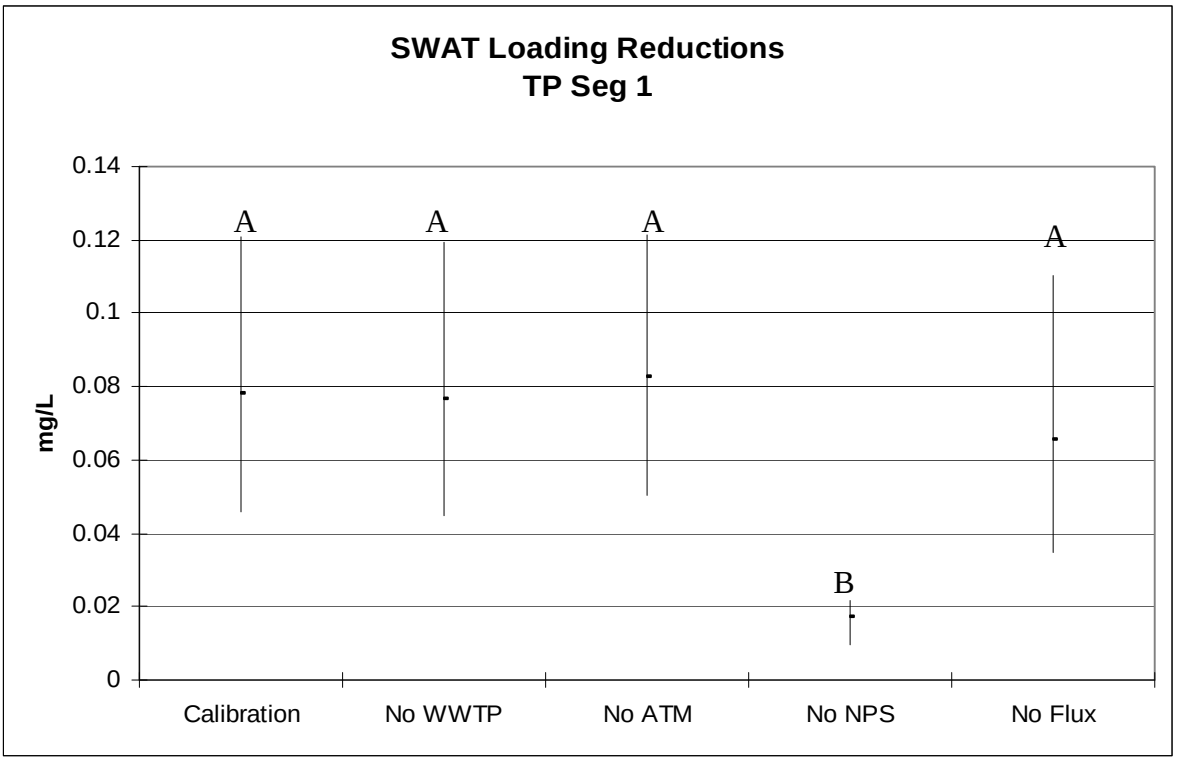

Figure 25: Eagle Mountain Reservoir Annual Chl'a' Segment 1 Median and Percentiles (1994-2003)

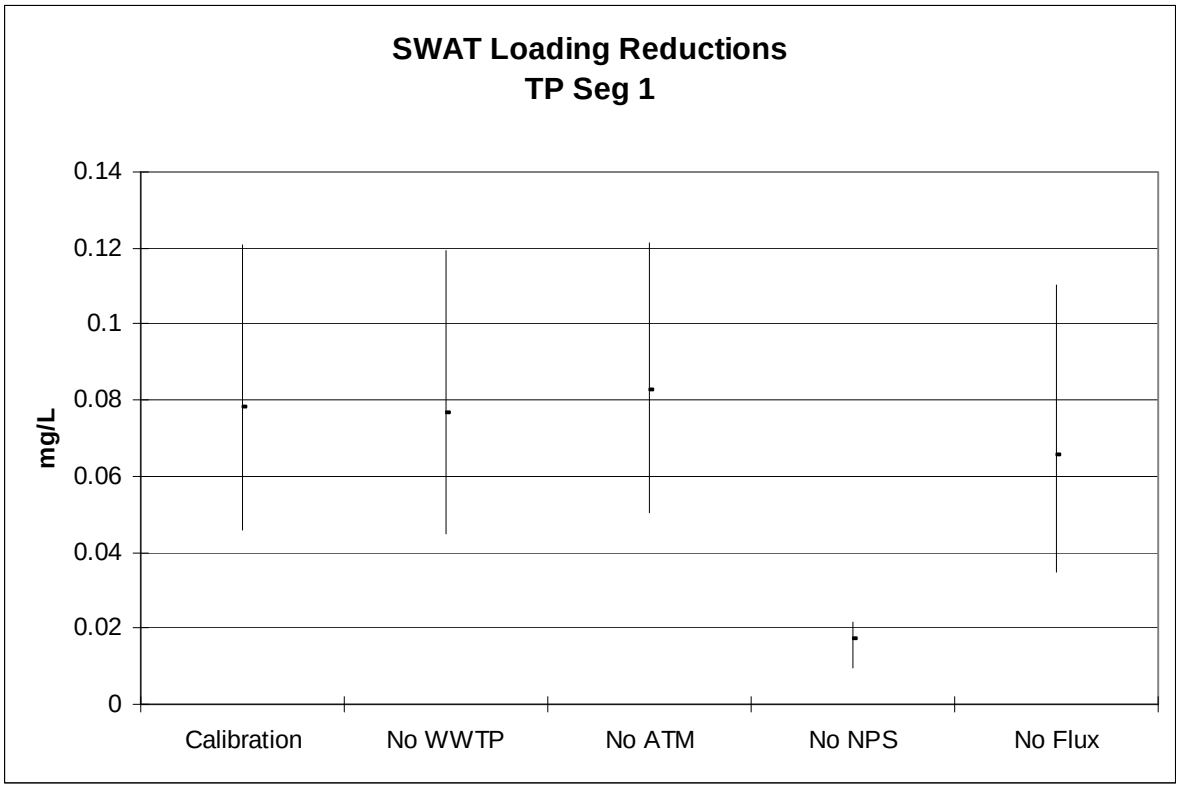

Figure 26: Eagle Mountain Lake Annual TP Segment 1 Median and Percentiles (1994-2003)

LOAD REDUCTIONS

Five load reductions were simulated during the calibration years by scaling the NPS file to create reductions ranging from 15% to 65%. As evident from Figures 26 and 27, a significant reduction in Chl'a' and TP concentration is not realized until about a 25% to 35% reduction in the watershed loading.

In order to narrow down the target load reduction, a fine resolution analysis was done for load reductions between 25% and 35%. 5 scalars were applied within this range and compared to the calibration model for a statistically significant reduction in Chl'a' and TP concentrations. As shown in Figure 29 and Figure 30, the concentrations for both parameters were not significantly reduced until somewhere between 28% and 30%. Therefore, a 30% reduction in P loading to the reservoir was recommended based on model results in order to have a significant impact on reservoir water quality.

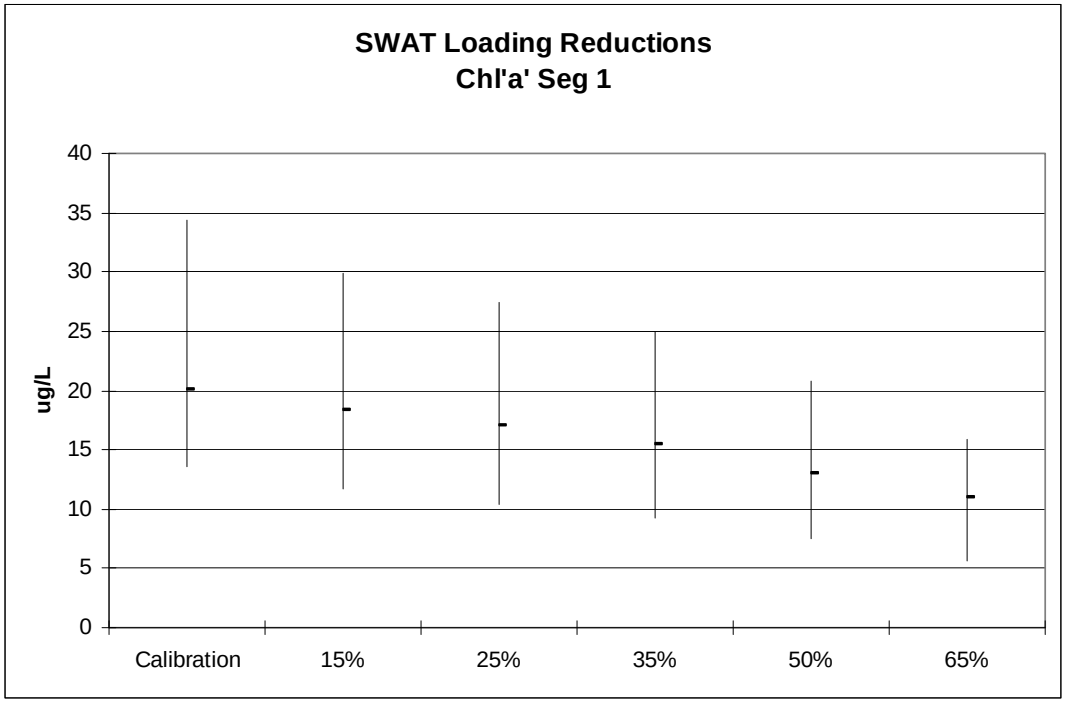

Figure 27: Eagle Mountain Annual Chl'a' in Segment 1: Reduction in SWAT *NPS File Loading – Median and Percentiles (1994 – 2003)

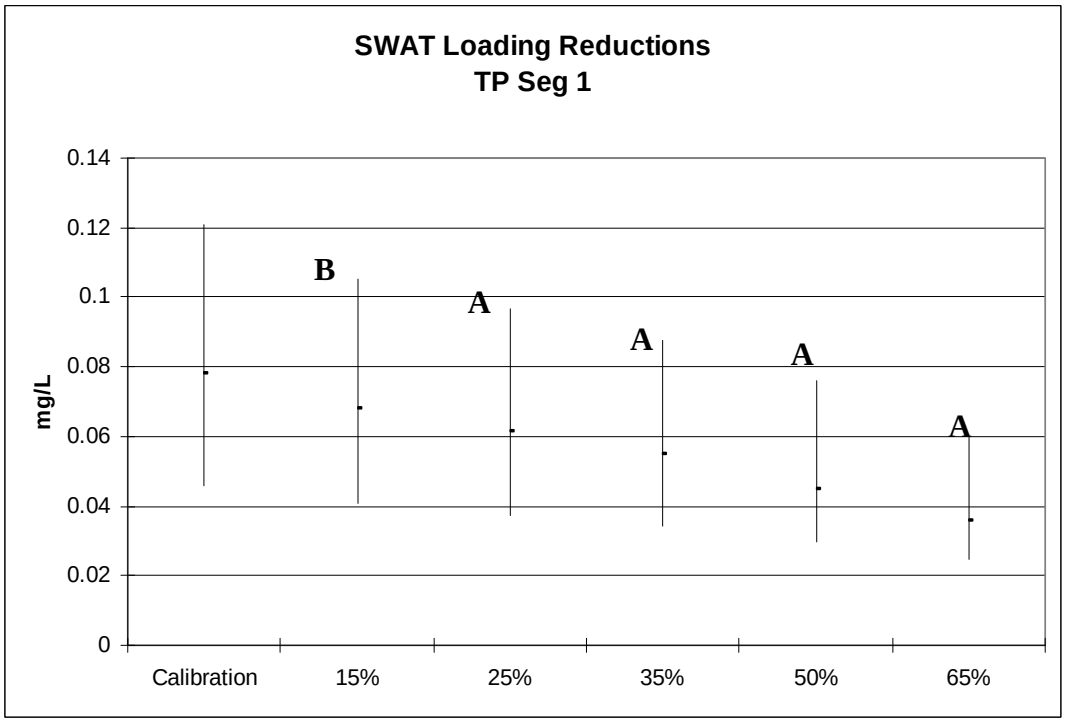

Figure 28: Eagle Mountain Annual TP in Segment 1: Reduction in SWAT *NPS File Loading – Median and Percentiles (1994 – 2003)

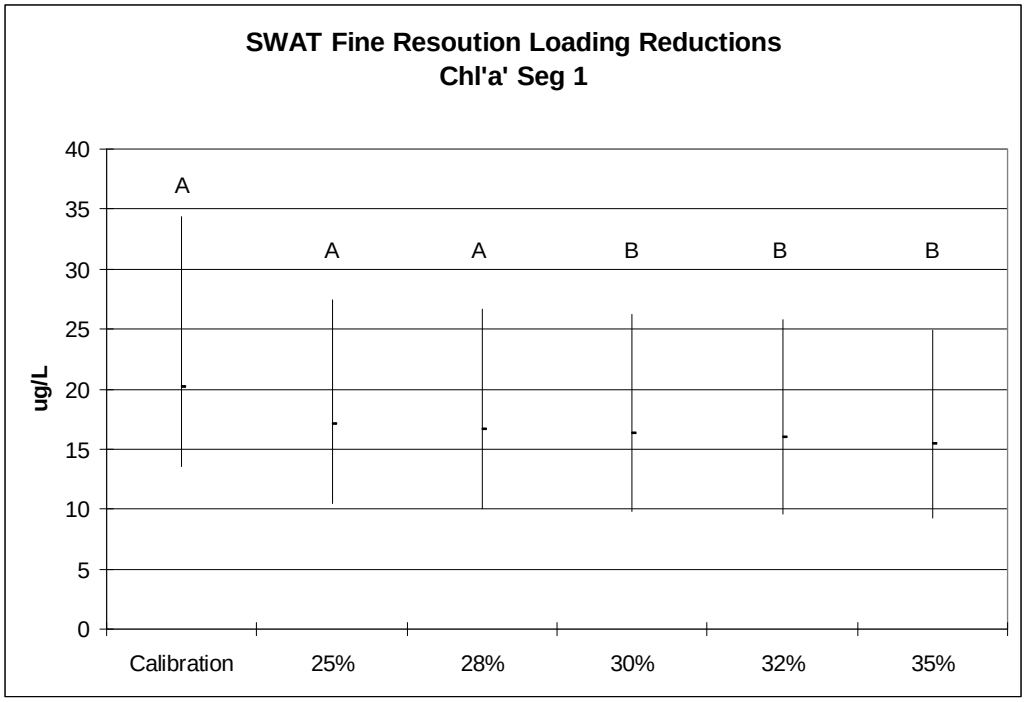

Figure 29: Eagle Mountain Annual Chl'a' in Segment 1: Fine Resolution Reduction in SWAT *NPS File Loading – Median and Percentiles (1994 – 2003)

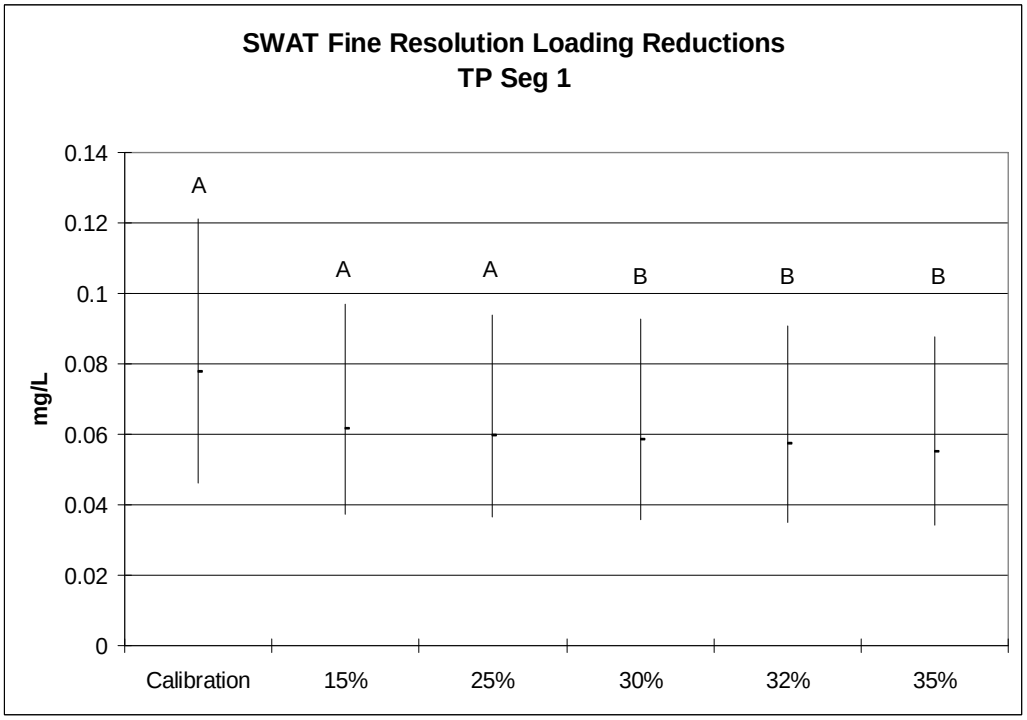

Figure 30: Eagle Mountain Annual TP in Segment 1: Fine Resolution Reduction in SWAT *NPS File Loading – Median and Percentiles (1994 – 2003)

BMP OPTIMIZATION ANALYSIS

Owens, J. Eagle Mountain Lake Simulation of Optimal Eagle Mountain BMP Analysis in WASP Technical Memorandum. October 11, 2011

The 10-year WASP model was initially used in the Eagle Mountain Project to provide direction on the degree of phosphorus reduction that would be necessary to translate into a reduction in Chl'a' that was meaningful. The daily watershed loading file (nps file generated by SWAT) was systematically reduced by a scaling factor from 15% to 65% to determine when Chl'a' was significantly ($p<0.05$) less than the calibration results at two sites in the main pool of the reservoir. This exercise determined that a 30% reduction was necessary to see a statistically significant reduction in Chl'a' at the Dam of Eagle Mountain Lake. The stakeholders on the project adopted a 30% total phosphorus reduction goal for the project.

It must be emphasized that the WASP simulation was done with a scaler on the NPS file that reduced the daily load by a set amount. Subsequent analysis by SWAT and the Economic Model used the target of 30% reduction to guide their efforts, however they were focused on 30% of the average annual load as a target. There has been some question as to whether implementing the Optimal solution based on a 30% total phosphorus reduction will actually result in the desired impacts in Eagle Mountain Lake. This exercise is aimed at testing the load reductions under various spatial and temporal conditions to see the resulting impact on reservoir water quality.

The Economic Model has selected an optimal solution of 12 BMPs that reduces the phosphorus loading to the target goal of approximately 30%. This solution was given back to the SWAT modelers who implemented the suite of BMPs. A new nps file was generated that reduced the phosphorus load generated from the watershed by 26.1%. One of the optimal BMPs in the suite was P-inactivation with alum, which is an in-lake BMP. Therefore, in conjunction with the new nps file, the flux rate in the WASP model was modified to simulate the alum treatment BMP. The flux scaler in the model was set to 32%, which simulated a 68% reduction in P phosphorus. The alum treatment should reduce the P load by 3.3% in addition to the 26.1% reduction made in the NPS loads for a total of 29.4% reduction in the total P load to the reservoir.

Figures 31 and 32 show time series plots of the TP and Chl'a' at the dam (Seg 1) for three sceanarios: calibrated model, Optimal solution with 12 BMPs and the systematic reduction of 30%. Both parameters show a reduction from the calibrated model and indicate similar results for the Optimal solution and 30% reduction scenario.

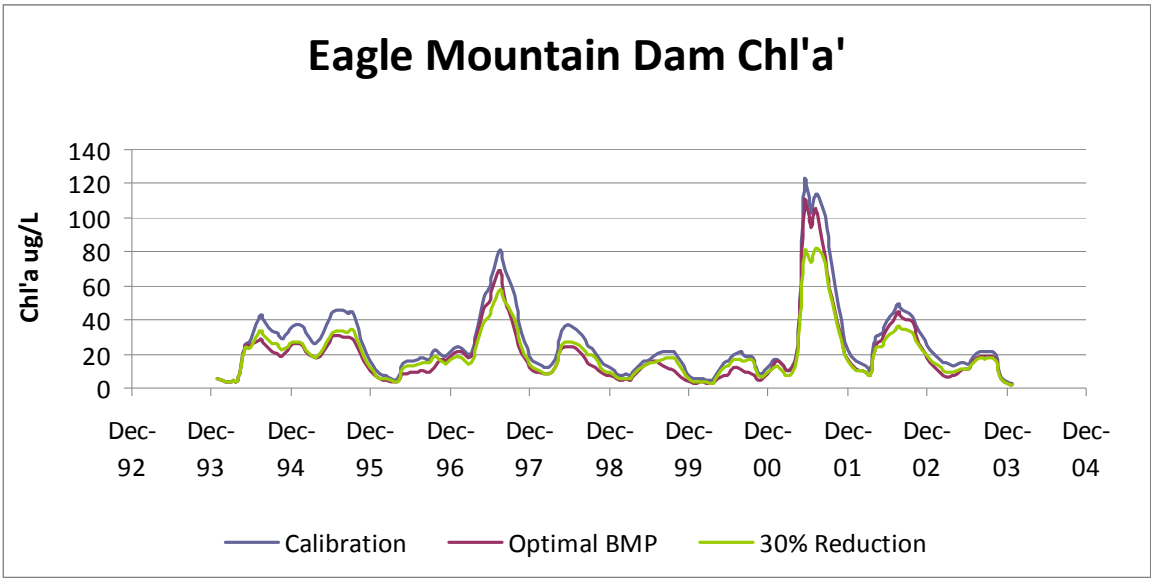

Figure 31. Eagle Mountain Lake Time Series Plot of Chlorophyll-a at Segment 1.

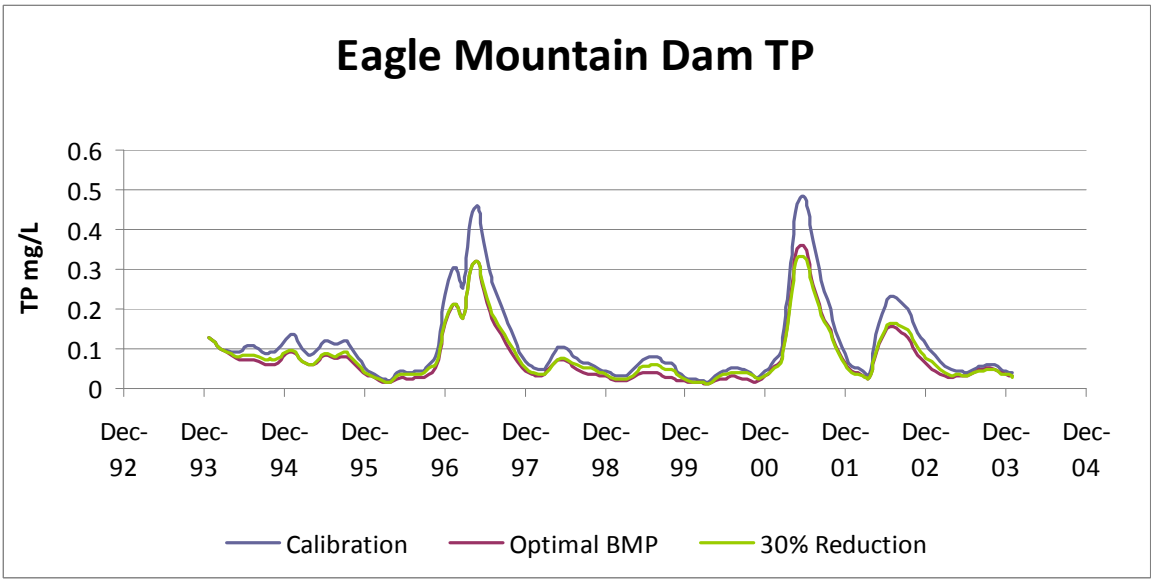

Figure 32. Eagle Mountain Lake Time Series Plot of Total Phosphorus at Segment 1.

Figures 33 and 34 compare the three scenarios by calculating the overall median and 75th and 25th percentiles. These medians were tested to see if they were statistically different from the calibration median ($p<0.05$) with a Kruskal-Wallis nonparametic multiple range test. This was the same technique employeed to test the systematic reductions at the beginning of this project. The results here show that at the dam (Seg 1) the Optimal Solution was significantly lower than the calibration median.

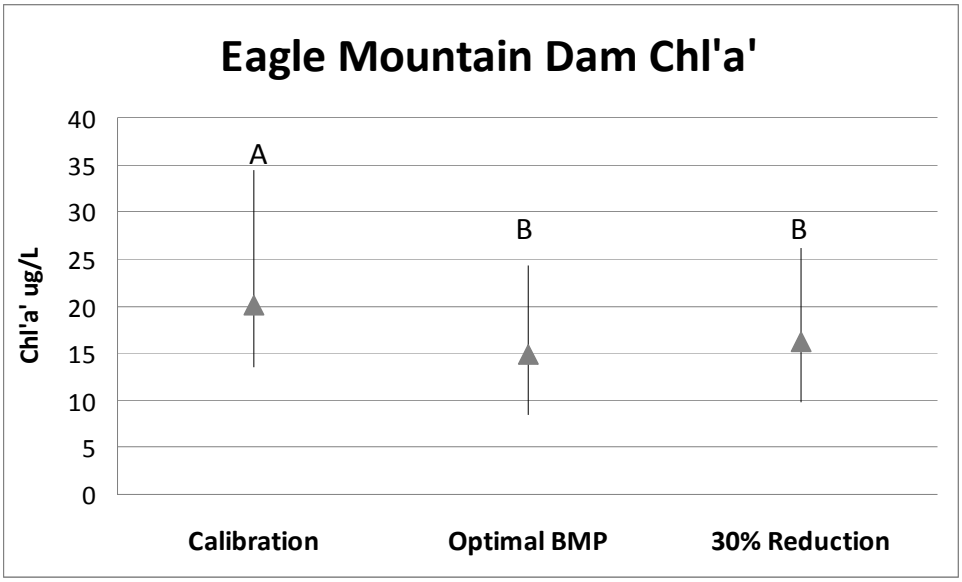

Figure 33. Eagle Mountain Lake Chlorophyll-a Segment 1 Median and Percentiles (1994-2003)

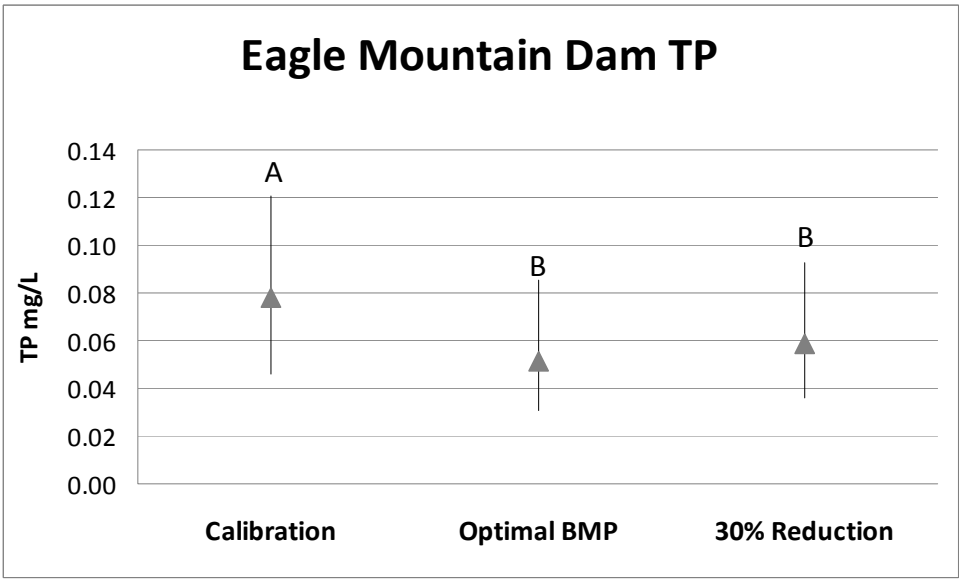

Figure 34. Eagle Mountain Lake Total Phosphorus Segment 1 Median and Percentiles (1994-2003)

In conclusion, the WASP modeling suggests that the Optimal Solution BMP scenario will reduce the phosphorus loading to a sufficient level to result in significant reductions in Chl'a' that were targeted by this project.

PIPELINE INFLUENCE ON REDUCTION SCENARIOS

Owens, J. Pipeline Influence on Eagle Mountain Reduction Scenarios Technical Memorandum. October 3, 2012

The 10-year WASP model simulating 1994-2003 was initially used in the Eagle Mountain Project to provide direction on the degree of phosphorus reduction that would be necessary to translate into a reduction in Chl'a' that was meaningful. The time period was chosen because it captured years with hydraulic variation and we had a solid database of water quality data to use for model calibration. Using the calibrated model, the daily watershed loading file (nps file generated by SWAT) was systematically reduced by a scaling factor from 15% to 65% to determine when Chl'a' was significantly ($p<0.05$) less than the calibration results at two sites in the main pool of the reservoir. This exercise determined that a 30% reduction was necessary to see a statistically significant reduction in Chl'a' at the Dam of Eagle Mountain Lake. The stakeholders on the project adopted a 30% total phosphorus reduction goal for the project.

In 2008, the Eagle Mountain Connection pipeline was completed allowing for the transfer of water from Cedar Creek and Richland Chambers to be pumped into Eagle Mountain. With the addition of a new source of water to the reservoir, the question was raised if a 30% reduction in nonpoint source total phosphorus would still reflect a statistically significant reduction in TP and chlorophyll 'a'.

In order to run the calibration model with the addition of pipeline flows, a new flow balance had to be created for the calibration years as if the pipeline had been in place. TRWD Engineering used Riverware to simulate the trib inflows, pipeline inflows and reservoir volume for Eagle Mountain for the time period of 1994-2003. This information was used to create a new flow balance for WASP that included pipeline inflows. The average annual trib inflow for the simulation period was 214,307 ac-ft and the average annual pipeline inflow was 19,805 ac-ft. Over the calibration period, there were three years in which the pipeline did not contribute any inflow to the reservoir. In the years the pipeline was used, the annual contribution ranged from 9%-27%. The average annual pipeline contribution was 11.41%.

Using Riverware created the quantity of water that the pipeline would discharge during the simulation years, however the quality of the water needed to be input. In order to calculate the nutrient load associated with the pipeline inflows, median nutrient concentrations from the pipeline sampling locations (RC-05, M) and (CC-04, M) were obtained from the 20 year trend study (Table 8). A blend of 65% RC and 35% CC was assumed for the entire simulation. Loading inputs were developed for NH3, NOx, OPO4, Org N, and Org P. The loads were put in as (kg/day) to segment 8.

Table 8. Median Nutrient Concentration of Pipeline Inputs to Eagle Mountain Lake Segment 8.

Median PL Concentrations (mg/L)								
	NH3	NOX	TKN	TN	TP	OPO4	Org N (calc)	Org P (calc)
CC	0.05	0.11	0.8	0.95	0.08	0.02	0.75	0.06
RC	0.05	0.18	0.69	0.88	0.06	0.01	0.64	0.05

Figures 35 and 36 show box and whisker plots of the TP and Chl'a' at the dam (Seg 1) for four different model runs: calibrated model (Cal), calibrated model with pipeline inflows (Cal_PL), calibrated model with 30% NPS reduction (Cal_30%), and calibrated model with pipeline inflows and 30% NPS reduction (PL_30%).

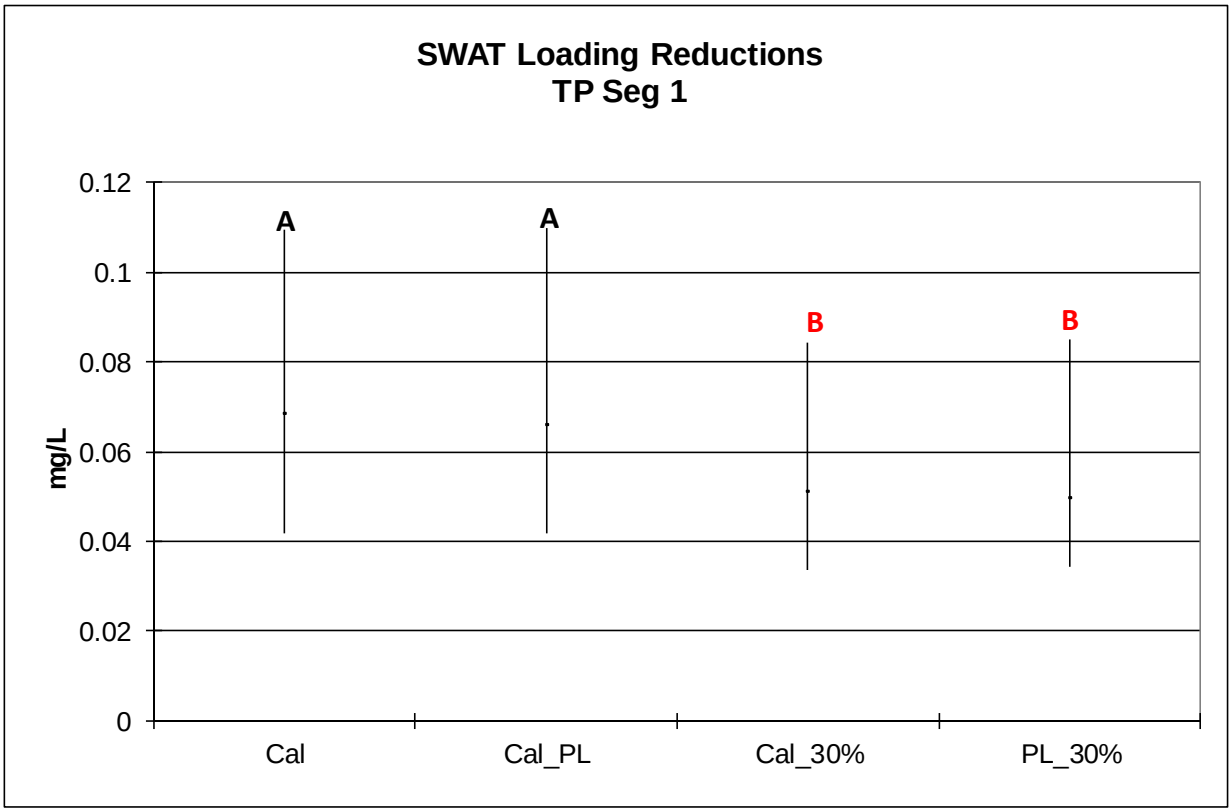

Figure 35 – Median +/- 25th percentile Total Phosphorus values from four modeled scenarios.

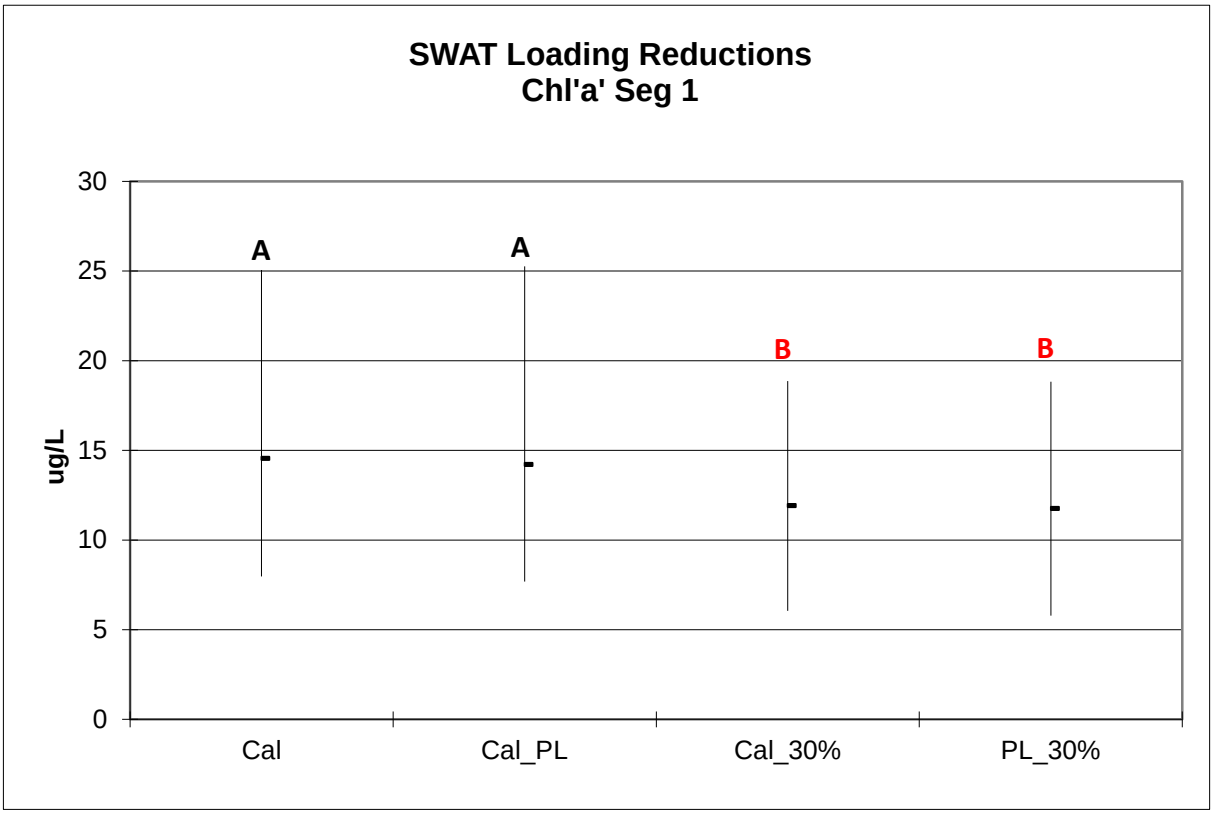

Figure 36: Median +/- 25th percentile Chlorophyll-a values from four modeled scenarios.

Monthly output from each scenario was log transformed and statistically analyzed using an ANOVA and Duncan's multiple range test. Each scenario in the chart has been coded with a letter to indicate the statistical results. The Calibration and Calibration with PL inflows scenarios are both labeled with an "A". This indicates that the model outputs from both of these scenarios are not significantly different. Both of the scenarios using the NPS with 30% reduction are labeled with a "B". This again indicates that the outputs from both of these scenarios are not significantly different. However, it does indicate the output from the 30% reduction scenarios are significantly different from both the calibration and the calibration with pipeline inflows.

In conclusion, the addition of East Texas pipeline inflows as they would have been implemented under the system operational guidelines for the calibration period would not require more than a 30% reduction in NPS loading to achieve a statistically significantly lower level of Chl'a and TP in Eagle Mountain Lake.

REFERENCES

Chapra, S. C. 1997. *Surface Water Quality Monitoring*. McGraw-Hill. 844 pp.

Erickson, M.J. and M.T. Auer. 1998. Chemical exchange at the sediment-water interface of Cannonsville Reservoir. *Lake and Reserv. Manage*. 12(2-3):266-277.

Ernst, M.R. 1995. *Estimation of Extinction Coefficients from Secchi Disk Measurements in Turbid Reservoirs*. AWRA. November. 61-70.

Harmel, R.D., R.J. Cooper, R.M. Slade, R.L. Haney and J.G. Arnold. 2006. Cumulative Uncertainty in measured streamflow and water quality data for small watersheds. *Trans. ASABE* 49(3) 689-701.

Nurnberg, G.K. 1988. Prediction of release rates from total and reductant-soluable phosphorus in anoxic lake sediments. *Can. J. Fish Aquatic Sci*. 45, 453-462

Sterner, R.W. and J.P. Grover. 1998. Algal Growth in Warm Temperate Reservoirs: Kinetic Examination of Nitrogen, Temperature, Light and other Nutrients. *Wat. Res*. 32(12) 3539-3548.

Thomann, R.V. and J.A. Mueller. 1987. *Principles of Surface Water Quality Modeling and Control*. HarperCollinsPublishers, Inc. 644 pp.

Walker, W.W. Jr. 1985. Statistical basis fro mean Chlorophyll a criteria. *Lake and Reserv. Mgnt*. 2:57-62.

APPENDIX – Eagle Mountain Lake Erosion Study

Eagle Mountain Reservoir

Part I: Channel and Gully and Part II: Sedimentation

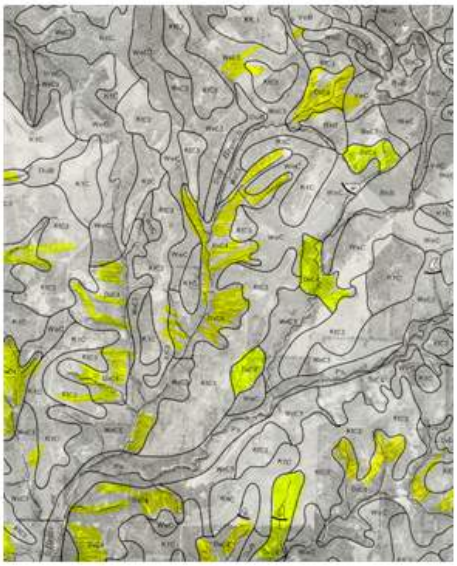

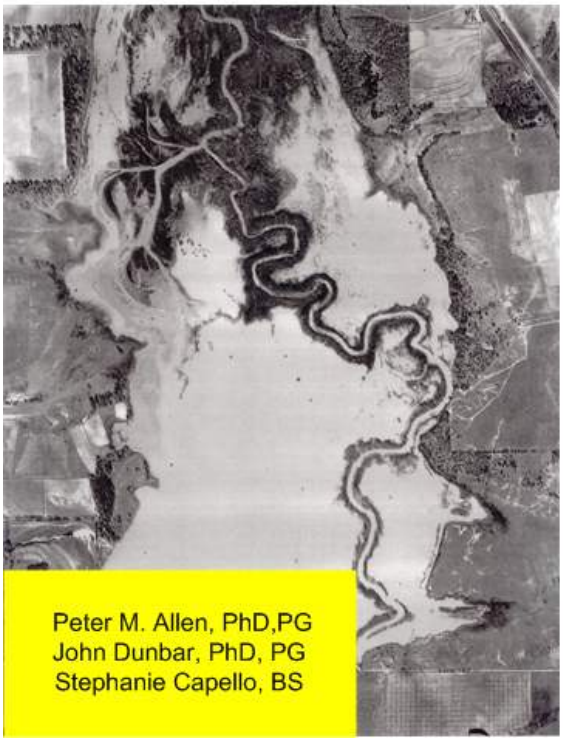

Peter M. Allen, PhD,PG
John Dunbar, PhD, PG
Stephanie Capello, BS

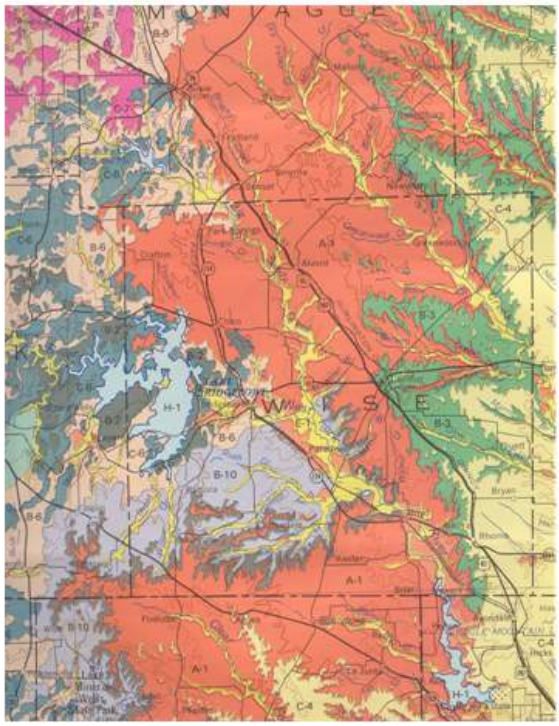

CHANNEL AND GULLY EROSION: PART I

Mean channel erosion in the Eagle Mountain Watershed is estimated to range from 115,124 to 748,031 tons per year. Apparent rates of combined gully and channel erosion based on best estimates would be 293,092 for present day conditions to around 748,031 for past conditions (impoundment to 1960's). This is based on five different methods of channel erosion assessment: (1) erosion assessment made for the basin based on NRCS field evidence (Griener, 1982) and USLE methodologies, (2) field assessment of channel erosion and SWAT generated channel lengths and dimensions, (3) field assessment of channel erosion and power functions utilized in SEDNET (4) using a weighted average of sediment yield by ecoregion and (5) literature review of channel erosion rates.

Project Area

Eagle Mountain Reservoir has a drainage area of approximately 5,102.3 sq. km. at USGS Gage Site 08045000. The reservoir began impoundment in February 1934. The capacity at conservation pool level is 178,400 acre feet at 649.1 feet above mean sea level elevation. The watershed trends approximately along strike of four major geologic units. From oldest to youngest these are: Paleozoic aged rocks, the Twin Mountain Formation, Glen Rose Formation, Paluxy Formation, and the Goodland Formation. For simplicity, a land resources map of the area is shown which simplifies the geologic map into general lithologic (rock types) units, Figure 1 and Table 1 .

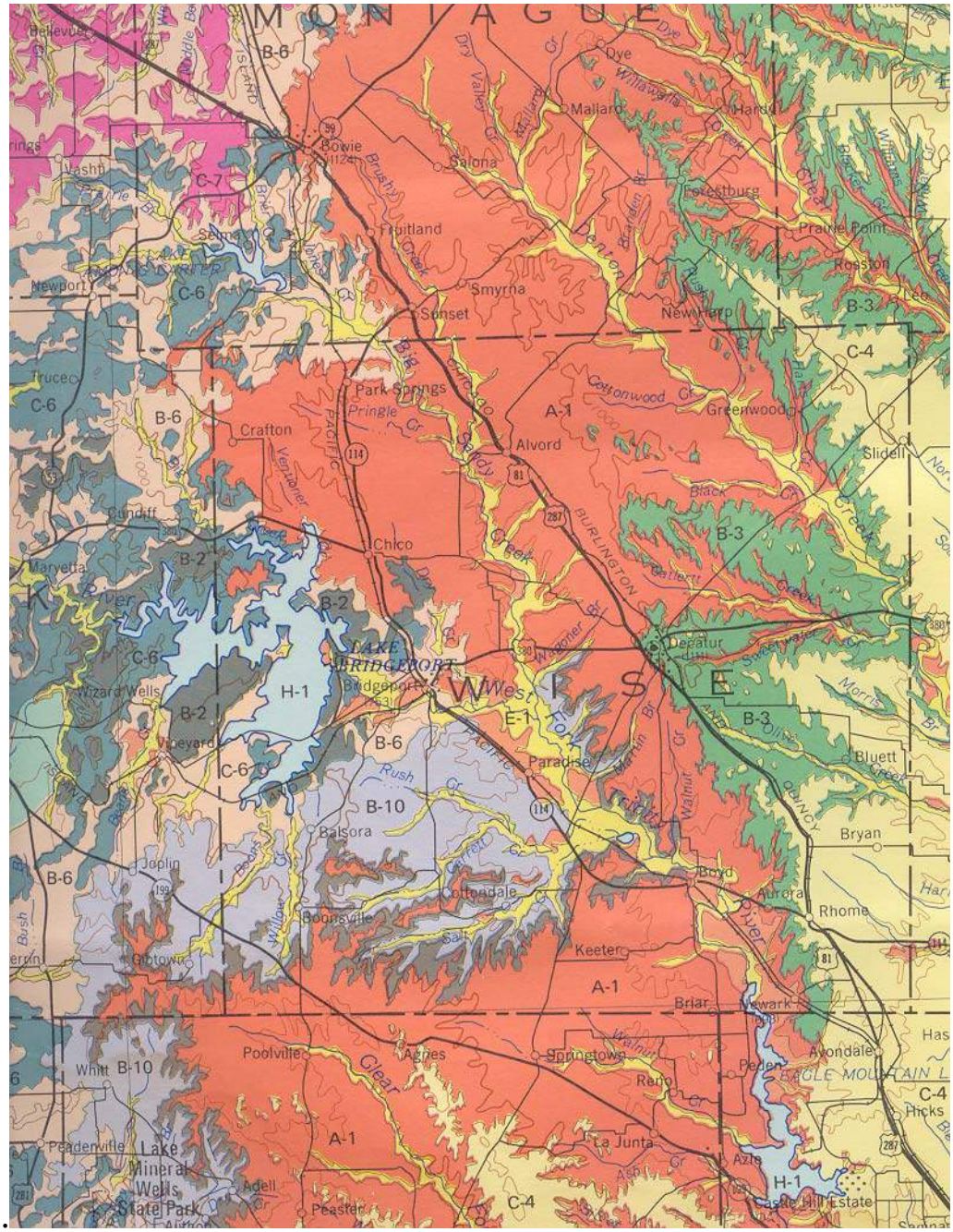

Figure 1. Land Resources Map of the Eagle Mountain Watershed. (From Kier et. al. (1977)

Table 1. Description of Land Resources Units in Basin (After Kier and others, 1977).

Map Unit	Substrate	Soils	Slope Stability	Plasticity
B-2	Limestone	Thin stony soils	High	Low
B-3	Soft Limestone	Thick to thin expansive clays and clay loams	High	Low
B-6	Clay mud and sandstone; local lignite; local thin limestone beds	Clay and sandy loams	Moderate	Moderate
B-10	Conglomeritic sandstone, quartz and flint and silty clay mud	Thin sandy soils	High	Low
D-8	Limestone and Marl	Thin clay loams	Moderate to High	Low to Moderate
A-1	Sand	Thick fine sandy loams	Low	Moderate

In general, it can be seen that the A-1 (Paluxy/Antlers Sand) area underlies most of the Watershed. In terms of aerial extent, the B-10 unit in the south and the B-6 Unit in the north make up the substrate of the rest of the basin. The B-10 unit is comprised of the outcropping area of the Twin Mountains Formation, and the B-6 unit is comprised of the outcropping area of the Paleozoic Bowie Group.

Physiography

The majority of the basin falls within the West Cross Timbers Physiographic Province. This area is nearly level to rolling, moderately dissected uplands. Stream valleys are narrow and have steep gradients. The majority of the area is in native grass pastures, improved grass pastures, or noncommercial forest areas used for grazing. Most of the pastureland, rangeland and woodland is grazed with beef cattle. There are a few dairies in the area. A smaller percentage of the land is farmed to peanuts, grain sorghum, small grains, or forage sorghums (from Griener, 1982).

Division of large landholdings into small farms began in the 1880's. Cotton was the leading cash crop producing up to 40,000 bales in 1910. By 1920, serious erosion was occurring, much of the topsoil was gone, and gullying was rampant (Ressel, 1989). It is assumed that this trend continued until the 50's and 60's at which time the NRCS began structural erosion control practices in the basin. At the same time, the number of cropping operations declined owing to the depression in the 1930's and then poor yields and market value for crops following this period. In Wise County as of 1983, there was only 11 percent of the land devoted to crops, the majority was in range and pasture.

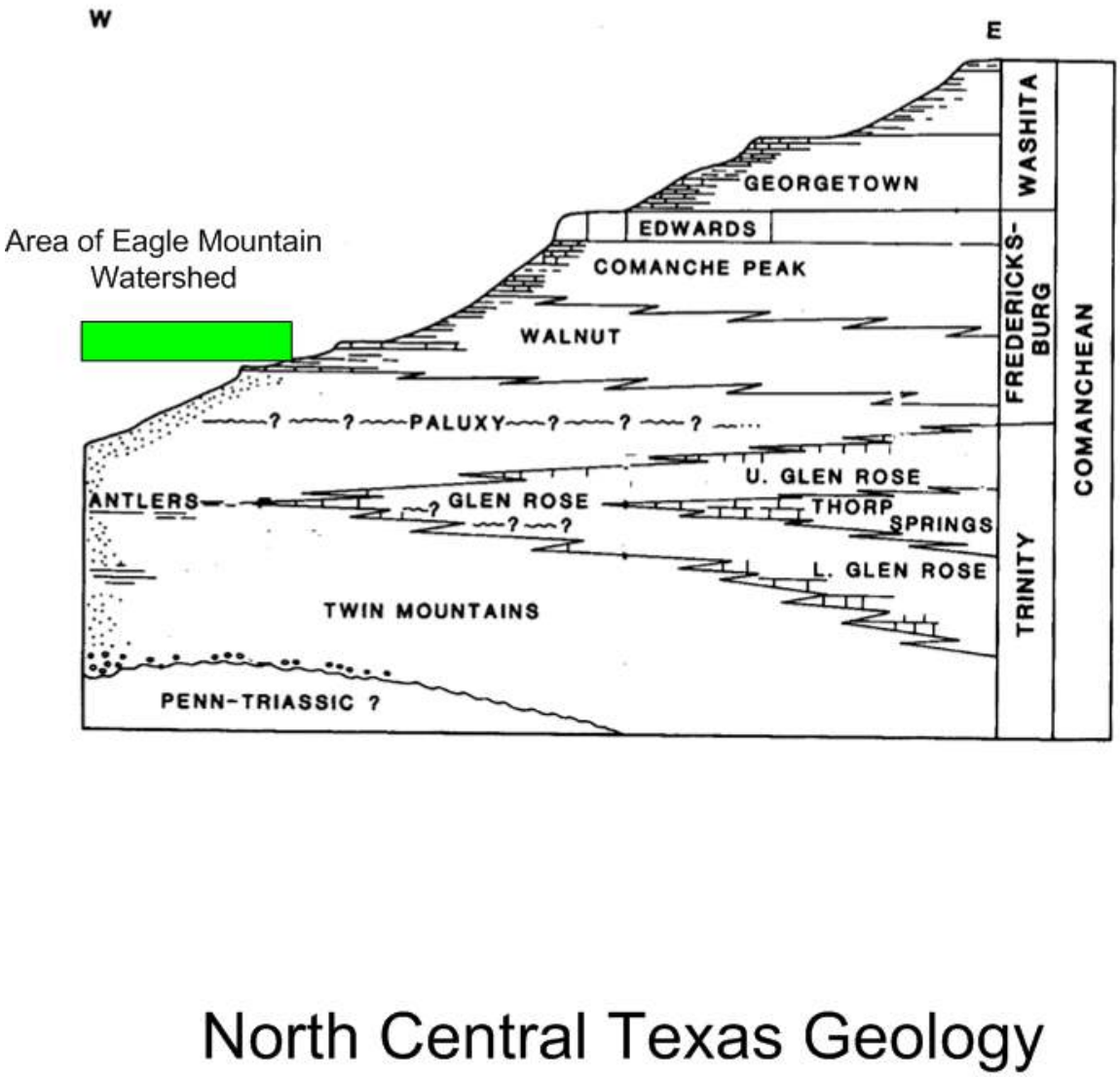

Figure 2. Diagrammatic Cross Section of Geology of Eagle Mountain Reservoir.

METHODS

Method 1.

Griener (1982) summarized sediment yield for 300 points within the State of Texas based on modeled and field observations by the NRCS. Gross gully and stream bank erosion was obtained from analyzing a national resource inventory in which 4753 primary sample units consisting of 160 acres in size were expanded to the watershed scale to arrive at estimates of annual gross erosion. A gully-stream delivery ratio was then used to compute the total erosion to the yield point from the watershed where:

$$DR = 69.49 \text{ X } 2.7128^{(.0000001644 \text{ X Acres})} \qquad (1)$$

Table 2. Sediment Erosion Results from Griener, (1982)

Cropland (ac.)	Pasture (ac.)	Range (ac.)	Urban (ac.)	Forest (ac.)	Misc. (ac.)	Total (ac.)
9991	184,045	298,990	44962	0	6206	544,194
Area Basin (ac.)	**Sheet and Rill Rate Tons/ac.**	**Gully and Streambank Rate (tons/ac)**	**Controlled (ac.)**	**Basin Sediment Yield Tons/ac. 1/**	**Ac. ft./sq. mi.1/**	**Previous Survey (1952)**
544,194	2.22	3.43	212,909	1.73	0.85	2.01

1/ Note the basin sediment yield is downstream of the reservoir and should not be confused with the sediment entering the reservoir.

According to Griener, the stream and gully erosion entering the reservoir would be 748,031 tons for the contributing area of 331,285 acres or 517.6 square miles. About 78 percent of the sediment would be from channel and gully erosion and 22 percent from the uplands. This was computed by multiplying the gross sediment yields by the sediment delivery ratios computed for the contributing drainage area of the reservoir after equations given in Griener (1982). The sediment delivery rate is 22% for sheet and rill and 66 % for channel and gully erosion. .

Method 2.

The SWAT model was run for the Eagle Mountain Watershed by the Spatial Sciences Lab at Texas A&M. The stream erosion component of the SWAT model utilizes routing reaches which are compiled by subwatershed. Field assessment of streams within the watershed was performed to assess the potential channel erosion rate of a sampling of stream reaches within the Eagle Mountain Watershed. Sampling methods were based on previous work by Windhorn (1999) and others. The lateral recession rate estimates were based on visual examination of banks in the field according to the following table.

Table 3. Field Evaluation Criteria for Channel Erosion Assessment after Wilkinson (1999) and studies in Arkansas, Colorado and Carolina.

Lateral Recession Rate (ft/yr.)	Average (ft./year)	Category	Description
0.01-0.12	.0675	Slight	Some bare bank but active erosion not readily apparent. Some rills but no vegetative overhang. No exposed tree roots.
0.2-0.8	.5	Moderate	Bank is predominantly bare with some rills and vegetative overhang. Some exposed tree roots. No slumps.
0.5-1.4	.94	Severe	Bank is bare with very noticeable vegetative overhang. Many tree roots exposed and some fallen trees. Slumping or rotational failures are present. Some changes in cultural features such as missing fence posts and realignment of roads.

At each location the channel was photographed and average site dimensions were taken with range pole and hand held laser. Accuracies are probably within a couple of feet. Two channel properties were calculated from the measurements; the width depth ratio and the entrenchment ratio. The width depth ratio is here defined as the ratio of the width of the active channel seen in the field to the depth of the active channel. This ratio is important in understanding the energy within the channel and the ability of the discharge frequency to move sediment. The mean width depth ratio was 5.9 and the range was from 2.6 to 14.

The entrenchment ratio is the ratio of the width at the active channel depth to the width at 2X the active channel depth. With a mean side slope of 65 degrees, this computed to a mean value of 1.27 (std. dev. .134) and a range of 1.07 to 1.66. According to Rosgen, a channel is by definition entrenched when the ratio is below 1.4. From 1.4 to 2.2 a stream is classified as moderately entrenched and above 2.2; slightly entrenched. All channel surveyed were entrenched. An entrenched stream will contain larger floods and thus be more prone to frequent channel erosion.

Based on the field evaluation forms Figure 4, and limited air photographic analysis, channel segments were classified by degree of erosion. These are found in the Excel spreadsheet in the Appendix. Actual erosion heights evident in the field are shown in Figure 3. The lower trend line indicates a rather nice increase in the height of bank erosion in the streams with increasing basin area. The average height of erosion was 1 meter. It can also be seen that the small drainage areas have a lot more variability. This is due to the more pronounced response small basins have to changing land use and climate; large basins are more buffered.

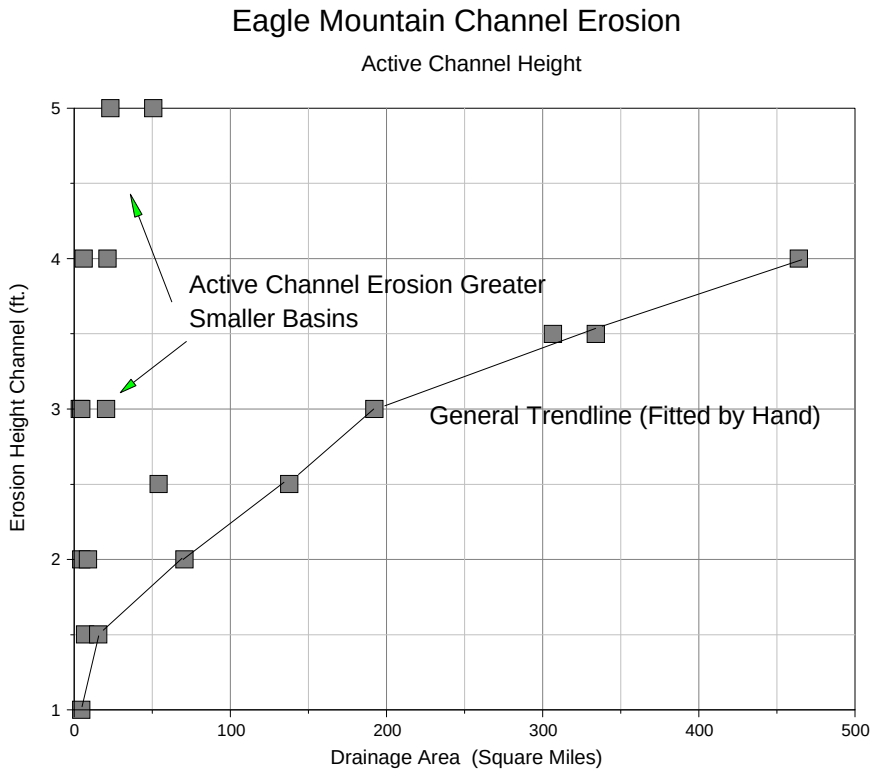

Figure 3. Field evaluation of channel bank erosion height and drainage area in Eagle Mountain Watershed.

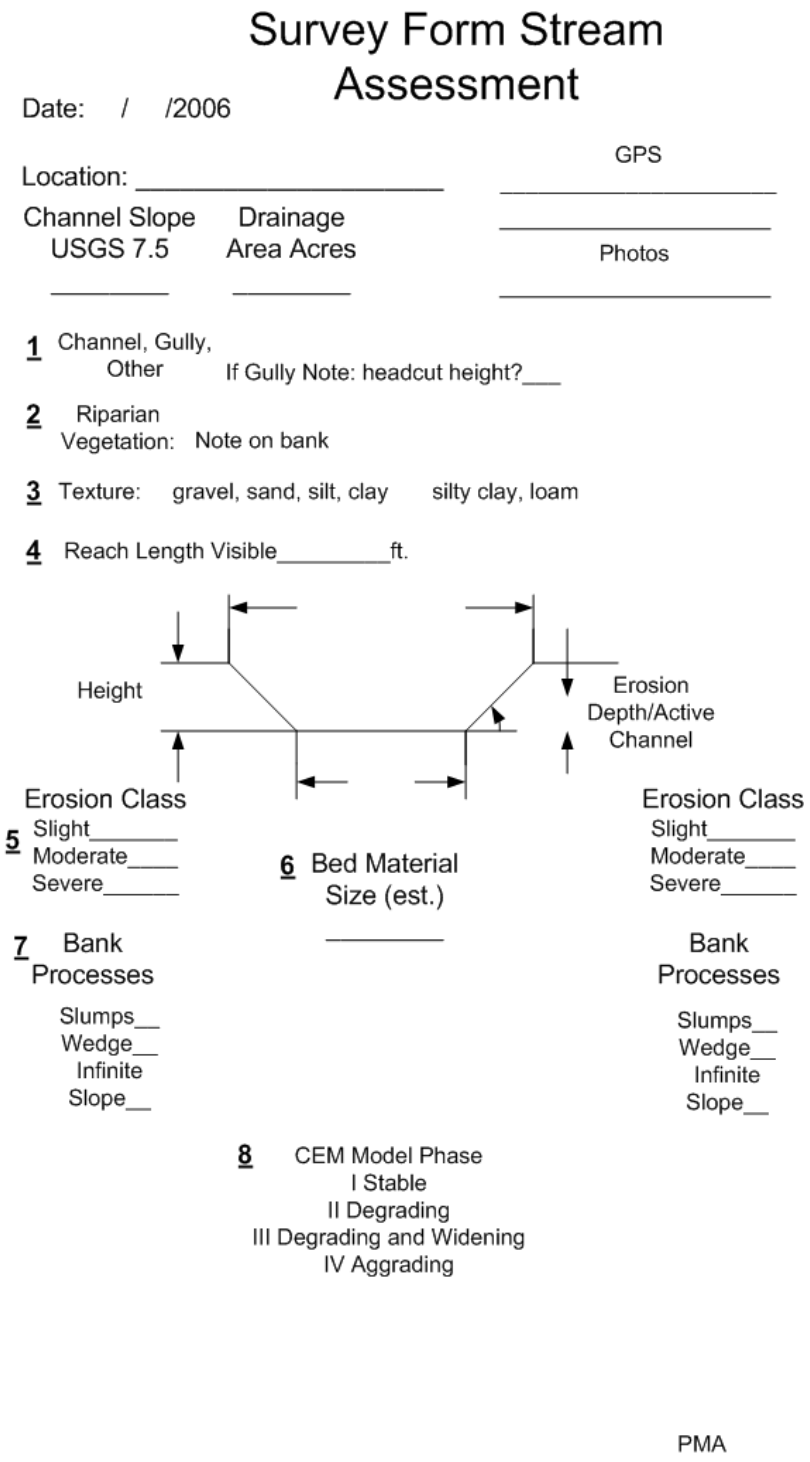

Figure 4. Channel Survey Form

Rates of erosion were used with the channel lengths from the SWAT model to assess overall erosion using the following equation. It is assumed, for purposes of this analysis that the channel lengths are adjusted for upstream reservoirs.

Tons/yr. = {Length x Eroding Height x Erosion Rate x Density x Vegetation } x Routing Factor (2)

For silts and sands (as was found in the majority of the sites) the mean bulk density measured from field samples was 86 pcf or .043 tons per cubic foot conversion. The vegetation factor is based on previous work by Julian and Torres (2005) and given below.

Table 4. Vegetation reduction factor for channel erosion adapted from Julian and Torres (2005).

Vegetation	Class	Reduction Factor
Bare	I	1.0
Grassy	II	.508
Sparse Trees	III	.185
Dense Trees	IV	.05

The routing factor is the sediment delivery ratio used by Griener (1982) for gully and channel erosion equation (1).

This calculation, when summed over the basin yielded 115,124 tons/year assuming no channel vegetation in the active channel depth of 1 meter..

Method 3.

An Australian method was utilized based on the stream power approach in which bank erosion is assessed as:

$$BE = .0001\ pg\ Q\ S\ (V\ F) \qquad (3)$$

Where: pg = the density of water and acceleration of gravity

Q = discharge in cms for the 1.58 year flood (used 2 year flood)

S = slope of the water surface (taken as the channel bottom slope)

VF = channel vegetation coefficient (Table 4).

BE= bank erosion rate in m/year

To calculate the total loss, equation (3) is used substituting the routing areas and slopes from the SWAT model . The erosion rate is multiplied times the channel length for each reach from the SWAT model as in Method 2.With the SEDNET method, the average value obtained was 148,255 tons/year. This estimate again uses no vegetation factor in the 1 meter of active channel erosion modeled.

Method 4.

The fourth method utilized used the percentage channel erosion rates established by Griener (1982) for Eagle Mountain Watershed and multiplied this number by the sediment yield established by Simon et. al. (2002) for the South Central Plains Ecoregion.

Table 5. Channel and gully erosion for the Eagle Mountain Reservoir.

Basin Area (sq. km)	25%	50%	75%	Percent Channel	Tons/year
1340.7	.48	1.23	3.17	.78	150,236
1340.7	.48	1.23	3.17	.78	384,979
1340.7	.48	1.23	3.17	.78	992,183

The percentiles are from Simon et. al. (2002) and are in units of tons/day/sq. km.

Gully Erosion Estimate

Since gully erosion was shown to be a significant process in the watershed based on Ressel (1989) and field evidence, gully erosion was modeled using methods developed in SEDNET (2002) where:

$$GC = ((1000\ A\ P\ R)/T) * G\ D$$

GC= tons per year

A = area of the internal catchment in km^2

P = soil density in $tons/m^3$

R = mean cross sectional area of a gully in m^2

T = time of gully contribution (100 years)

GD = gully density in km/km^2

Air photo assessment was made to determine gullying in the basin using a 1973 NRCS photo base to be consistent across the basin, (Figure 5). It was found that the majority of gullies observable from the photographs were within one mapped soil series or the Duffau Gullied Land Complex 3-8% slopes. This is a fine sandy loam with 44-56% silt and clay, and a K factor of 0.49. The area attributed to this soil for this calculation was 11,600 acres or approximately 47 sq. km. The soil

density was taken as 1.5 tons per sq. meter and an average cross sectional area of 18.5 sq. meters. The time used in assessing the yield was from the time of early cropping in the area or 100 years. This computed to a value of 166,731 tons per year.

Gully Contribution to Sediment Yeild

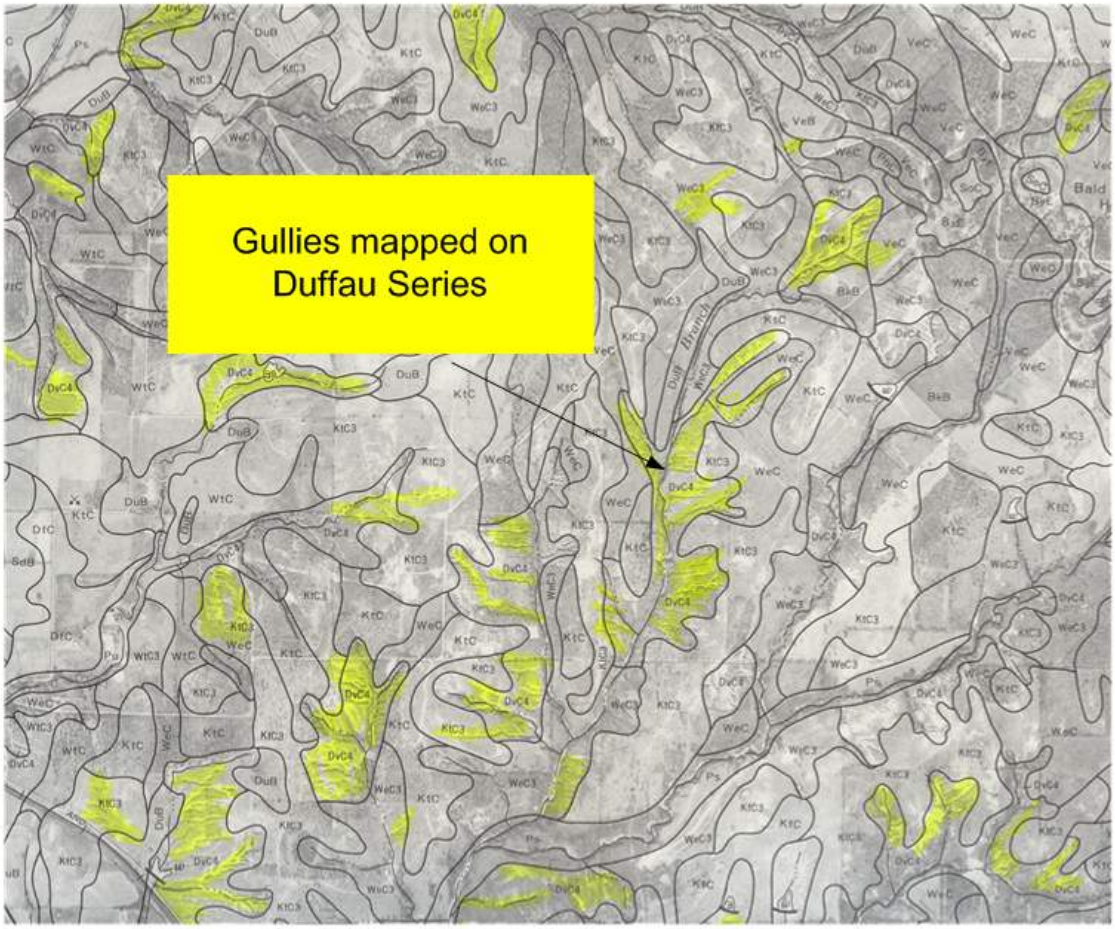

NRCS (1989)

$$\text{Gully Tons/Year} = \frac{1000 * km^2 * tons/m^3 * m^2}{Years} \quad \text{Gully Density } (km/km^2)$$

Figure 5. Example of observed gully erosion and SEDNET equation for computation of annual gully yield in tons per year.

Analysis of Bed Material Transport

In an effort to assess the sand contribution to the reservoir on an annual basis, a simple set of calculations was made in which the flow duration curve was combined with an average bed material transport rate. The result of this calculation is the average daily bed material transport in tons per day.

A combination of three equations were used for evaluate bedload transport; Bagnold, Colby, and Molinas and Wu, (Yang, 1996). The flow duration curve was established for the USGS Gage at Boyd (08044500). The results indicate sand transport at this site would be on the order of 545 tons per day or an annual yield of 200,000 tons of sand.

Assumptions

- Alluvial Soil Pulexas is 70 percent silt/clay and 30 percent sand
- Average transport per year 60,000 tons sand at Boyd gage on Trinity based on Bagnold, Colby and Molinas transport functions
- Assume transport limited (eg. sand supply is not a limiting factor)

Therefore:

Assuming a mass balance from the eroded soil, calculating movement of the sand fraction at 60,000 tons (1,395,349 cubic feet) requires that the silt clay fraction would be 140,000 tons or 3,255,814 cubic feet to equal the ratios in the original soil.

This combined amount is 200,000 **tons per year** of channel erosion based on transport assumptions. This would be equal to a lateral channel erosion rate of 0.4 ft per year from one 3 foot high active channel area or in the slight to moderate range.

Literature Review Rates

River bank erosion occurs through a combination of mass failure, fluvial entrainment, and sub aerial weathering and weakening and thus is a complex process. Literature review of channel erosion rates is somewhat limited as monitoring bank and bed erosion is time consuming and is typically done on small reaches and thus applicability to other geographic areas with different climates, soils, bed material, and vegetation or discharge regimes is always suspect. Such literature still is important in that it shows the range of erosion actually measured in the field and is shown below.

Table 6. Example of measured erosion rates in stream channels.

Stream Channel	Method and Material	Results
Laubel et. al. 1999 (113.5 sq. km basin in Denmark)	Erosion pins in clayey till and glacio-fluvial deposits	Lower bank 11 mm year or 0.02 cubic meters per meter
Allen and others 2005 (Texas Blackland; Ash Creek)	Erosion pins in clay alluvium; one month	18 mm average; 0.24 cubic meters per meter channel; approximately 0.11 tons per foot channel;
Phillips and others 2005 (42-46,000 sq. km. in Texas, Trinity River)	Historic air photographs; silt sand to clay	30.2 ha over 52 km or 17.4 tons per foot ; 87.6% of annual sediment load; lateral erosion dominant
Wolman 1959 (10 sq. km. catchment Maryland)	Resurvey and pins; sand silt	450-600 mm year (525)
Prosser and others 2000 (46 sq. km. basin Australia)	Erosion pins and pin surveys in clay	13 $\pm$ 2 mm year or .037 cubic meters per meter
Hooke 1980; worldwide averages; Martin (2005)		Bank m/yr = 0.0245 $DA^{0.45}$; m/yr = .0475$DA^{.4}$
Wohl 1999 (literature); variable sizes	Surveys in sedimentary rock	2-38 mm (20)
Booth and Henshaw (2000) Washington State; 0.1-20 sq. km.	Sand to clay	Less 20 mm to 1 meter year (510) Wide variation, vegetative influences.
Zaimes, et. al. 2005; Iowa 1-3rd order streams	Assumed loam	Severe erosion pasture 143-95 lbs/ft.; pasture no cattle stream and forest; 4.2 to 2.74 lbs/ft.
Couper and Maddock, 2001: cohesive channel; 389 sq. km.	Erosion pins	13-181mm/year

The average rate from the literature is **183 mm (7 inches) per year**. This includes a mean rate for Maryland and for urban streams in Washington State. Two simple equations for worldwide lateral channel erosion give rates ranging from 550mm to 700mm per year (22-28 inches/yr.). From field evidence, these rates seem excessive. A rate using only the sub aerial clay erosion rates is about **17 mm (0.6 inches) per year or per flood** minimum. This is for surficial erosion and does not include bank failure. This rate is for bare clay soil.

The calculated average rate for bank erosion in this study was about 122 mm (4.8 inches or .4 feet) per year per foot of channel. Therefore, based on the literature and specifically studies in silt and sand material by Zaimes, et. al. (2005) and Wolman (1959), this annual loss rate seems reasonable.

Summary of Channel Erosion Calculations

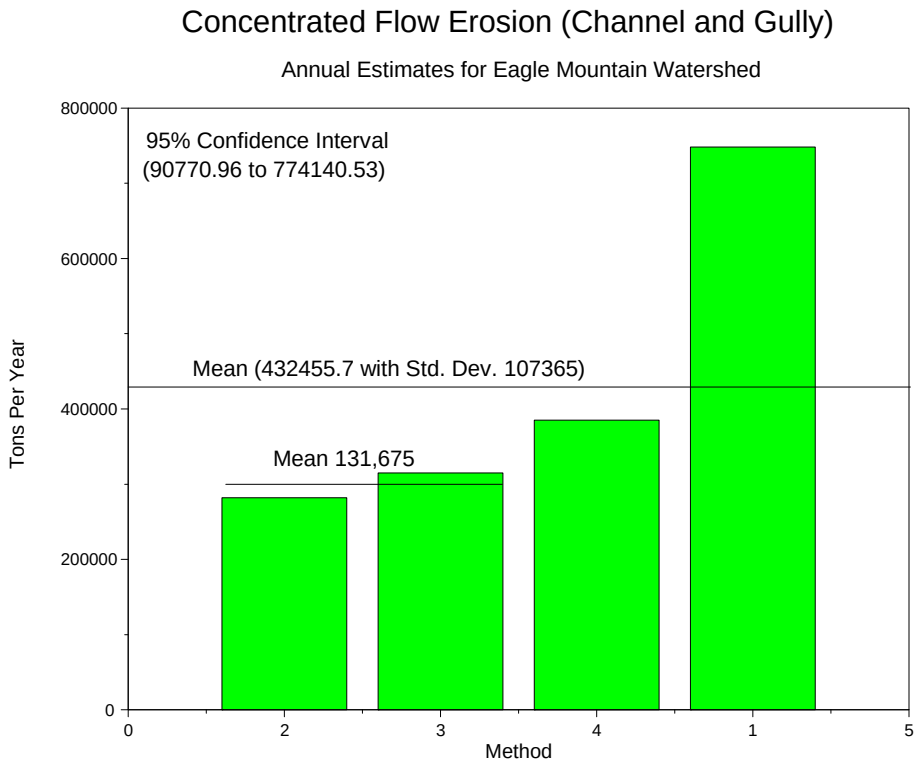

Table 7. Channel and gully erosion summary.

Method	Modeled Channel & Gully Erosion (tons/year)
Method 1.	748,031 (adjusted for upstream reservoirs)
Method 2.	115,124 channel + 166,732 gully = 281,856
Method 3.	148,225 + 166,732 gully = 314,957
Method 4.	384,979 (50 percentile)
Mean (Methods 1-4)	**432,455.7 (without Griener 327,264; lowest two methods 131,675)**

The high number from the Griener report is based on land use and work up until the early 1970's. It is believed that this rate is not active today but probably represents an acceptable upper limit to the channel and gully erosion which occurred in the basin under past land use and conservation practices. Today, based on field surveys of channels, it is thought that methods 2 and 3 are probably more representative of rates. The inferred gully erosion rate is based on long term trends and as a mean long term value, overestimates today's rates and underestimates past rates.

Discussion

If the following is assumed based on the reservoir surveys:

- 427.33 Ac. ft./year
- 98 lbs per foot lake delta

- 26 lbs per foot lake pro delta
- 80 percent lake pro delta silts and clays
- 20 percent lake delta sands
- 86 lbs per foot average watershed density
- weighted average 40.4 lbs per foot
- channel and gully 78 percent total and sheet and rill 22 percent total (Greiner,1982)

Ratio soil in watershed/soil in reservoir = 2.13

So: 427.3/2.13 = 200.6 ac. feet

Therefore 200.6 ac. feet year from watershed @ 86 lbs cubic foot =

375,759.2 tons/year

Gully and Stream Erosion = **293,092.17 tons/year (78%)**

Sheet and Rill = **82,667.03 tons/year (22%)**

If we subtract the amount of calculated gully erosion (166,731 tons/year) from 293,092.17, this leaves 126,361 tons per year of channel erosion. The average channel erosion from method 2 and 3 is 131,675 tons/year which within 5% of the average of methods 1 and 2. Using the above defined rates, this infers a ratio of 44% gully, 34% channel and 22% sheet and rill. It would be expected that this ratio would change based on land use and conservation measures as well as climate.

Historic Aerial Photographs

Historical photographs of processes were not accurate enough in scale to indicate channel migration rates. In general, older photographs are only accurate to about plus or minus 5 meters when rectified and therefore, it is difficult to establish rates without a lot more work and larger photographs (special order). However, inferences obtained from the time series photographs are valuable. In general, the trends across the watershed appear to confirm that from the time the reservoir was built and began filling, the watershed was probably near peak erosion rates with the majority of sediment coming from gullied terrain. As in much of the State, the Soil Conservation Service, (NRCS), began massive soil erosion management throughout the late 1950's. Although crude, the reservoir flux seems to reflect the positive impact of management within the watershed. Figures 6 and 7 illustrate the gully activity and figure 8 is the most illustrative of the temporal channel photographs.

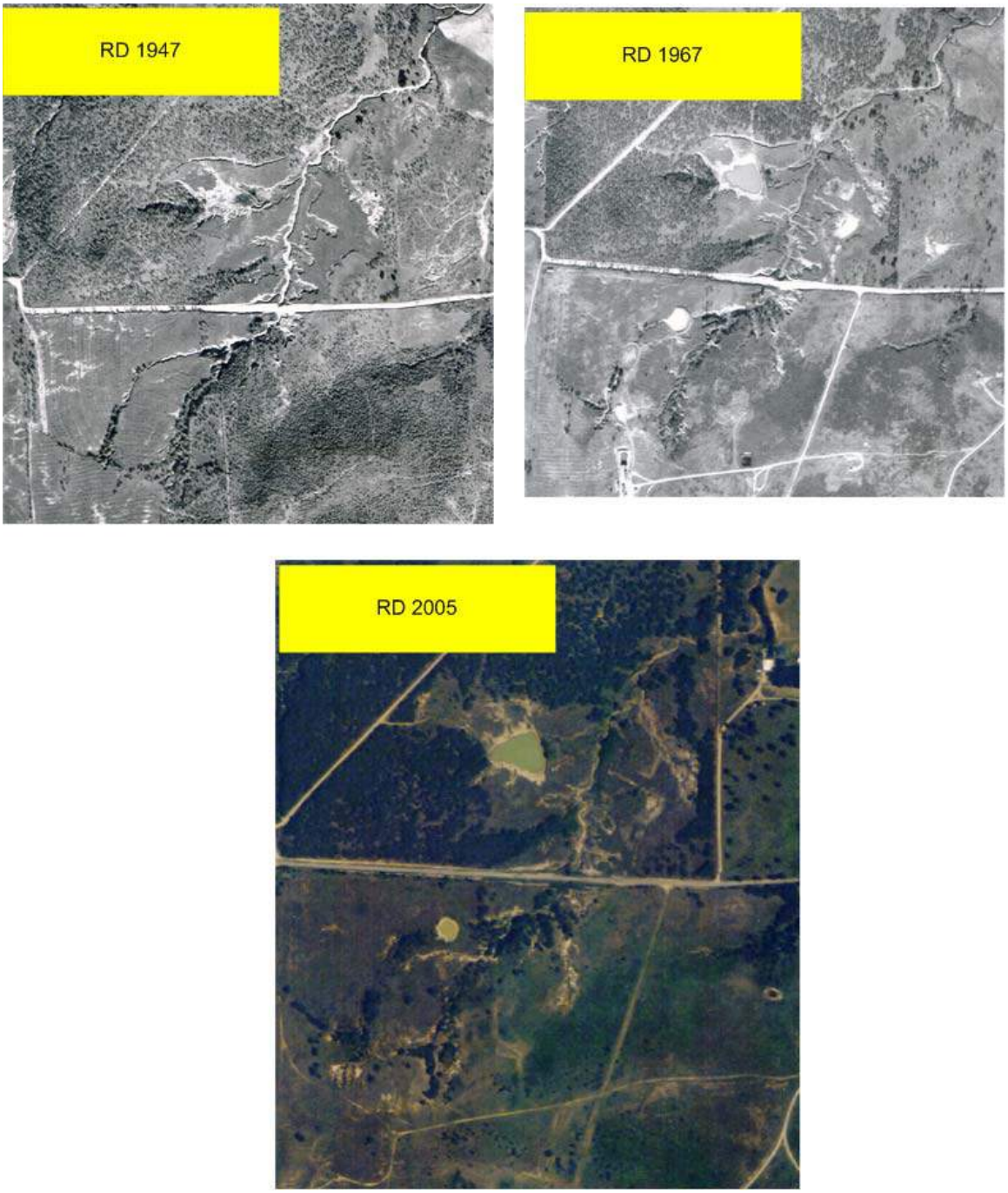

Figure 6. Historical air photographs illustrate the active gully system in the Duffau series soils were active in 1947 and through 1967.
Gully activity has lessened in recent times to changes in land use practices and conservation methods.

Gully Erosion
RD Location

Figure 7. The same gully system (in Figure 6) as seen from the field survey. The gully is temporarily stabilized. Note new floodplain.

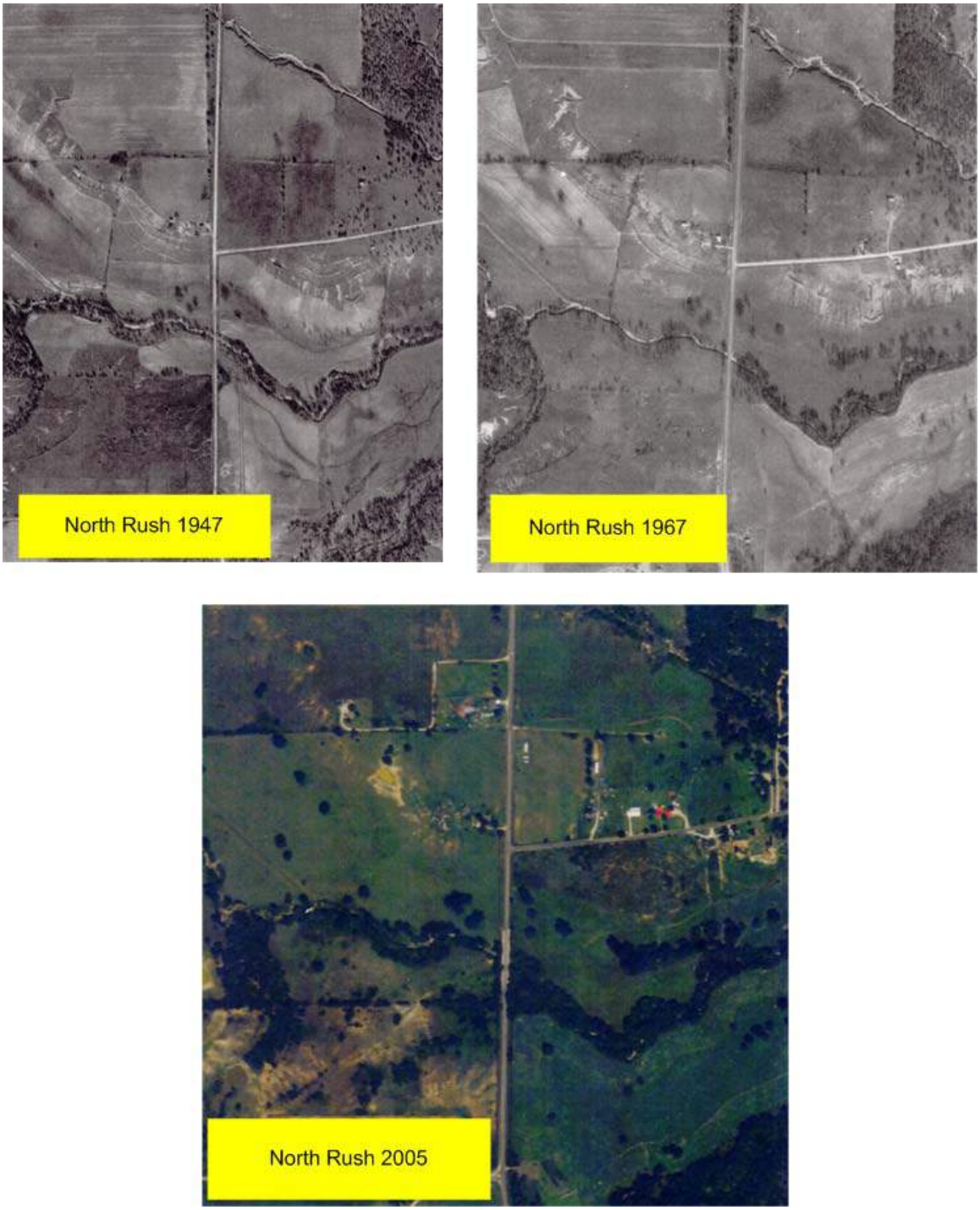

Figure 8. Illustrates similar trends in processes of advanced channel and gully erosion through the 60's and lessened erosion due to land use and management under current conditions.

Conclusions

1. Current estimates indicate an average annual sediment yield of about 200.6 ac. feet from the watershed to the reservoir. Analysis of reservoir flux over time (Dunbar and Allen Part II) indicates that this rate may have reached twice this amount or approximately 845 ac feet per year from the watershed or 4.2 times this amount during the 40's. This would be roughly the same order of magnitude that the Griener estimate is above the average of methods 1 and 2. Therefore, for current rates of channel erosion the average of methods 1 and 2 appear reasonable; for maximum rates, the Griener number would appear to be a good estimate.

2. Average annual rates indicate a ratio of 44 percent gully, 34 percent channel and 22 percent sheet and rill erosion. This is based on an average gully loss rate that would have reached a maximum during the 40's and diminished from the 1960's to present.

3. Average annual sand transport at the lower Boyd gage on the Trinity River is estimated to be 60,000 tons a year. Most of this material ends up in the delta area of the reservoir.

4. Material from sheet and rill erosion and the silt clay fraction from gully and channel erosion are carried into the lake as pro-delta deposits. This is of course the amount remaining in suspension after subtracting over bank deposition which is computed as part of the sediment delivery ratios.

4. Annual flux of gully and channel erosion to the reservoir cannot be computed with current methods. Modeling and monitoring of these rates is advocated for future assessment of BMP's

5. The large standard deviation in rates is due in part to the added complexity of routing and eroding cohesive (clay) and non-cohesive (silts and sand) sediments and the accuracy of current empirical models. Better assessment of the actual aerial extent of the higher density delta deposits to the less dense pro delta deposits would improve these estimates.

6. Air photographic analysis infers that the highest yields were in the 30's to 60's and rates have diminished since this time owing to changes in land use and conservation practices within the basin. This is supported by sediment resurveys.

Future Considerations/Concentrated Flow Erosion

In the case of all surveys and modeling efforts, better results can be obtained with better data inputs. With regard to the Eagle Mountain Reservoir, the following suggestions are made in an effort to better calibrate the modeling efforts and make assessment of future management and land use scenarios more precise.

1. **Channel Erosion Assessment**: It is recommended that erosion pins and scour chains or monitoring sites be installed on major stream channels. A statistical sampling of stream erosion based on field data by soil/geology could give a far better assessment of erosion loss rates. In addition, within these areas, it is recommended that submerged jet test be done to assess Tc and K values by alluvial soil type so that the results can be directly put into the model and calibrated. It is estimated that only about 6 such tests would be needed in order to quantify these initial values. The erosion pins and scour gages can be quickly installed, left for a period of a year, and then resurveyed. Data loggers which record water levels can also be installed easily and can be downloaded once every 6 months and used to enhance routing as well as verify time series tractive force. New loggers are cheap ($500.00) and easy to install (and hide) owing to their small size. Battery life is also

enhanced (up to several years). Gully erosion could be quantified by surveying small impoundments (Figure 9.)

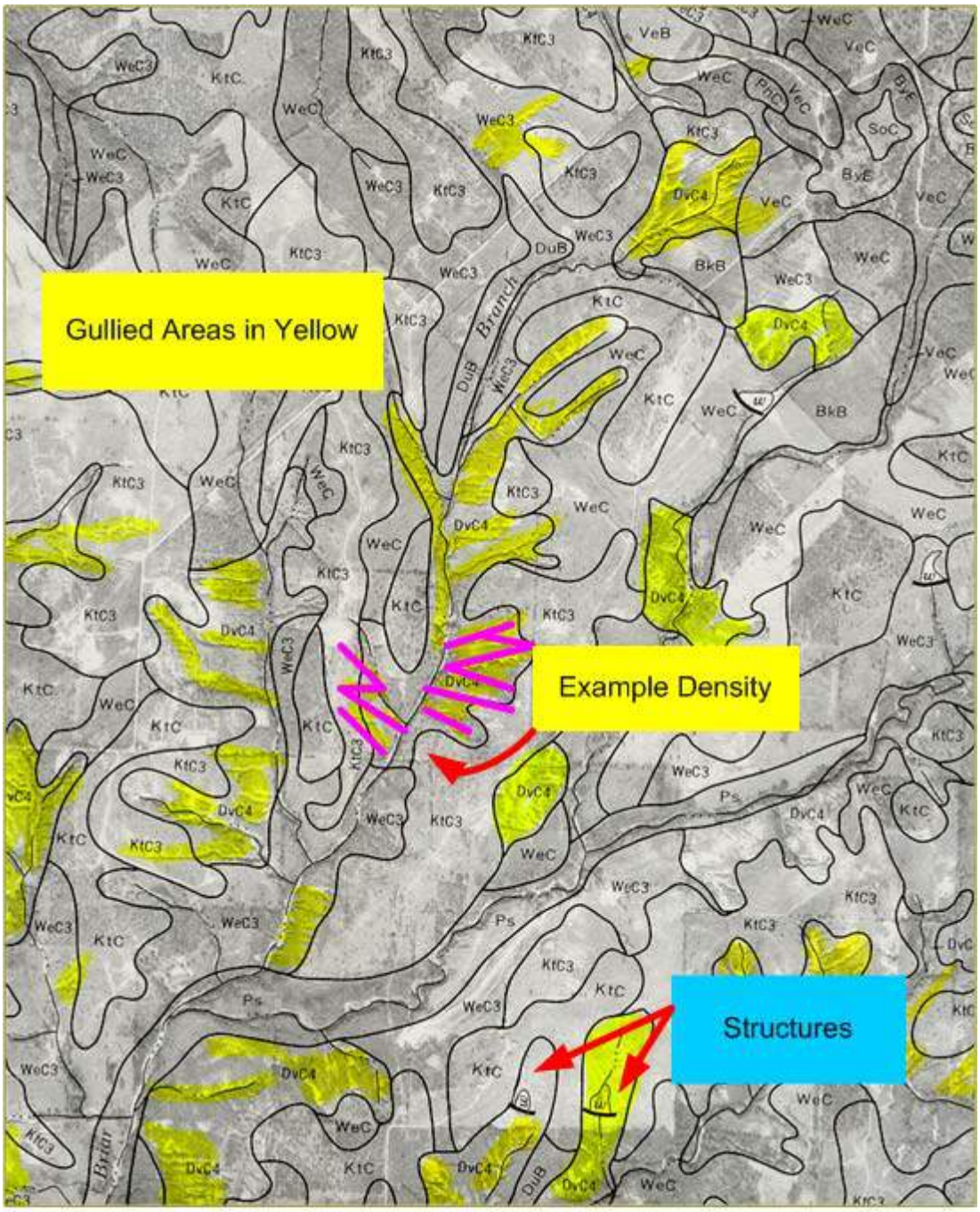

Figure 9. Survey of structures downstream from active gullies in the watershed would provide an estimate of erosion rates.

2. **Land Use Change**: It appears as if the Eagle Mountain watershed area has progressed from intensive agriculture to more recent pasture and rangeland. Land use and climate changes will affect stream and gully erosion. While the SWAT model can assess the sheet and rill and ephemeral gully erosion (MULSE), more information is needed on rates of channel and gully erosion. Work is currently being done on the SWAT model to enhance these capabilities in terms of predicting change. What is needed is verifiable data to calibrate the model so that inferences regarding management practices in this domain are reasonable for judging viable economic alternatives.
3. **Long Term Basin Erosion/Floodwater Surveys**: Surveys of floodwater structures in the upper basin can also give better estimates of sheet/rill and ephemeral gully erosion for model calibration. This can be done quickly and with high precision. These should be chosen by soils/geologic province, age of structure, and land use changes within the sub-watershed.
4. **Short Term Sediment Transport Monitoring/Turbidity Sensors**: Installation of turbidity sensors on major tributary inputs to the lake with some preliminary calibration could give excellent data for future model calibration and assessment of watershed trends. These systems are now quite reasonable and require, after calibration, minimal field time to download or can be attached to cellular phones or hard-lined to the office.

RECONNAISSANCE SEDIMENT SURVEY: PART ii

Historically**,** three different methods have been used to estimate reservoir sedimentation rates from acoustic surveys. The oldest method is the range line method, which involves carefully repeating water depth measurements along selected cross-sections after 5 or 10 years. Because of the great expense of doing this work, the cross-sections were spaced several thousand feet apart along the long axis of the reservoir. The sedimentation rate was determined from the average change in cross-sectional area along the range lines. This produced reasonably good estimates of the change in volume, but not particularly good estimates of the total volume. When GPS navigation became available, it became standard practice to collect many profiles spaced a few hundred feet apart, to better constrain the total volume. Because no profiles are precisely repeated in these modern surveys, sedimentation rates are determined from the difference in total volume. The change in volume between surveys is usually a small faction of the total volume. Hence, the accuracy of sedimentation rates determined from the apparent change in total volume given by the modern surveys is probably no better or perhaps worse than that of the old range line method.

To solve this problem we proposed the sub-bottom profiling method for directly measuring the sediment volume (Dunbar et al., 1994; 1999). In this approach, the sediment thickness is mapped directly by using low-frequency acoustic profiling instruments that image both the water bottom and base of sediment, determining the sediment volume in one survey. In the past ten years, we have used this method to survey 4 large water supply reservoirs and 23 small PL-566 flood control reservoirs. The method produces accurate estimates of the total sediment volume, the current percent of sediment fill, and the average sedimentation rate over the life of the reservoir. It does not provide information about how sedimentation rates change over time or the modern sedimentation rate.

On July 18 and 19, 2006 we conducted a reconnaissance sub-bottom acoustic profiling and coring survey of Eagle Mountain Lake. The goals of this survey were to determine (1) the extent to

which the thickness of post-impoundment sediment fill can be mapped by sub-bottom profiling, (2) the profile spacing needed to achieve a given accuracy in future surveys, and (3) an estimate of the dry bulk density of the post-impoundment sediment.

Historical Survey Data

Since its impoundment in 1928, Eagle Mountain Lake has been surveyed 7 times (Table 8). In most cases the exact methods used in these surveys are not known, but it is safe to assume that different methods were used throughout. Manual methods were likely used to measure water depth along sparse range lines in the earliest surveys. The 1960 survey was probably done with an acoustic fathometer and optical positioning methods. The more modern surveys were done with acoustic fathometers and electronic positioning. The profile spacing used in these surveys probably varied from thousands of feet in the earliest surveys to 500 ft in the 2000 Texas Water Development Board (TWDB) survey. There is an unknown level of error in each of these surveys.

These uncertainties aside, the overall pattern of survey results shows a trend of decreasing volume over time at an average rate 468.8 acre-ft/yr (Figure 10). The pattern indicates an initial period of rapid sedimentation from 1928 to 1952 (1,270 acre-ft/yr), followed by a much lower rate between 1960 and 2000 (24.2 acre-ft/yr) (Figure 11). These combine to produce an apparent long-term average sedimentation rate of 427.3 acre-ft/yr, which is not representative of either modern or past depositional rates. The apparent large change in sedimentation rate over the life of the reservoir indicated by historic surveys is consistent with the history of land use changes in the watershed described in Part 1 of this report and is likely real. However, repeat surveys between 1952 and 2000 show both negative and positive changes in volume with time. This suggests that the average apparent rate since 1960 of 24.2 acre-ft is probably not significant relative to the errors in the survey. What ever it is, the modern sedimentation rate is likely to be small relative to pre-1960s rates, but the accuracy of the surveys is not sufficient to say with certainty that it is larger than zero.

Table 8. Survey information of reservoir volume with time. (1/ From Ernst 2006).

Source	Date	Volume (Ac.Ft.)
Original Survey 1/	1928	212,500
TWDB Report 126 1/	1934	190,000
USDA Rept. 1143	1939	205,175
USDA Rept. 1143	1952	182,000
Texas Board Water Eng. 1/	1960	182,700
Rutledge and Others 1/	1968	189,522
Rutledge and Others 1/	1988	177,520
TWDB Survey 1/	2000	181,732

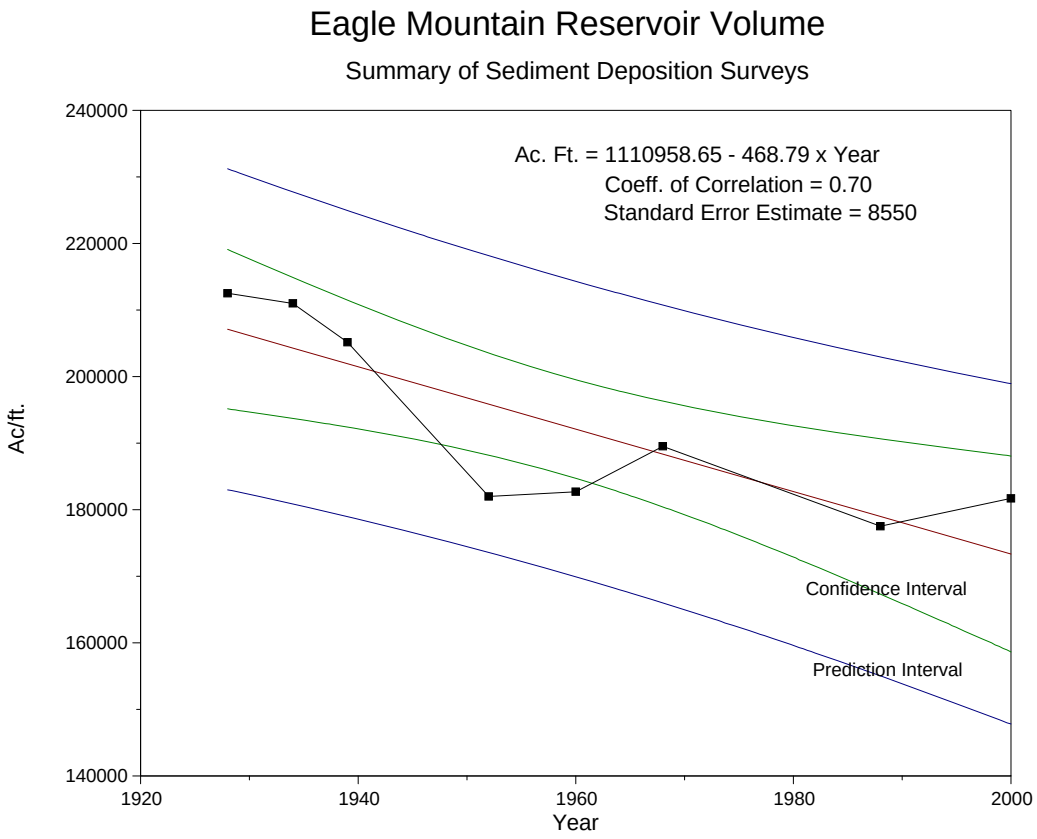

Figure 10. Apparent water storage capacity of Eagle Mountain reservoir versus time from historic bathymetric surveys.

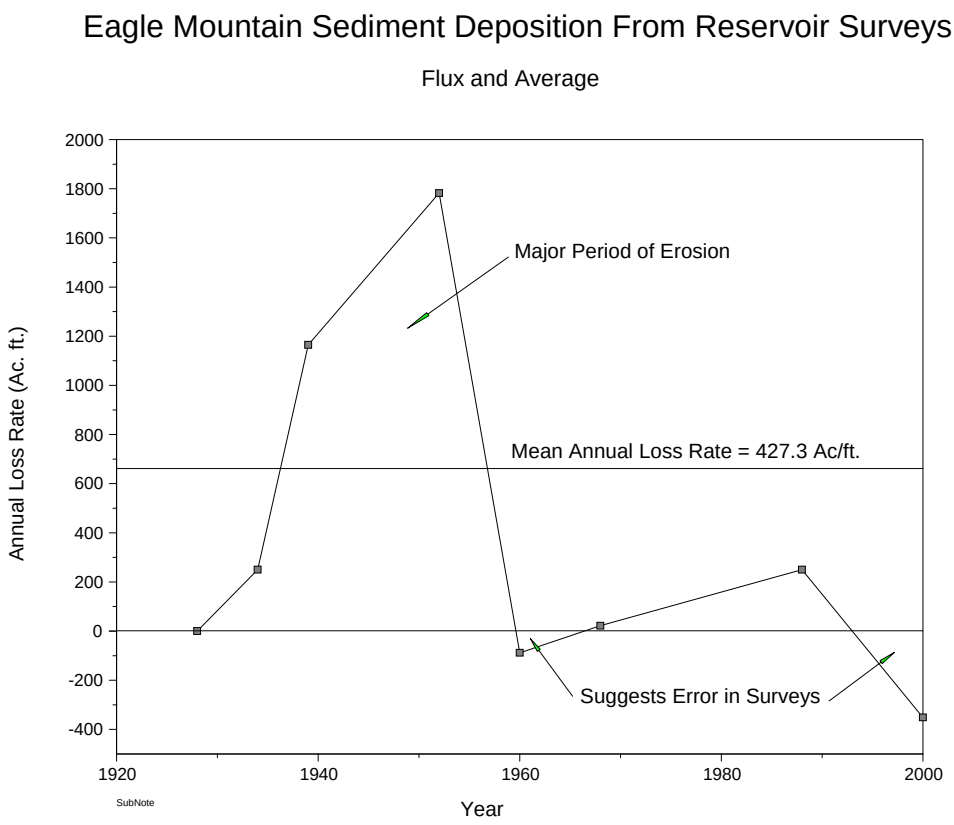

Figure 11. General Flux in Reservoir Volume computed from Table 8.
The high flux at the beginning of reservoir filling is attributed to land use practices and erosion of reservoir banks; differences in survey methodologies and accuracy is thought to be responsible for the apparent more recent flux.

Reconnaissance survey of Eagle Mountain Lake

Acoustic profiling methods

To test the applicability of the sub-bottom profiling method to Eagle Mountain Lake, we collected acoustic data using a four-frequency acoustic profiler rented from Specialty Devices Inc., of Wylie, Texas (SDI). This particular profiler collects acoustic records using 200, 50, 25, and 3.5 kilohertz transducers. Other frequency combinations are available. The recordings at each frequency are made in a rapid, round-robin sequence, which in effect, samples the same profile at the four frequencies simultaneously. During post processing, the same profile can be viewed at each frequency separately, and the best frequency can be selected to pick the water bottom and base of sediment at each point in the reservoir.

During the two-day reconnaissance survey, we collected a total 63.8 km of profile data. These data consisted of a profile along the axis of the reservoir, several shorter axial lines to either side of the long profile and several profiles perpendicular to the axis of the reservoir. The northern

limit of the long axial profile was determined by the northern-most point we could reach before running aground in the survey boat. We used this profile (marked in red in Figure 12) to determined profile spacing requirements for future surveys. The shorter profiles were used to sample the local range of sediment thicknesses in order to optimally site core locations.

Acoustic Data Analysis

In post survey processing of the acoustic data, we identified the base of sediment fill on the acoustic profiles, using the sediment cores that reached the pre-impoundment surface as a guide. Then the water bottom and base of sediment were manually traced along each profile to access the range of sediment thickness and the extent to which the base of sediment could be mapped. For the purpose of estimating the error in future surveys versus profile spacing, the water depth and sediment thickness along the axial profile were exported for use in a custom analysis program.

We estimate the potential error in reservoir surveys versus profile spacing by comparing the cross-sectional areas of water and sediment along an axial profile at different sub-sample intervals. The concept is that each point on an axial profile represents a possible sample point along a regular survey profile collected perpendicular to the reservoir axis. Therefore, the axial profile is a sample of the variability of water depth and sediment thickness between the profiles of any future survey. To the extent to which the water depth and sediment thickness vary linearly between survey profiles, the survey will accurately reflect the true volumes of water and sediment. To the extent that water depth and sediment thickness deviate from linear trends between profiles, the survey will be in error.

To estimate the potential spatial sampling error associated with a given profile spacing, we first compute the cross-section area of the water and sediment along the axial profile at full resolution. Because the sample points are spaced only 1 m or less apart on the recorded profile, we assume that the resulting areas represent the true cross-sectional areas. We then sub-sample the profile at the specified larger sample interval, by interpolating between measured points. The result is a cruder version of the full-resolution cross-section. We then compute the cross-sectional area of the sub-sampled section and the percent difference between the sub-sampled and full-resolution areas. For a given sub-sample interval, the percent error changes somewhat as the set of sample points are shifted back-and-forth along the profile, depending on how well they happen to align with the peaks and troughs in the profile. To quantify this variation, we systematically sweep through the full range of possible shifts and compute the standard deviation in the percent error. To estimate the spatial sampling error for a continuous range of potential profile spacings, we have the program sweep through a series of potential spacings and report the results in graphical form.

Vibracoring methods

As part of the reconnaissance survey we also collected 6, continuous sediment cores to verify acoustically determined sediment thicknesses and to determine the dry bulk density of the sediments. Cores, 3 inches in diameter, were collected using a vibracore system that slowly vibrates the core tube into the sediment. This limits compaction and disruption of the sample. The core locations were distributed over the length of the reservoir that could be reached by boat.

The specific core location within each area was selected to best represent the thicknesses observed in that part of the reservoir as determined from the acoustic profiles (Figure 12).

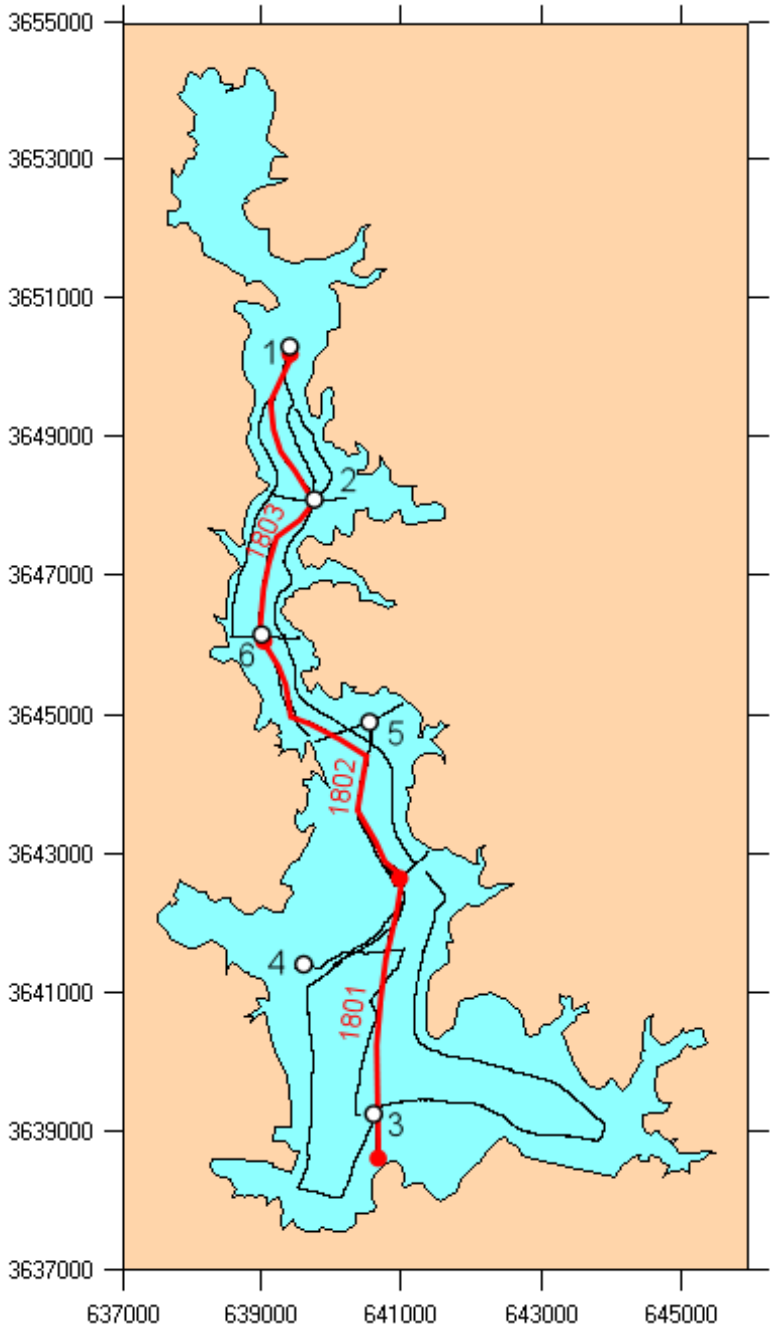

Figure 12. Map of reconnaissance survey data collected in Eagle Mountain Reservoir

Acoustic profile lines are shown in black and red. The axial profile marked in red is used to estimate survey accuracy versus profile spacing in future surveys. It was collected in three

segments (1801, 1802, and 1803), the ends of which are marked with red circles. White circles mark the 6 core locations. Geographic coordinates are in UTM Zone 14, meters.

Core Analysis

The goal of the coring operation was to determine the thickness and dry-bulk density of the post-impoundment sediment present at representative sites throughout the reservoir. To identify the base of post-impoundment sediment in the cores, we relied on visual examination of the sampled material, and measurements of the sediment water content and sediment strength versus depth in the cores. After the cores were brought back from the field, they were cut in half longitudinally and sub-sampled in 5-or 10-cm slices, depending on core length. During the sub-sampling operation, the strength of the sediment was determined using a pocket penetrometer that measures the force required to drive a 2.5 cm diameter disk into the sediment. The sediment within each sub-sample was weighed wet, dried for 48 hours at 106º C, reweighed, and stored for potential future analysis. The wet and dry weights of the samples were used to compute water content versus depth within the cores. From the average water content fraction of sampled sediment *wc*, we estimate the average dry-bulk density ρ_{db} of the sediment within each core using the formula

$$\rho_{db} = \frac{\rho_w \rho_g (1 - wc)}{\rho_g (wc) + \rho_w (1 - wc)}, \quad (1)$$

where ρ_w is the assumed density of water (1000 kg/m^3) and ρ_g is the assumed density of the sediment grains.

Two slightly different grain densities were assumed, depending on the texture of the sediment. The post-impound sediment in two of the cores (1 and 4) was sand with only minor amounts of organic material. For these cores we assumed a grain density ρ_g = 2.65 g/cm^3, which is the density of quartz. The post-impoundment sediment in the remaining cores (2, 3, 5, and 6) consisted of silty-clay, with a significant organic component. For these cores we assumed that a mineral grain density of 2.65 g/cm^3, which includes quartz at 2.65 g/cm^3 and clays, which range from 2.6 to 2.7 g/cm^3. We assumed the organic component of the sediment has a density of 1.1 g/cm^3, which is midway in the range of 0.9 to 1.3 g/cm^3 reported densities for solid organic particles without pore space in soils (Pilatti et al., 2006). To estimate the average organic content, we made a composite sample from cores 2, 3, 5, and 6 and determined the mass loss on ignition by cooking the sample at 450 ºC for 2 hours. This resulted in a 6.5% reduction in mass. Combining this result with the assumed component densities yields an average grain density of 2.55 g/cm^3 for the organic-rich, silty-clay sediments in Eagle Mountain Lake.

Results of Reconnaissance Survey

Base of sediment mapability

Analysis of the reconnaissance acoustic profiles indicates that the base of pre-impoundment sediment is clear and mapable in the parts of the reservoir we could reach by boat (Figure 13). The long axial profile shows significant bathymetric relief and change in sediment thickness, with the maximum thickness reaching 2.7 m (Figures 14). Over the 68.3 km of reconnaissance profiles, the average sediment thickness is 0.71 m, with a standard deviation of 0.63 m. In some

areas of thick, possibly gassy sediment, the 50 and 24 kilohertz signals did not penetrate to the base of sediment. In these cases, the lower-frequency 3.5 kilohertz signal did image the base of sediment (Figure 15). If a full-scale sub-bottom profiling survey is conducted on Eagle Mountain Lake, at these one signal frequencies lower than 25 kilohertz will be required.

Because of the low-water conditions during the reconnaissance survey, we were not able to collect profiles in the northern-most reach of the reservoir, were a substantial delta has formed over time (Figure 16). The delta has apparently grown throughout the reservoir's history. It is likely that thick sediment deposits occur within the delta and that it represents a significant portion of the total sediment load to the reservoir. However, a large part of the modern delta is well vegetated and above water most of the time. Hence, even at normal pool conditions it will not be possible to survey the delta using the sub-bottom profiling method. If a full-scale sub-bottom profiling survey is conducted, the amount of sediment contained in the delta will have to be determined by some other method.

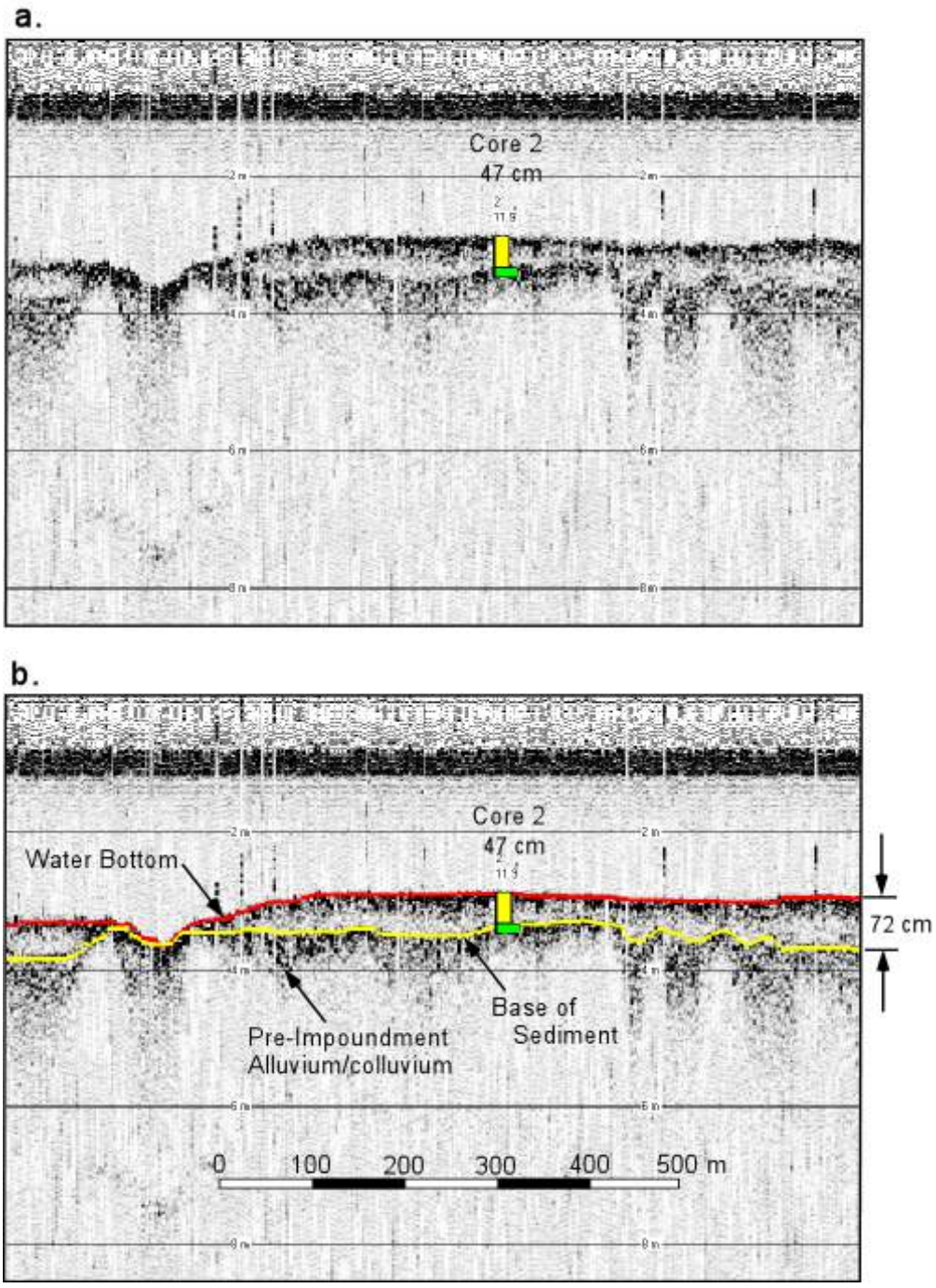

Figure 13. Close up view of profile 1803.

(a) Uninterrupted view of the 50 kilohertz data, with Core 2 projected onto the line from 11.2 m off line. The 47 cm sediment thickness (yellow) observed in the core corresponds to a clear and easily traceable sub-bottom surface in the 50 kilohertz data. (b) The same 50 kilohertz displace with the water bottom (red) and base of sediment (yellow) traced.

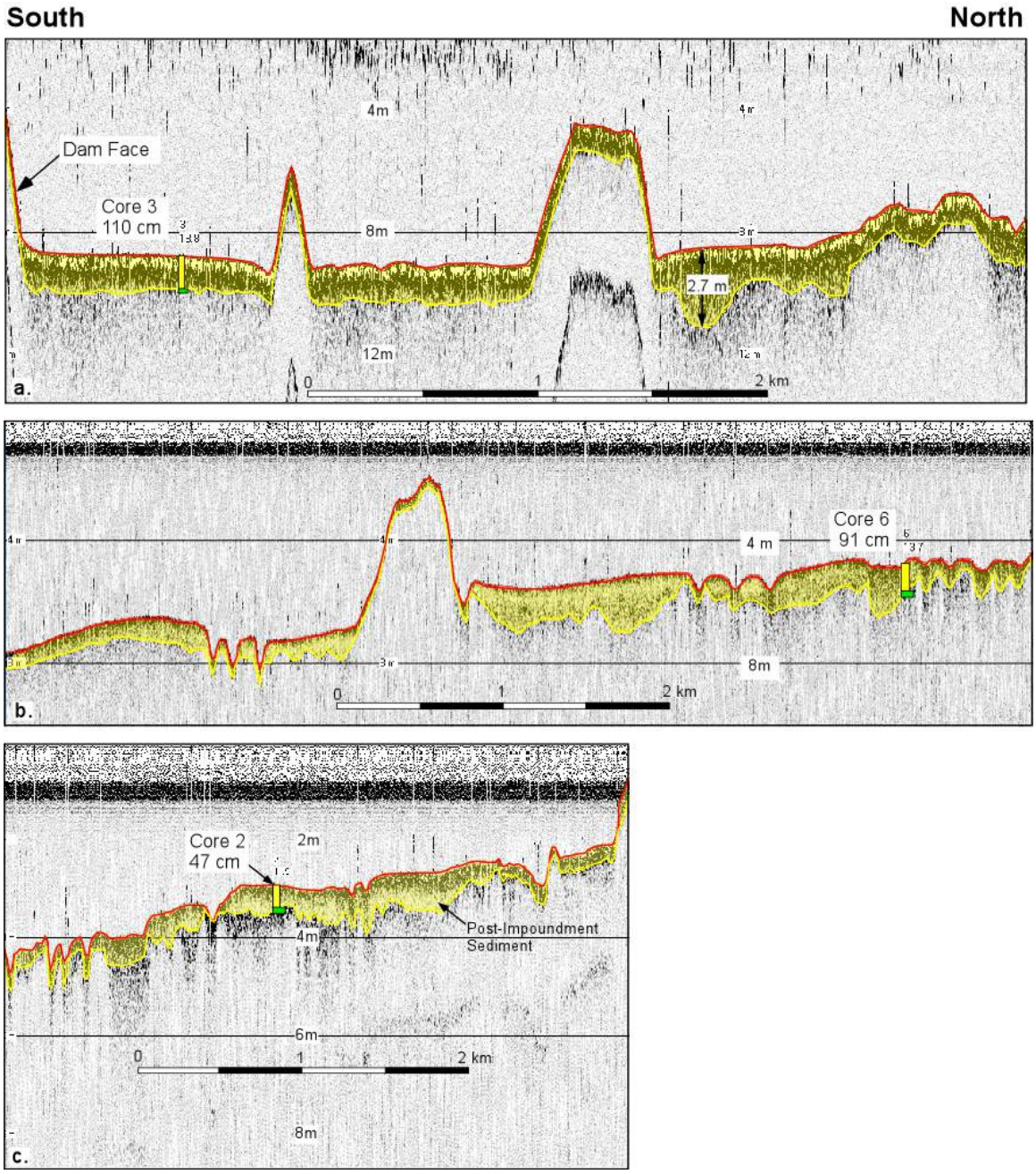

Figure 14. Long axial profile.

The 14.6-km long profile was collected in 3 segments from south to north (Figure 12). (a) Profile 1801 starts at the dam and exists north. The base of thick sediments along this reach is best shown using the 25 kilohertz signal. Core 3 verifies the interpreted base of sediment on the south end. (b) Profile 1802 is the middle segment. The base of sediment is best shown using the 50 kilohertz signal. Core 6 verifies the interpreted base of sediment on the north end. (c) Profile 1803 is the north segment of the long profile. The

50 kilohertz signal is shown. Core 2 verifies the sediment thickness in the middle of this profile.

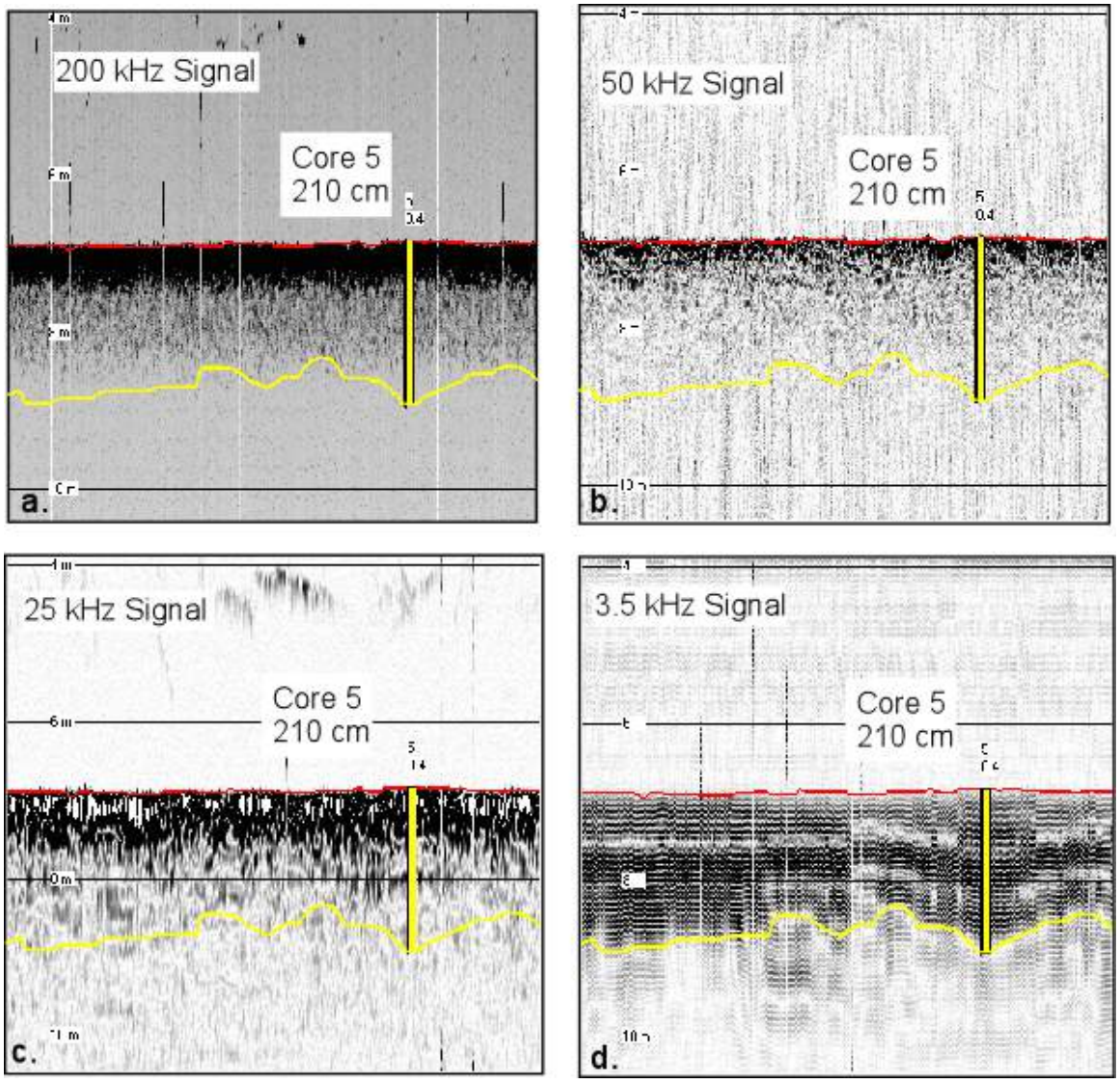

Figure 15. Penetration of difference signal frequencies.

(a) 200 kilohertz signal. (b) 50 kilohertz signal. (c) 25 kilohertz signal. (d) 3.5 kilohertz signal. In this case only the 3.5 kilohertz signal penetrates the full thickness of cored sediment.

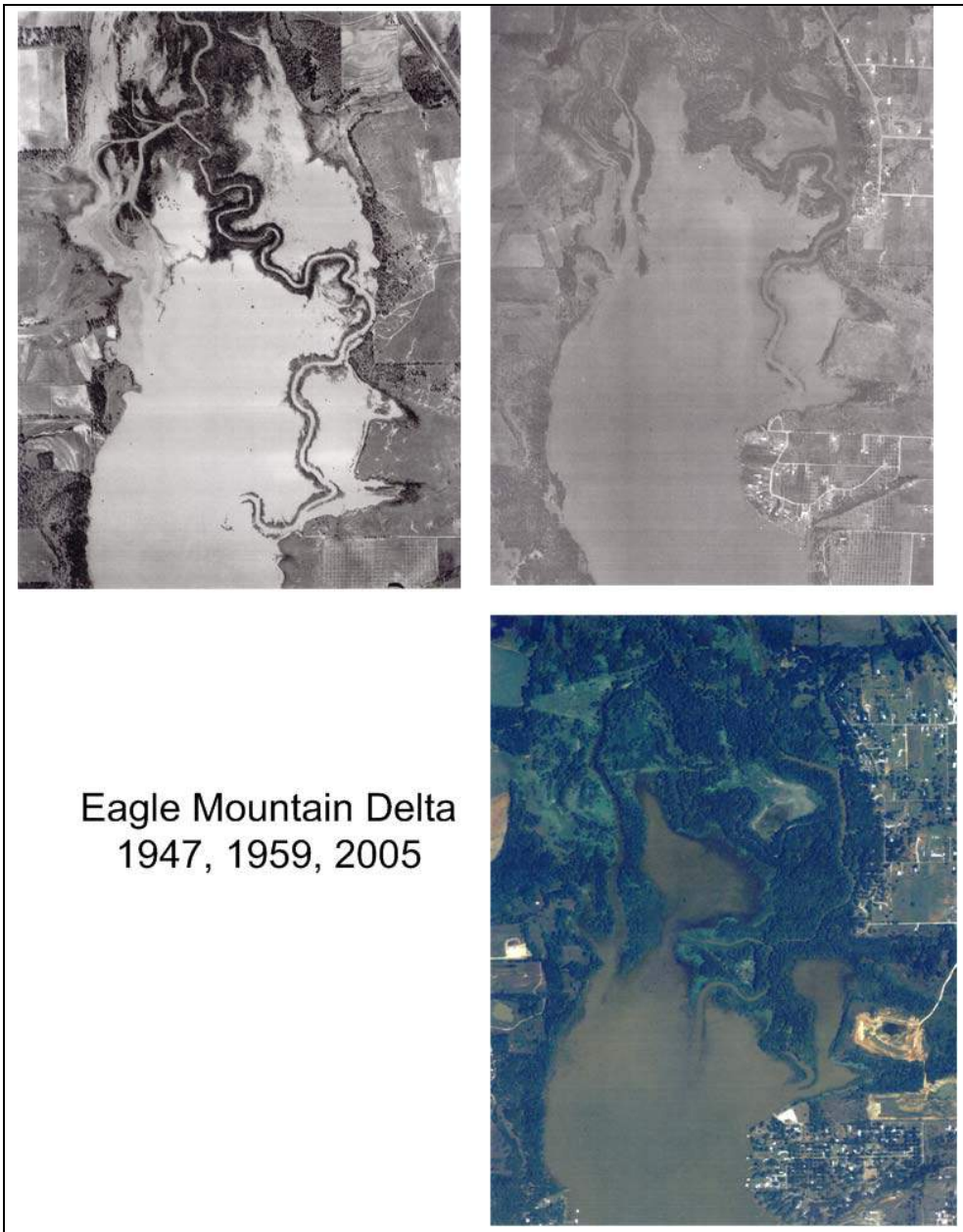

Figure 16. Growth of Eagle Mountain reservoir delta.

It is assumed that most of the delta growth is from sand transport out of the supplying watershed. The silts and clays are carried further into the pro-delta area of the lake.

Estimated Survey Error versus Profile Spacing

We used the variability of water depth and sediment thickness over the long axial profile to estimate the accuracy of volumetric surveys versus the profile spacing. To do this we sub-sample the measurements along the profile at different possible survey profile spacings ranging from 10 m to 1000 m and compare the cross-sectional areas of the re-sampled profiles with that of the full-resolution profile. Examples of the resulting sub-sampled profiles are shown in Figure 17. Figure 18 shows the predicted relationship between bathymetric survey profile spacing and error in water volume. From this relationship, the profile spacings needed to achieve possible target error levels of 0.5, 1, 2, and 4% are 120, 240, 520, and 1000 m, respectively. Similarly, Figure 19 shows the predicted relationship between the profile spacing of a acoustic sub-bottom surveys and the error in sediment volume. The profile spacings need to achieve possible target error levels of 2, 4, 6, 8, and 10% accuracy are 170, 320, 410, 525, and 990 m, respectively.

Core Analysis

We also estimated the dry bulk sediment density (dry weight of sediment per unit volume of wet sediment) by analyzing the 6 sediment cores collected throughout the reservoir (Figure 12). A summary of the coring results is given in Table 9. Of the 6 cores collected, 5 penetrated the post-impoundment sediment column and sampled the rep-impoundment material. The post-impoundment thickness ranged form 23 to 210 cm and averaged 87 cm thick. The dry bulk density of the post-impoundment sediment is bimodal. In Core 1 and Core 4 the post-impoundment sediment was sand with an average dry bulk density of 98.1 lbs/ft^3. Both of these cores were collected near the mouth of tributaries. In the remaining 4 cores, the post-impoundment sediment was silty-clay with an average dry bulk density of 25.2 lbs/ft^3.

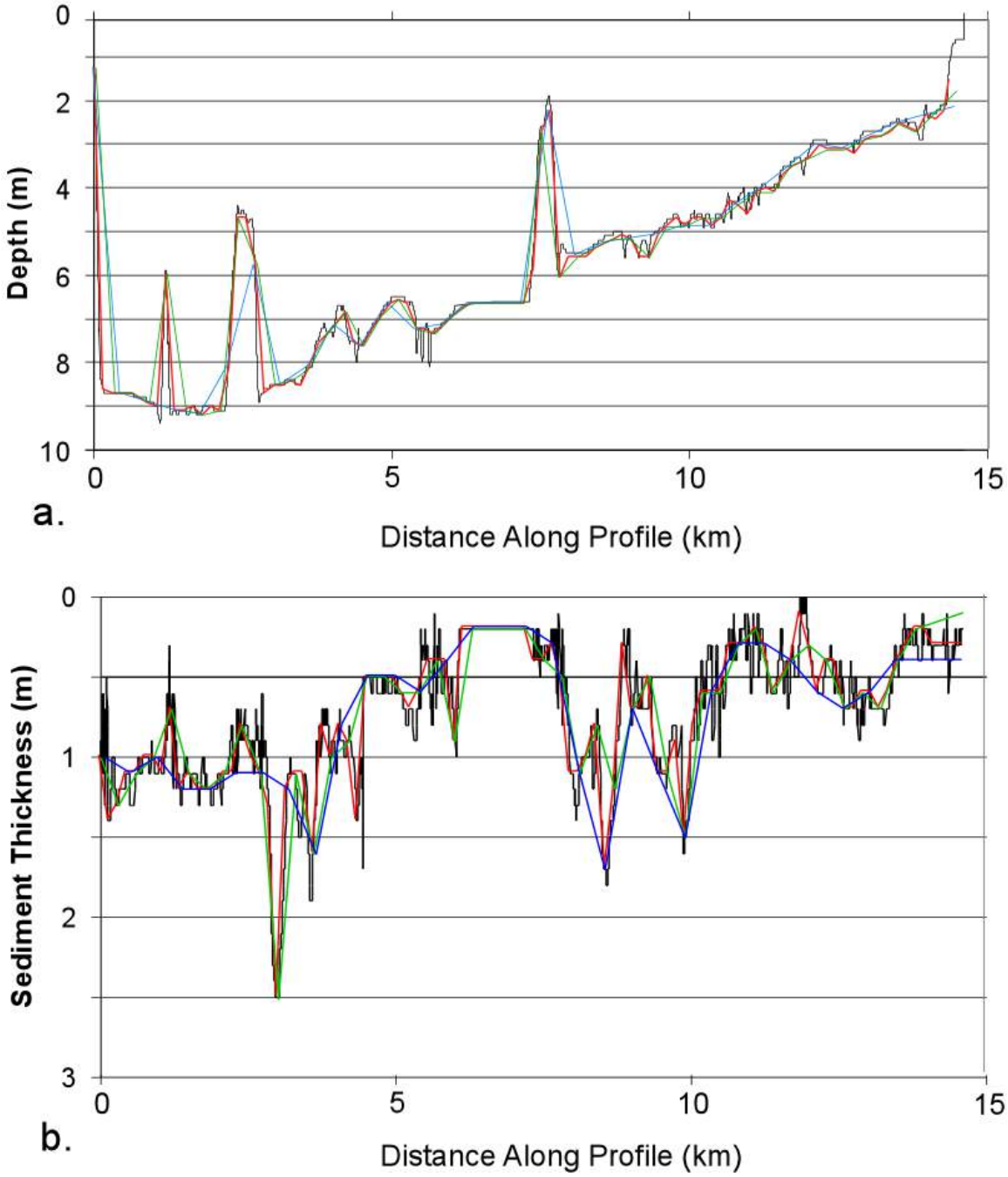

Figure 17. Sub-sampling of the long axial profile.

(a) Water depth along the axial profile is shown at full-resolution (black), Sub-sampled at with points every 150 m (red), 300 m (green), and 450 m (blue). (b) Sediment thickness variation along the profile re-sampled at the same 150, 300, and 450 m intervals.

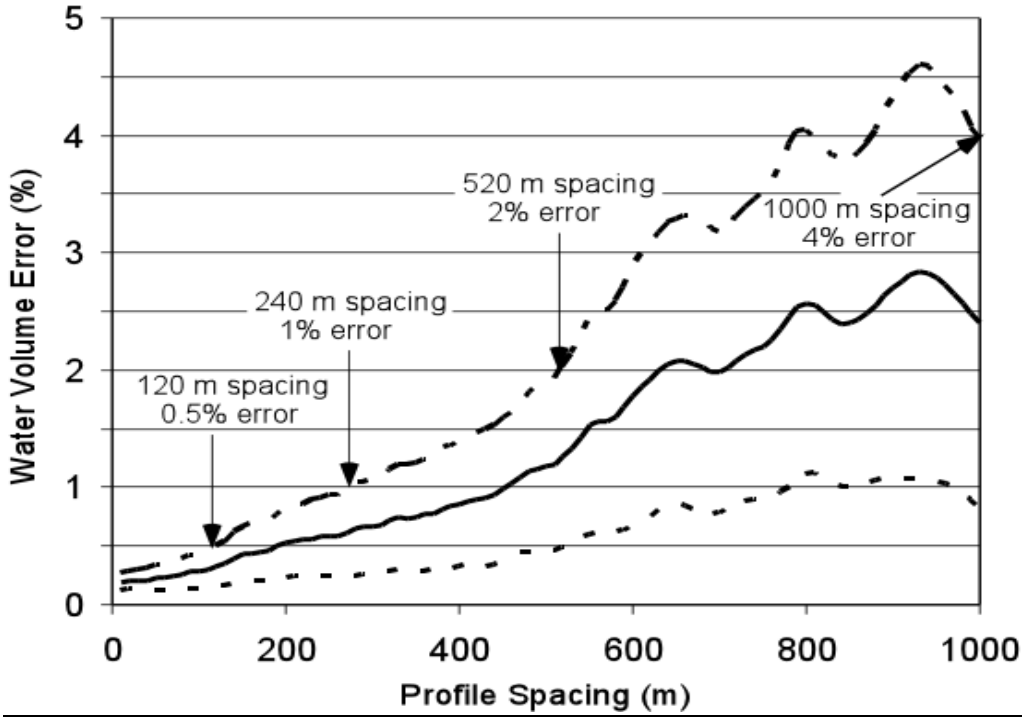

Figure 18. Relationship between bathymetric profile spacing and error in water volume for hydrographic surveys of Eagle Mountain Reservoir.
The solid line is the expected error. The upper and lower dashed lines are 1 standard deviation maximum and minimum error estimates, respectively.

Table 9. Coring results for Eagle Mountain Reservoir.

Core No.	Post-Imp. Thickness (cm)	Pre-Imp. Sample (cm)	Post-Imp. Texture	Dry Bulk Density (lbs/ft^3)
1	23	7	Sand	89.7
2	47	8	Silty-Clay	25.6
3	110	20	Silty-Clay	23.3
4	40	30	Sand	106.4
5	210	Not Sampled	Silty-Clay	26.4
6	100	20	Silty-Clay	25.3

Discussion

One of the main goals of this reconnaissance survey was to determine if the thickness of the post-impoundment sediment could be mapped using the sub-bottom acoustic profiling method. The results indicate that the method works in Eagle Mountain Reservoir and it would be technically feasible to use the method in the main part of the reservoir to determine the total sediment accumulation since impoundment. A sub-bottom survey with profiles spaced 1000 m apart would be sufficient to constrain the total sediment accumulation in the main part of the reservoir to approximately 10%. An alternate method, such as coring or ground-penetrating radar, would have to be used to measure the amount of sediment in the delta. However, it is not clear that the results of such a survey would be of any value in terms of defining the modern sedimentation problem. The review of the results from prior surveys, plus documented changes in land use, both suggest that the sediment rate has dropped dramatically since the mid 1950s. Hence, an estimate of the average sedimentation rate over the life of the reservoir would not be of much value in terms of constraining the modern sedimentation rate.

The results of the reconnaissance survey were also used to estimate the profile spacing required to achieve a given level of accuracy. This analysis indicates that the 2000 TWDB survey, which was likely conducted with a 500 ft (152 m) profile spacing, had sufficient resolution to constrain the water volume to within ±0.5%. This sound good, but at the apparent post-1960 sedimentation rate of 24.2 acre-ft/yr, the capacity is expected to have decrease only 0.08% since the 2000 TWDB survey. At this rate another 70 years of deposition will be needed before a repeat survey of the same resolution could determine that the sedimentation rate was greater than zero. Clearly, this is not an option either.

One point that should not be missed is that if the modern sedimentation is so low that it cannot be easily measured by standard surveying methods, then it is not causing rapid loss of water storage capacity. The question is: how can we check to see if it really is as low as it appears? One possibility is to measure the sediment accumulation since 1964 at a small number of points in the reservoir by Cesium-137 analysis. If the sedimentation rate is as low as 24.2 acre-ft/yr, the average accumulation would be 3.5 cm since 1964. In the reconnaissance survey, we found that some places had 3 to 4 times the average sediment accumulation. Hence, it should be possible to find a few points in the lake at which the 1964 peak in Cesium-137 deposition occurs as deep as 10 to 15 cm below the bottom, but in most places the peak would occur within the first 5 cm. If the average sedimentation rate is significantly higher than the apparent rate, the 1964 peak in Cesium-137 will be found deeper than these expected depths. Hence, Cesium-137 dating would be a cheap and quick way to see if excess sedimentation is currently a significant problem in Eagle Mountain Reservoir.

Recommendations Part II.

Given the results of the reconnaissance survey we have the following recommendations:

1. If a sub-bottom acoustic profiling survey is conducted of Eagle Mountain Lake, it should be done with the knowledge that it will constrain the average sedimentation rate over the life of the reservoir, but this rate is likely significantly different than the modern rate.

2. If a sub-bottom profiling survey is conducted it should be done using a system that includes a 3.5 and/or a 12 kilohertz transducer to penetrate to the base of 3 or more m of sediment.

3. The profile spacing of a full-scale sub-bottom survey should be no larger than 1000 m, to constrain the total sediment volume to within 10%.

4. Any full-scale sub-bottom survey should be augmented by an extensive coring and/or ground penetrating radar survey of the delta region.

5. An alternative approach that could be used to constrain post-1960 sedimentation rate would be to perform Cesium-137 analysis on the top 20-25 cm of each core and possible on additional core collected in the delta region in the northern-most part of the reservoir.

Bibliography:

Laubel, A., Svendsen, L.M., Kronvang, B., Larsen, S.E., 1999. Bank erosion in a Danish lowland stream system. Hydrobiologia, 410: 279-285.

Phillips, J.D., Slattery, M.C. and Musselman, Z.A., 2005. Channel adjustments of the lower Trinity river, Texas, downstream of Livingston dam. Earth Surface Processes and Landforms. 30: 1419-1439

Wolman, M.G., 1959. Factors influencing erosion of a cohesive riverbank. Amer. Journal of Science: 257:204-216.

Prosser, I.P., Hughes, A.O., and I.D. Rutherfurd. Bank erosion of an incised upland channel by sub aerial processes: Tasmania, Australia. Earth Surface Processes and Landforms, 25:1085-1101.

Hooke, J.M., 1980. Magnitude and distribution of rates of river bank erosion. Earth Surface Processes, 5:143-157.

Wohl, E.E., 1999. Incised bedrock channels (In) Incised River Channels: processes, forms, engineering, and management (eds.) S. Darby and A. Simon, Wiley, pp. 187-218.

Booth, D. and Henshaw, P.C. (2000) Rates of channel erosion in small urban streams. (In) M. Wigmasta, ed. Stream Channels in Disturbed Environments: AGU Monograph Series.

Zaimes, G.,N., Schultz, R.C., Isenhart, T.M., Mickelson, S.K., Kovar, J.L., Russell, J.R., Powers, W.P., 2005. Stream Bank Erosion Under Different Riparian Land-Use Practices in Northeastern Iowa. AFTA Conference Proceedings. pp. 1-10.

Couper, P. and I. P. Maddock, 2001. Subaerial river bank erosion processes and their interaction with other bank erosion mechanisms on the River Arrow, Warwickshire, UK., Earth Surface Processes and Landforms, 26, pp 631-646.

Dendy, F. E. and Champton, W. A. 1969. Summary of Reservoir Sediment Deposition Surveys Made in the United States Through 1965. USDA Misc. Publication No. 1143.

Mark Ernst 2006. Personnel Communication of Reservoir Volumes.

Pilatti, M. A., Ghiberto, P. J., and Imhoff, S. (2006) Application of general relationship between soil particle density and organic matter to mollisols of Santa Fe (Argentina), (abstract) presented at the 18th World Congress of Soil Science, Philadelphia, Pennsylvania, July 9-15, 2006.

Kier, R.S., Garner, L.E., Brown, L.F., 1977. Land Resources of Texas. Bureau of Economic Geology, Austin, Texas, 42p.

Ressel, D.D. (1989) Soil Survey of Wise County. USDA, NRCS. U.S, govt. Prointing Office, Wash. DC., 198 p.

Richardson, E.V., Simons, D.B., Lagasse, P.F., River Engineering For Highway Encroachments. Office of Bridge Technology, FHWA NHI, Report 01-004. Washington, DC.

Yang, C.T., 1996. *Sediment Transport, Theory and Practice*. McGraw Hill. N.Y., 396p.

Appendices

Eagle Mountain Subbasins

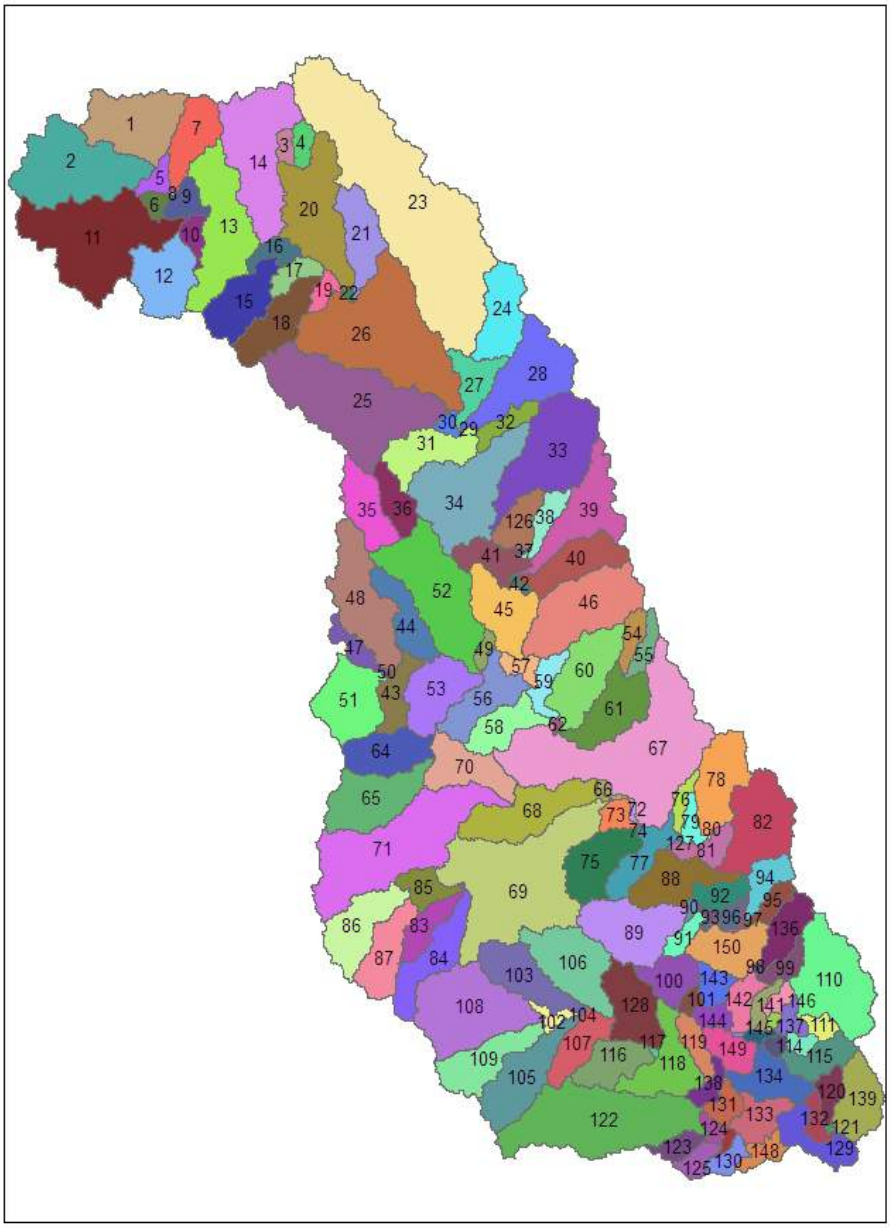

Eagle Mountain Field Locations.

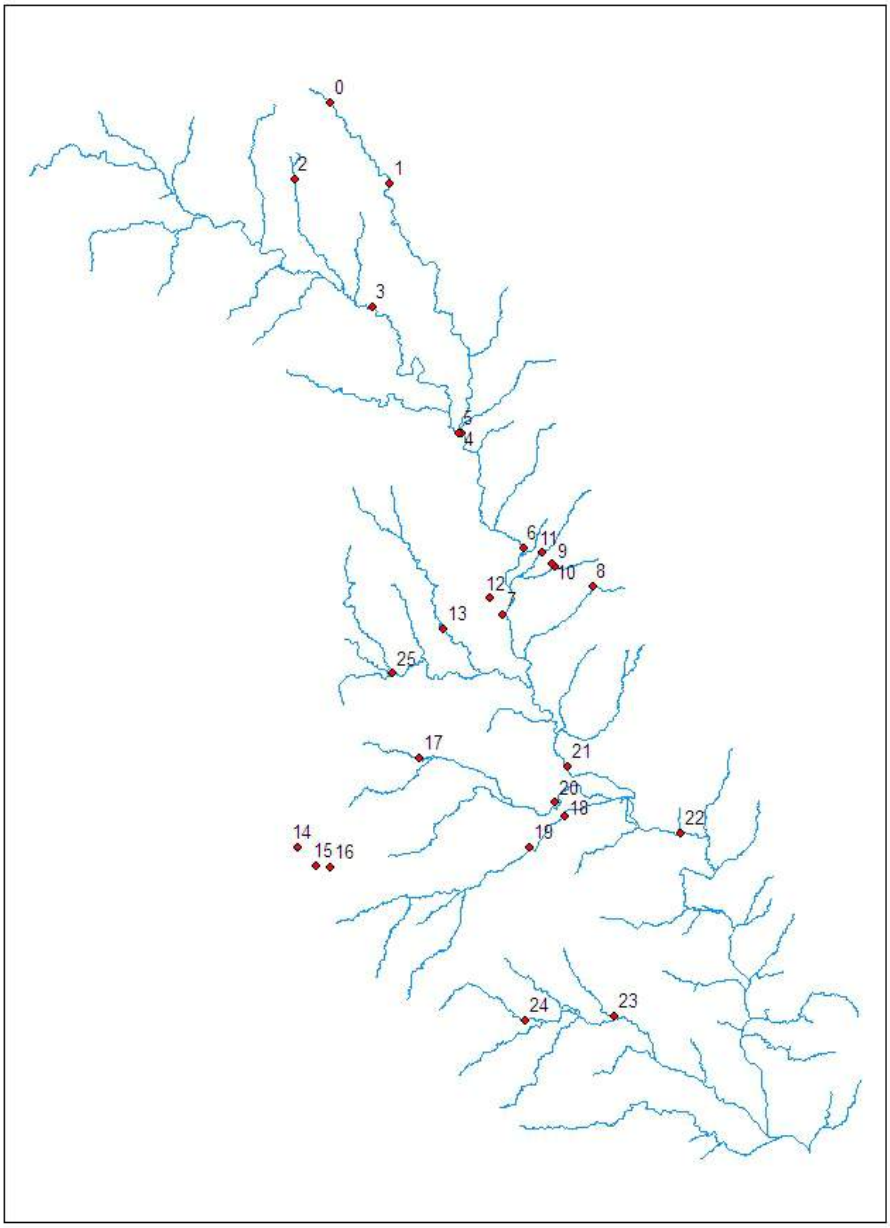

Location Field Coordinates and Photo Numbers

Location Number	Map Numbers	Photos	GPS Coordinates
1	0	1-4	N 33 343.229/W 97 45.6009
2	1	5-9	N 33 31.011/W 97 46.834
3	2	10-11	N 33 31.210/W 97 51.376
4	3	13-15	N 33 26.144/W 97 47.751
5	4	16-17	N 33 21.108/W 97 43.607
6	5	18-19	N 33 21.106/W 97 43.715
7	6	20-21	N 33 15.530/W 97 40.743
8	7	22-23	N 33 13.919/W 97 41.755
9	8	26-29	N 33 14.987/W 97 37.474
10	9	30-31	N 33 15.776/W 97 39.270
11	10	32-35	N 33 15.882/W 97 39.385
12	11	36-38	N 33 16.321/W 97 39.863
13	12	39-41	N 33 14.554/W 97 42.356
14	13	42-45	N 33 13.355/W 97 44.605
15	25	46-49	N 33 11.392/W 97 02.29 (?)
16	14	50-51	N 33 04.780/W 97 51.552
17	14	52	N 33 04.051/W 97 50.687
18	16	53-58	N 33 03.993/W 97 50.039
19	17	59-63	N 33 08.290/W 97 45.805
20	18	64-65	N 33 05.900/W 97 38.962
21	19	66-70	N 33 04.686/W 97 40.621
22	20	71-76	N 33 06.447/W 97 39.394
23	21	77-80	N 33 07.854/W 97 38.815
24	22	81-86	N 33 05.180/W 97 33.526
25	23	87-91	N 32 57.986/W 97 36.726
26	24	92-96	N 32 57.841/W 97 40.946